

DISSERTATION

THE USE OF METAGENOMIC SEQUENCING AS A TOOL FOR PATHOGEN DISCOVERY WITH
FURTHER INVESTIGATION OF NOVEL REPTILIAN SERPENTOVIRUSES

Submitted by

Laura L. Hoon-Hanks

Department of Microbiology, Immunology, and Pathology

In partial fulfillment of the requirements

For the Degree of Doctor of Philosophy

Colorado State University

Fort Collins, Colorado

Summer 2019

Doctoral Committee:

Advisor: Mark Stenglein

Gregory Ebel
Daniel Sloan
Sushan Han

Copyright by Laura L. Hoon-Hanks 2019

All Rights Reserved

ABSTRACT

THE USE OF METAGENOMIC SEQUENCING AS A TOOL FOR PATHOGEN DISCOVERY WITH FURTHER INVESTIGATION OF NOVEL REPTILIAN SERPENTOVIRUSES

Infectious diseases play a significant role in the health of all organisms, from the largest mammals to the smallest bacteria. The consistent identification of pathogens has been propelled by generations of perceptive scientists and the development of important biological tools for microbe detection. In recent years, a new technology has surfaced that has changed the face of pathogen discovery: next generation sequencing and metagenomics. This sequencing technology allows for unbiased sampling of genetic material from all organisms within a given sample, independent of our pre-conceived suspicions of the pathogens most likely to be present. Therefore, metagenomic sequencing has become a powerful tool for investigating both known and newly emerging infectious diseases that evade classical methods of diagnosis.

The preliminary goal of this dissertation was to present metagenomic-based pathogen discovery projects that highlight the benefits and limitations to this technology. First, we assessed meningoencephalitis of unknown origin (MUO) in dogs, a suspected autoimmune disease, but for which an underlying infectious agent remains a possibility. We did not detect any infectious agents associated with disease, further supporting the hypothesis of an autoimmune pathogenesis. Second, we assessed two cases of malignant catarrhal fever (MCF)-like disease in free-ranging mule deer. In the U.S., MCF is most commonly associated with ovine herpesvirus-2 infection, however, we identified caprine herpesvirus-2 (CpHV-2) in both cases. CpHV-2 is an uncommon cause of MCF and has not been previously described in mule deer. Therefore, metagenomics aided in the identification of a known but unexpected pathogen of disease. Lastly, we investigated an outbreak of granulomatous nephritis in a collection of seahorses. We identified a novel paramyxovirus and parvovirus, but no clear association between infection and disease was drawn for case and control animals. Therefore, additional examination of these viruses will be necessary to determine their association with disease. In this case, metagenomics provided a new thread of

investigation but did not provide a definitive answer. This is a common outcome with metagenomic projects and highlights its use as an investigatory tool upon which future experimentation can be based.

The second goal of this dissertation was to further characterize a virus discovered by metagenomic sequencing through confirmation of disease causality and epidemiologic investigation of species susceptibility and disease. Recently, a novel serpentovirus was discovered by metagenomic sequencing in association with fatal respiratory disease in pythons. Investigations of this virus included genome characterization, tissue tropisms, viral nucleic acid localization to areas of disease, and potential mechanisms of pathogenesis. However, these studies only provided circumstantial evidence linking serpentovirus infection to disease. In attempt to confirm disease causality, we conducted experimental infections in ball pythons (*Python regius*) with a serpentovirus known as ball python nidovirus (BPNV). Three ball pythons were inoculated orally and intratracheally with cell culture isolated BPNV and two were sham inoculated. Antemortem choanal, oroesophageal, and cloacal swabs and postmortem tissues of infected snakes were positive for viral RNA, protein, and infectious virus by qRT-PCR, immunohistochemistry, western blot and virus isolation. Clinical signs included oral mucosal reddening, abundant mucus secretions, open-mouthed breathing, and anorexia. Histologic lesions included chronic-active mucinous rhinitis, stomatitis, tracheitis, esophagitis and proliferative interstitial pneumonia. Control snakes remained negative and free of clinical and histologic disease throughout the experiment. Our findings establish a causal relationship between serpentovirus infection and respiratory disease in ball pythons and shed light on disease progression and transmission.

Following an established disease causation, we sought to characterize the epidemiologic features of serpentovirus infection in captive snakes. We performed a large longitudinal study of serpentovirus infection with the aim of generating an improved understanding of the course and clinical outcome of infection, assessing the susceptibility of different types of snakes to infection and disease, surveying viral genetic diversity, and defining effective management practices. We collected 777 antemortem choanal or oral swabs from 639 snakes from 12 collections across the United States. These included snakes from 62 species, 28 genera, and 6 families: Pythonidae (N=414 snakes), Boidae (79), Colubridae (116),

Lamprophiidae (4), Elapidae (12), and Viperidae (14). Infection was more common in pythons (40% infected), and in boas (10% infected) than in other types of snakes, which had infection rates of 0-1%. Pythons were more likely to exhibit signs of respiratory disease: 85 of 144 infected pythons displayed signs of mild to severe respiratory disease, but only 1 of 8 infected boas did. Infected snakes had increased mortality: the percentage of infected pythons that died of respiratory disease during the course of this study ranged from 45 to 75% in two different collections. Genetically distinct serpentoviruses, including divergent genotypes, were detected in pythons, boas, and colubrids, suggesting a potential species barrier between snakes of different families. In some cases, nearly identical viruses were found to infect pythons of different genera, indicating host plasticity amongst python serpentoviruses. Older snakes were more likely to be serpentovirus-positive, but males and females were equally likely to be infected. Neither age nor sex were statistically associated with disease. Longitudinal sampling of forty pythons over 28 months revealed serpentovirus infection is chronic, and definitive evidence of viral clearance was not observed. We followed offspring of infected parents and found that vertical transmission either does not occur or occurs at a much lower efficiency than horizontal transmission. Management strategies that could reduce the spread of serpentoviruses include rapid physical separation of infected snakes, testing snakes multiple times over several months to ensure true negative results, and rigorous quarantine when introducing pythons into a collection.

Our findings regarding serpentovirus infection in snakes provide a solid foundation for future investigations of related serpentoviruses. In addition to snakes, serpentoviruses have also been identified in lizards and turtles in Australia. Serpentovirus infection in lizards has been associated with a respiratory disease similar to that seen in snakes, but disease causation is only circumstantial. We further develop our understanding of serpentovirus-associated disease in lizards by describing novel serpentoviruses in a collection of veiled chameleons with respiratory disease-associated mortalities. Over the course of 1 year, a reptile collection lost 24 of 30 veiled chameleons. Clinical signs included wheezing and vertical head tilting with gasping, increased mucus in the oral cavity, anorexia, and reduced water intake. Histopathology included severe proliferative and mucinous interstitial pneumonia, tracheitis, and rhinitis. Tissue pools from

3 chameleons were evaluated by metagenomic sequencing and two novel serpentoviruses were detected; coinfection with both serpentoviruses was found in 1 chameleon. Antemortem oral swabs were sampled from the remaining 6 live chameleons in the collection and were tested for serpentovirus infection by PCR. Five of 6 chameleons were serpentovirus positive, one of which was exhibiting mild signs of respiratory disease. Genomic assessment revealed approximately 50% nucleotide identity between each of the chameleon serpentoviruses, as well as to other reptile serpentoviruses in snakes, lizards, and turtles. These findings further support the hypothesis that serpentoviruses cause disease in lizard species. In the future, serpentovirus should be considered a possible differential for respiratory disease in chameleons.

ACKNOWLEDGMENTS

There is an immense community of people that I would like to thank for the support and encouragement I have received throughout this process. First, I would like to thank Craig Kuchel for instilling in me a love of science at an early age. I would like to thank the Samuels' laboratory at the University of Montana for creating such a wonderful and encouraging environment in which to learn and appreciate research. Their continued support has been immensely important to my growth as a scientist. I would like to thank Dr. Paula Schaffer, Dr. Chad Frank, Dr. EJ Ehrhart, Dr. Gary Mason, Dr. Colleen Duncan, and the pathology residents at CSU for making my residency a fruitful and fulfilling experience. I wouldn't have made it this far without their help. I would like to thank Dr. Mark Stenglein for welcoming me into his laboratory and providing me endless support, valuable training, and the freedom to pursue to my research interests and career goals. The path to a Ph.D. is long and arduous, but training under him has been a truly rewarding experience. I would like to thank Marylee Layton, Shaun Cross, and Justin Lee for always providing me with lab assistance and advice. I would like to thank Lauren Keuchter and Case Rogers for being wonderful mentees and contributing to my research projects. I would like to thank my committee members, Dr. Greg Ebel, Dr. Dan Sloan, and Dr. Sushan Han for giving me guidance during this process.

Thank you to my family for their never-ending patience and encouragement throughout my education. I wouldn't be here without them and am incredibly grateful to have such a wonderful (Bobo) family. Thank you to my friends for keeping me sane and reminding me of the importance of work-life balance. Thank you to Alex Smiley for his limitless tolerance and forgiveness when I put my career above all else. His support has been invaluable.

Finally, I would like to thank all my collaborators and the reptile owners that have made this work possible and truly meaningful. Working with them has given me a new appreciation for reptiles and those who advocate for their health and welfare.

TABLE OF CONTENTS

Abstract	ii
Acknowledgments.....	vi
List of Tables	ix
List of Figures.....	x
Chapter 1: Introduction	1
1.1: Review of Pathogen Discovery Methods and Recent Advances.....	1
1.2: Respiratory Diseases of Reptiles	9
Chapter 2: Metagenomic Sequencing as a Tool for Pathogen Discovery	16
2.1: Rationale for Included Metagenomic Studies	16
2.2: Metagenomic Investigation of Idiopathic Meningoencephalomyelitis in Dogs (<i>Canis lupus familiaris</i>).....	16
2.2.1: Introduction	16
2.2.2: Materials and Methods	17
2.2.3: Results	24
2.2.4: Discussion.....	26
2.3: Metagenomic Investigation of Meningoencephalitis of Unknown Origin in Free-Ranging Mule Deer (<i>Odocoileus hemionus</i>)	29
2.3.1: Introduction	29
2.3.2: Materials and Methods	30
2.3.3: Results	31
2.3.4: Discussion.....	33
2.4: Metagenomic Investigation of Granulomatous Nephritis of Unknown Origin in Lined Seahorses (<i>Hippocampus erectus</i>).....	34
2.4.1: Introduction	34
2.4.2: Materials and Methods	35

2.4.3: Results	36
2.4.4: Discussion.....	38
2.5: Conclusion	40
Chapter 3: Respiratory Disease in Ball Pythons (<i>Python regius</i>) Experimentally Infected with Ball Python Serpentovirus	42
3.1: Introduction.....	42
3.2: Materials and Methods	43
3.3: Results.....	50
3.4: Discussion.....	61
Chapter 4: Epidemiologic Investigation of Ophidian Serpentoviruses in Captive Snake Populations	65
4.1: Introduction.....	65
4.2: Methods and Materials	66
4.3: Results.....	73
4.4: Discussion.....	88
Chapter 5: Respiratory Disease in Veiled Chameleons (<i>Chamaeleo calypttratus</i>) Associated with Serpentovirus Infection.....	94
5.1: Introduction.....	94
5.2: Case History.....	94
5.3: Methods and Materials	96
5.4: Results.....	100
5.5: Discussion.....	106
Chapter 6: Concluding Remarks.....	110
6.1: Learning from Metagenomic Studies	110
6.2: The Value of Establishing Disease Causation	111
6.3: Going Forward: The Future of Serpentovirus Research.....	113
References.....	115
Appendix.....	132

LIST OF TABLES

Table 2.1. MUO Case Summary	19
Table 2.2. Average reads per deer sample and sequencing analysis summary	31
Table 2.3. Infectious agents detected by metagenomic sequencing in seahorses with and without nephritis.....	38
Table 3.1. List of oligonucleotides used during qRT-PCR for detection of BPNV or GAPDH and used for sequencing library generation	47
Table 4.1. Primer sets targeting serpentoviruses	72
Table 4.2. Prevalence of serpentovirus by snake species, family, and total	75
Table 5.1. Animals sampled for serpentovirus testing from a single collection.....	98
Table 5.2. Summary of sequencing depth and aligning reads to VCSV and VCOrV	102
Table 5.3. General features of veiled chameleon orthoreovirus genome	104
Supplemental Table 2.1. Average reads per canine sample and sequencing analysis summary	132
Supplemental Table 2.2. Positive control sequencing analysis summary	132
Supplemental Table 2.3. Oligonucleotides used in this study	133
Supplemental Table 4.1. Summary table of each study collection	133
Supplemental Table 4.2. Snakes screened for serpentoviruses by metagenomic sequencing	137

LIST OF FIGURES

Figure 2.1. CpHV-2 detected by PCR in brain, spleen, and RPLN of two mule deer.....	33
Figure 3.1. Antemortem findings in ball pythons infected with BPNV	51
Figure 3.2. Postmortem findings in ball pythons infected with BPNV	53
Figure 3.3. Histopathology of ball pythons infected with BPNV.....	54
Figure 3.4. Western blot of BPNV nucleoprotein.....	55
Figure 3.5. IHC of the respiratory tract and cranial esophagus in BPNV-infected ball pythons.....	56
Figure 3.6. IHC of the gastrointestinal tract in BPNV-infected ball pythons.....	57
Figure 3.7. Relative viral RNA in antemortem swabs.....	58
Figure 3.8. Relative viral RNA in postmortem tissues	59
Figure 3.9. Immunofluorescence of DPHT cells inoculated with infectious swabs and tissues.....	60
Figure 4.1. Oral (top) and choanal (bottom) swabbing of captive snakes	69
Figure 4.2. Captive pythons in some collections have a high prevalence of serpentovirus infection	74
Figure 4.3. Excessive oral and nasal mucus production in a serpentovirus-positive snake.....	77
Figure 4.4. Clinical disease varies by individuals within each snake genus and amongst snake families ..	78
Figure 4.5. Infected snakes are statistically more likely to experience mortality than uninfected snakes ..	79
Figure 4.6. Gross and histologic pulmonary lesions in a serpentovirus-positive green tree python from collection A (snake A26)	79
Figure 4.7. Serpentovirus infection is statistically associated with age but not sex; clinical signs are not statistically associated with age or sex.....	80
Figure 4.8. Serpentovirus phylogeny reveals at least two distinct evolutionary lineages	82
Figure 4.9. The progression of serpentovirus infection and disease in a single collection (A) over 28 months	86
Figure 4.10. Phylogeny and proposed horizontal transmission in collection A	87
Figure 5.1. Proliferative and catarrhal interstitial pneumonia and rhinitis in veiled chameleon (VC1)....	101
Figure 5.2. Cladogram of veiled chameleon serpentovirus and other reptilian serpentoviruses	103

Figure 5.3. Phylogenetic tree of veiled chameleon orthoreovirus and orthoreoviruses of reptiles, mammals, and birds..... 105

Figure 5.4. Gel electrophoresis of serpentovirus PCR..... 106

CHAPTER 1: INTRODUCTION

1.1: Review of Pathogen Discovery Methods and Recent Advances

Since the discovery of microorganisms and the development of the germ theory, there have been pathogen hunters: those adventurous scientists in search of microscopic agents of disease. The prominent discoveries made by Koch, Pasteur, Hooke, Leeuwenhoek, and others instilled in scientists a fascination with the microbial world and highlighted the role organisms play in health and disease [1,2]. The first portion of this introduction provides a brief overview of conventional and recently developed tools used for pathogen discovery.

1.1.1: Conventional Methods of Detecting Infectious Agents

Although the field of infectious disease has greatly advanced since the days of early microbial discovery, some methods, albeit improved, have remained a staple in the identification of pathogens. The original tool these scientists employed was the microscope, a means of visualizing the microbial world [1]. Today, microscopic examination of tissues is still an essential component of disease investigation. The identification of lesions associated with infectious disease or the direct visualization of a microbe can be the first step in pathogen detection. However, the sensitivity and specificity of this tool is limited. Light microscopy is generally considered a poor method for pathogen detection when used on its own. Typically, organisms need to be large enough, occur in high enough numbers, or cause detectable lesions to be identified. One study found that light microscopy missed nearly 50% of infectious agents in HIV patients, but that sensitivity was significantly increased with the use of electron-based imaging [3]. Transmission electron microscopy (TEM) has been a key component of many pathogen discoveries, including Ebola virus, severe acute respiratory syndrome virus (SARS), and lymphocytic choriomeningitis virus [4–6]. This tool is useful for its unbiased approach that does not require prior information of the pathogen, lending it to the detection of known and novel pathogens [7]. Additionally, it does not require live or intact organisms and it can identify multiple pathogens at once [7]. However, identification can often only be achieved at

the family level and some pathogens share morphologic characteristics that can limit interpretation or misidentify the organism [7–9]. Furthermore, the use of EM requires specific sample preparation techniques that are not always widely available and extensive training is necessary for accurate interpretation of images [7]. Microscopy is a valuable first step in the identification of diseases with infectious origins, but for more specific classification of pathogens additional exploration is required.

Culture techniques have long been an essential tool for microbiologists [10]. Unfortunately, the challenge with culture is that many pathogens are either fastidious, and therefore difficult to culture, or completely unculturable. This is true for eukaryotic, prokaryotic, and viral pathogens alike. Examples include *Helicobacter heilmannii*, *Tropheryma whippeli*, *Bartonella* species, Kaposi sarcoma-associated herpesvirus, hepatitis viruses, hantavirus, aquatic pathogens, and *Laboulbeniales* fungus [11–14]. Therefore, although culture remains an important tool for microbiologists, its use in pathogen discovery has waned with advancements in molecular techniques [15–19].

In 1983, Kary Mullis developed a new technology known as polymerase chain reaction (PCR), an invention that changed the course of science [20]. Several molecular-based methods for pathogen discovery have some foundation in PCR. This technique is a rapid, low-cost method that requires minimal equipment and training, has portable options for use in the field, and for which data can be generated in real-time. The specificity and sensitivity of PCR assays is dependent on design but can often be tailored to meet the goals of the assay. In singleplex assays primers and probes can be designed to unique genomic regions of an organism for high specificity. These assays can also be designed with degenerate primers and probes or in highly conserved regions that may allow for reduced specificity but increased sensitivity to groups of related organisms [21]. Furthermore, these same principles can be applied to multiplex assays that allow for the simultaneous screening of numerous microorganisms. This can be particularly useful in medicine where different infectious agents can result in similar diseases [22].

Detection microarrays have also been used for pathogen detection as a scale-up from multiplex PCR. These are designed as numerous oligonucleotide probes, complementary to sequences of interest, attached to a solid substrate. The addition of fluorescently labeled DNA of interest allow for visualization

of increased fluorescence at sites of hybridization [23]. Unfortunately, these assays suffer from the same issues as other types of microarrays, including background fluorescence, transient or inappropriate hybridization with non-complementary DNA, secondary structure preventing hybridization, and the need for continuous updating of probe sequences based on available genomic data [23].

Serology and immunoassays (e.g. immunohistochemistry/fluorescence, western blot, enzyme-linked immunosorbent assays) have been used for the detection of infectious agents based on the presence of antigen or the development of antibodies as an immune response to infection [24–26]. These assays are particularly useful in assessing active infection with a pathogen (e.g. acute and convalescent sera) or assessing exposure (current or historical) to an infectious agent by seroconversion. Serologic assays were essential to the identification of the SARS coronavirus in the 2003 Hong Kong outbreak [27]. RNA/DNA in situ hybridization (ISH) has also become a widely-used tool for the detection of nucleic acids in specimens, including for infectious agents such as papillomavirus, herpesvirus, and pathogenic fungi [28–32]. ISH allows for the localization of specific nucleic acid sequences in fixed specimens by hybridization of a labeled probe to a target sequence by complementary base pairing. It is akin to immunochemical assays but relies on complementary nucleic acid interactions rather than antigen-antibody interactions.

Proteomics refers to characterization of the proteome, including the structure, function, and interactions of organismal proteins. Proteomic techniques are diverse, including chromatography, protein microarray, protein gel electrophoresis, isotopic labeling, x-ray crystallography, mass spectrometry, and NMR spectroscopy [33]. Proteomics have been used for the identification of prokaryotic and eukaryotic pathogens as well as understanding the structure and pathogenesis of infectious diseases [33–36].

Molecular-based methods, such as PCR, microarray, serology, and proteomics are useful in the identification of known or closely related pathogens but can fall short at the identification of divergent or novel organisms. Targeted assays require prior understanding of the agent of interest and are therefore limited by our current knowledge of pathogen sequences and composition. These limitations have impacted our understanding of infectious disease. For example, in a large analysis of human encephalitis cases, targeted methods failed to detect an infectious agent in up to 70% of suspected cases [37–39]. This finding

highlights the need for an unbiased method of infectious agent identification for improved detection of pathogens in human and animal health.

In recent years, such a method has come to light: next generation sequencing. With the increasing availability and affordability of sequencing methods, this cutting-edge technology has become an integral tool to the pathogen hunter and is paving the way for a new era of pathogen discovery.

1.1.2: Development of Sequencing Technology

The development of sequencing technology could only begin after the discovery of the DNA structure [40], therefore, its history is relatively short. First-generation sequencing methods included ‘chemical cleavage’ and ‘chain termination’ sequencing [41,42]. Chain termination methods (also known as dideoxy or Sanger sequencing) are still used today and were instrumental in the sequencing of the human genome [43,44]. Sanger sequencing is founded on the use of chain-terminating nucleotide analogs that lack a 3’ hydroxyl group, resulting in base-specific termination during primed DNA synthesis. With a known concentration of fluorescently labeled nucleotide analogs added to the reaction, the nucleotide sequence can be derived by base-specific termination sites. For nearly 30 years, Sanger sequencing technology dominated the field and was considered the gold standard. Modern versions of this technology generate long reads (up to ~1000 bp) with high accuracy, but are restricted by low-throughput and high cost per sample for the depth of data generated [45].

Recently, the commercial availability of massively parallel sequencing platforms has transformed sequencing technology, allowing for high-throughput genomic analysis known as next-generation sequencing (NGS) [46]. The most widely used method of NGS is “sequencing by synthesis” that tracks the addition of fluorescently labeled nucleotides as DNA is copied in a massively parallel fashion on a flowcell [47]. This and other similar methods have allowed for an unprecedented throughput, scalability, and speed of sequencing with relatively low cost and high precision. Reads lengths are short (typically 75-300 bp), which may be limiting, but the achievable depth and accuracy of sequencing data can offset this weakness [45]. Additional technologies have since been developed, including single-molecule and nanopore-based

methods, resulting in amplification-independent sequencing, long-read sequencing (multiple kilobases), sequencing of RNA, and the portability of sequencing technology [48–50].

1.1.3: Metagenomics: The Technique

In the field of pathogen discovery, one of the most important aspects of NGS technology is the development of metagenomics. Metagenomic sequencing refers to the sampling of all extracted nucleic acids from all organisms present within a single complex sample; this allows for an unbiased approach to the detection of infectious agents [51]. The process of metagenomic sequencing begins with the extraction of RNA or DNA from a sample. If short-read sequencing is being performed, nucleic acids are fragmented to an appropriate size (usually 150-300 bp) by chemical, physical, or enzymatic fragmentation. Fragmentation is not required for long-read systems (e.g. Oxford Nanopore). Nucleic acids are then prepared as a “library” of double stranded DNA sequences that are tagged (e.g. 5’ and 3’ adapters) for compatibility with the desired sequencing platform. When multiple samples are being prepared for a single NGS run, sequences derived from each sample are indexed with unique barcodes, allowing for post-sequencing sorting of data. Amplification may or may not be necessary during library preparation, depending on the quantity of nucleic acids, the method of adapter ligation, and the sequencing platform being used. Libraries are then loaded onto a sequencer and massively parallel sequence analysis is performed [52].

Following the generation of sequencing data, the results are analyzed. Typically, a stepwise data analysis pipeline is utilized. First, if multiple samples prepared simultaneously, sequences are demultiplexed based on unique barcodes to identify the sample of origin. Adapter sequences are then removed, followed by filtering-out of low quality and duplicated reads. The remaining unique reads contain both host and non-host sequences. In most cases of pathogen discovery, host nucleic acids are not of interest and can therefore be removed by the exclusion of sequences that align to a provided host genome. The loss of sequencing data at this step can be minimized by kits that allow for depletion of host nucleic acids (e.g. ribosomal RNA) during library preparation rather than data analysis [53]. Once host sequences have been

removed, remaining sequences are assembled into longer contiguous sequences (contigs) based on individual read overlap. Contigs, as well as individual reads that were not assembled, are then queried against a database of nucleotide and protein sequences to identify possible pathogen-derived sequences.

1.1.4: Unbiased Metagenomic Sequencing for Detecting Infectious Agents

During the rapid advance of high-throughput sequencing technology, the use of sequencing platforms in the field of infectious disease has drastically increased. This is most apparent in the field of virology, in which new viruses are continuously being discovered; the result being massive expansion of the viral genome database and enlargement of taxonomic groups of known and novel viruses [16,54,55]. This includes both general discovery of viruses, independent of their role in disease, as well as specific investigations of pathogenic agents.

Large-scale metagenomic-based surveys have recently redefined entire taxonomic groups of viruses. As an example, Shi et al. (2016 and 2018) recently employed a meta-transcriptomic approach to sample 220 different invertebrate species spanning nine animal phyla and 186 different vertebrate species of amphibians, reptiles, and fish [56,57]. The goal was to identify new viruses that could elucidate the history of RNA virus evolution and provide a more thorough understanding of viral diversity. In these two studies, nearly 1700 new viruses were discovered, highlighting the power of this technology and the sheer breadth of organisms that have yet to be discovered.

On a smaller scale, but no less significant, are investigations into specific diseases of human and animal health [14,22,54,58,59]. Examples include a novel arenavirus identified in transplant-associated diseases, which has subsequently increased our awareness of potential pathogens spread through transplantation [60]. Another novel arenavirus, Lujo virus, was detected in only 72 hours following an outbreak of hemorrhagic fever in southern Africa, indicating the speed at which diagnoses can be made with this technology [61]. Additionally, portable sequencing methods have made rapid on-site detection of viruses possible during infectious disease outbreaks, including in the 2014-2015 large-scale Ebola virus outbreak [50]. Furthermore, veterinary diseases that have long-been identified as infectious but have evaded

classical methods of diagnosis have been identified with sequencing technology. Examples include novel reptarenaviruses as the causative agents of inclusion body disease in pythons and boas [62,63]; a novel borna virus in proventricular dilatation disease in psittacine birds [64]; and novel serpentoviruses associated with respiratory disease in pythons (see Chapters 3-5) [9]. These are just a few examples of the use of this technology as a tool for pathogen discovery and detection. With continued advancement in the field, it is certain we will see a sustained increase in the number of pathogens discovered in the years to come.

1.1.5: The Shortcomings of Metagenomics in Pathogen Characterization

Although the methods of pathogen discovery have become more advanced, our ideas of confirming causative relationships have been modified very little. Koch's postulates, established in 1891, describe the necessary steps to establish disease causation: a microbe must be present in every case of disease, that same microbe must be absent in cases of other disease (i.e. disease specific), and following isolation in pure culture the microbe must induce the same disease in a naïve host [65]. This proposal has been applied to the field of infectious disease for over 100 years and remains the gold standard for proof of disease causation. However, these can be difficult or impossible to apply in cases of unculturable pathogens, chronic diseases, diseases associated with latent infections, or diseases in which animal models are unavailable.

With the discovery of viruses and the introduction of new technologies this standard was modified to include slightly relaxed standards for establishing probable causation [66–68]. To account for the differences between viruses and other known pathogens, Rivers (1936) proposed that viruses must be regularly associated with a specific disease and that the association could not be incidental. Rivers also suggested experimental inoculations without the requirement of isolation in culture as an additional way of determining causality. Following the invention of PCR, Fredericks and Relman (1996) proposed that the identification of pathogen-specific nucleic acid sequences in most cases of disease, and at the sites of disease pathology, could support causation. Caveats were applied to this: few or no pathogen sequences should be present in a non-diseased host or tissue, sequence detection should diminish as the disease

resolves or increase during relapse, and sequences should be present prior to the onset of disease (incubation period of infection). Although these amendments to Koch's postulates broaden our abilities to establish causation, there are still exceptions to these criteria. Exclusions include infectious agents that cause disease in distant tissue sites separate from infected tissues (e.g. *Clostridium botulinum* and *Clostridium tetani* [69,70]), immune-mediated disorders secondary to infectious agents (e.g. Guillain-Barré syndrome, rheumatic heart disease, Sydenham's chorea, and chronic Lyme disease [71–73]), latent or chronic infections (e.g. human papillomavirus and herpesvirus [74,75]), and comorbidities [76,77].

More recently, Lipkin outlined a scale of certainty relating to disease causation [16,22]. Level 1, a possible causative relationship, is characterized by the detection of a microbe in one of more individuals with disease. This could include isolation of the microbe, detection of microbial nucleic acid or proteins, an adaptive immune response to the microbe, or visualization of the microbe. Level 2, a probable causal relationship, is characterized by biological plausibility of a causal relationship. This can include microbes or microbial components found in host cells with evidence of disease, precedent for a similar disease caused by a similar agent, antibody response indicating recent exposure in a diseased individual, or evidence of similar microbial infection in other individuals with the same disease. Level 3, a confirmed causal relationship, is characterized by fulfilling Koch's postulates or by the mitigation/prevention of the disease using targeted therapies.

These standards, although difficult to apply in some cases, provide a general guideline for terminology and practice. This is increasingly important in an age where microbe discovery is outpacing the basic science associated with disease causality.

In Chapter 2, we present three metagenomic-based studies in which we investigate diseases suspected of infectious origin in which identification of a causative agent failed by conventional methods. These examples were specifically chosen to illustrate the principles of metagenomic-based pathogen discovery and the limitations and benefits of these types of projects.

Furthermore, in the age of rapid virus discovery, subsequent studies are essential for the characterization of potential etiologic agents. Therefore, in Chapters 3-5 we take a pathogen discovery

project steps beyond those described in Chapter 2. First, in Chapter 3, we fulfill Koch's postulates and establish a causal relationship between the metagenomically-discovered ball python nidovirus (now classified as a serpentovirus) and respiratory disease in ball pythons [9,78]. Although the confirmation of a causal relationship is an essential step in disease characterization, it does not denote the significance of a pathogen in the scheme of global health. Consequently, in Chapter 4 we assess this group of respiratory-disease causing serpentoviruses of snakes in the context of epidemiologic significance and species susceptibility. Lastly, in Chapter 5, we describe an additional pathogen discovery project in veiled chameleons, in which a novel divergent serpentovirus is discovered in association with respiratory disease. Identifying new related viruses associated with similar disease further expands our knowledge of this growing clade of reptile pathogens.

The remainder of the Introduction will provide a discussion of respiratory diseases in reptiles. This will include justification for the study of reptile diseases, a summary of common respiratory pathogens, and an overview of novel viruses in the *Nidovirales* order that have recently been associated with disease.

1.2: Respiratory Diseases of Reptiles

1.2.1: Justification for the Study of Reptile Diseases

Reptile populations are on the decline worldwide [79,80]. The primary factors influencing these declines include habitat loss and pollution, the introduction of invasive species, infectious disease, unsustainable capture for the pet trade or killing for components of the carcass, and global climate change [79–82]. The role of infectious diseases in the decline of reptile and amphibian species can be significant [83–85]. Therefore, it is of increasing importance to evaluate the danger emerging diseases could pose to captive and wild populations, especially those already threatened or endangered. Additionally, the trafficking of reptiles to non-native countries is world-wide, and each year hundreds of thousands of non-native reptiles are imported into the United States for use in the pet trade [86]. Imported reptiles can pose a risk to human and animal health through the introduction of infectious agents to naïve populations,

including native reptile species [87]. Therefore, not only is it important to study emerging infectious disease in captive populations for the health of individual animals, but the investigation of diseases can have broader implications for the global health and conservation of reptile species.

1.2.2: Infectious Causes of Respiratory Disease in Reptiles

Respiratory disease in reptiles can present with a wide range of symptoms and lesions. Clinical signs vary depending on the location (upper versus lower respiratory tract). Clinical findings in the upper respiratory tract can include ocular, nasal, and oral exudate (serous to mucinous to purulent), erythema, swelling, and petechiation of the mucus membranes, erosion and ulceration of mucosa, swelling and inflammation of the conjunctiva, and accumulation of edema [88]. If severe enough, these lesions can result in dyspnea, especially if glottal or tracheal obstruction occur. However, tachypnea, dyspnea, wheezing, open-mouthed breathing, head tilting, and respiratory distress are typically signs of more advanced respiratory disease, likely involving the lower respiratory tract. Infectious and non-infectious causes have been documented in respiratory disease of reptiles [88]. Non-infectious causes include trauma (e.g. collision with or irritation from enclosure walls, bite wounds, vehicular trauma), neoplasia, nutritional disease (e.g. hypovitaminosis A), and environmental toxins or pollutants [88]. Infectious disease can be associated with bacterial, fungal, parasitic, or viral organisms [89].

1.2.2.1: Bacteria

Numerous bacterial species have been isolated from the respiratory tract of reptiles, including *Pseudomonas*, *Klebsiella*, *Salmonella*, *Proteus*, and *Aeromonas* species [90–92]. These have been described in cases of disease as well as normal flora of the oral cavity [90–92]; their detection in the lower respiratory tract is more consistent with disease but is often considered secondary in nature. In contrast, *Mycoplasma* and *Mycobacterium* have been associated with upper and lower respiratory disease in multiple reptile species [93,94]. Infections can be subclinical; environmental factors or causes of immunosuppression are often implicated in the development of clinical disease from a subclinical status.

Chlamydia pneumoniae has also been reported in systemic disease of both reptiles and humans, including lesions within the respiratory tract [95].

1.2.2.2: Fungi

Fungal infections are generally considered opportunistic and occur more commonly in immunocompromised animals. However, in recent years there have been increased reports of fatal fungal infections in animals, including chytridiomycosis in amphibians (*Batrachochytrium dendrobatidis* and *B. salamandrivorans*), white-nose syndrome in bats (*Pseudogymnoascus destructans*), and snake fungal disease (*Ophiomyces ophioidiicola*) [84,96,97]. In snakes, *O. ophioidiicola* typically causes skin infections, but the fungus has been found in the respiratory tract and can cause systemic disease [98]. Other fungal infections that have been detected in the respiratory tract of reptiles include *Chrysosporium*, *Aspergillus*, *Fusarium*, *Cryptococcus*, dermatophytes, and *Chamaeleomyces* [88,99].

1.2.2.3: Parasites

Protozoa (amoeba and apicomplexans), trematodes (renifers, spirorchids and hemiurids), nematodes (ascarids, filaroides, *Rhabdias*), pentastomids, and mites have all been associated with the respiratory tract of reptiles [100]. Parasitic infections are common in wild reptiles, or reptiles that have been brought into captivity from the wild [101,102]. However, as some parasitic life cycles require intermediate hosts, these infections can be less common in captive species [103]. In many cases, parasitic infections can remain chronic and subclinical for long periods of time until a predisposing factor results in disease development [104].

1.2.2.4: Viruses

Infection of the respiratory tract has been associated with several viral agents. In turtles, lizards, and crocodylians, the most common viral agents associated with respiratory disease are herpesviruses, ranaviruses, adenoviruses, and reoviruses [105]. In snakes, ophidian paramyxoviruses (also known as

ferlaviruses) have been a primary cause of significant respiratory disease, especially vipers [106,107]. Infections in snakes typically result in interstitial and proliferative pneumonia with or without intraepithelial inclusions [107]. Similarly, orthoreoviruses have been documented to cause respiratory disease in snakes [108]. Histologic lesions in orthoreovirus-infected snakes include proliferative interstitial pneumonia and tracheitis with syncytial cell formation [108]. Reptarenaviruses and sunshine virus (paramyxovirus) have also been associated with respiratory disease in snakes but are more consistently associated with neurologic disease [62,109,110]. Recently, a novel virus in the order *Nidovirales* has been discovered in association with severe and fatal respiratory disease in pythons [9,111,112]. This virus will be the focus of the remainder of the Introduction and will provide a background to the studies described in Chapters 3-5.

1.2.3: Nidoviruses: A Review

The nidoviruses (order *Nidovirales*) are a large and diverse group of single-stranded positive-sense RNA viruses that include notable human and veterinary pathogens [113–118]. Historically, the order *Nidovirales* has included the families *Coronaviridae* (infect mammals and birds), *Arteriviridae* (mammals), *Roniviridae* (crustaceans), and *Mesoniviridae* (insects) [113]. Subfamilies of the *Coronaviridae* family infect mammals (toroviruses) and fish (bafiniviruses) [113].

In general, nidoviruses have been separated based on genome size into small (~13-16 kb; e.g. arteriviruses) and large genomes (greater than 20 kb; e.g. coronaviruses, roniviruses, mesoniviruses) [116,118–120]. Despite the differences in size, nidoviruses generally share a similar genome structure. The two largest open reading frames (ORF1a and ORF1b) begin after the 5' untranslated region and cover approximately 60-75% of the genome [121]. The ORFs overlap at the 3' end of ORF1a in a region containing a single nucleotide (-1) ribosomal frameshift signal [116,121,122]. These ORFs encode non-structural proteins associated with the replicase complex. The number and organization of ORFs located downstream of ORF1b differ between viruses; these include structural or accessory proteins and are expressed from a nested set of subgenomic RNAs [121]. A recently discovered nidovirus from a planarian now represents the largest nidovirus genome (and RNA virus genome) recorded to date (41 kb). The

planarian nidovirus includes a single large 5' ORF1 [123]. Therefore, although most nidoviruses share general genome structures, this standard is likely to further transform with the unearthing of new viruses and expansion of the order.

In contrast to a conserved genome structure, virion morphology, as observed by electron microscopy, differs significantly amongst groups of nidoviruses due to the range of structural proteins expressed by each. Coronaviruses are spherical thickly-enveloped particles (~140 nm diameter) with long surface projections [124]. Arteriviruses are also spherical, but significantly smaller (~40 nm) and with short indistinct surface projections [117]. Mesoniviruses are spherical and approximately 50 nm in diameter with short spike surface projections [115,120]. Toroviruses and roniviruses are curved-rod or bacilliform in shape, ranging from 100-160 x 37-45 nm (toroviruses) and 150-200 x 25 nm (roniviruses), with surface spikes similar to (toroviruses) or smaller than (roniviruses) projections of coronaviruses [125–127].

The *Nidovirales* order contains numerous known human and veterinary pathogens. Significant arteriviruses include equine arteritis virus (EAV) and porcine reproductive and respiratory syndrome virus (PRRSV) that generally present as respiratory or reproductive-associated disease and persistent infections in hosts [117]. Simian hemorrhagic fever virus (SHFV) and lactate dehydrogenase elevating virus (LDV) can also cause lifelong asymptomatic infections of hosts or result in systemic or neurologic disease, respectively [117]. Coronaviruses generally result in gastrointestinal disease, respiratory disease, or multi-organ disease in mammals and birds [124]. Gastrointestinal pathogens include transmissible gastroenteritis virus and porcine epidemic diarrhea virus; respiratory pathogens include infectious bronchitis virus, bovine coronavirus, severe acute respiratory syndrome coronavirus, and Middle East respiratory syndrome coronavirus; multi-organ disease pathogens include feline infectious peritonitis virus and murine hepatitis virus [124]. Toroviruses have been associated with more mild but sometimes fatal diseases, primarily in ungulates [127]. Disease is typically localized to the gastrointestinal tract, but infection of the respiratory tract has also been documented [127,128]. Roniviruses are associated with fatal respiratory (gill-associated) disease of shrimp [119]. Overall, nidoviruses are most commonly associated with the respiratory, gastrointestinal, and reproductive tracts, suggesting common pathogenic features amongst the order.

1.2.4: Nidoviruses of Reptiles

Historically, nidoviruses have been known to infect mammals, birds, fish, crustaceans, and insects. With the increasing availability and affordability of NGS as a diagnostic and research tool, this order has seen marked expansion in the recent years due to the discovery of novel viruses by metagenomic methods. New taxonomic classification of the *Nidovirales* order has resulted in seven suborders: *Arnidovirineae* (arteriviruses), *Cornidovirineae* (coronaviruses), *Mesnidovirineae* (mesoni- and medioniviruses), *Ronidovirineae* (euroni- and roniviruses), *Abnidovirineae* (abyssoviruses), *Monidovirineae* (mononiviruses), and *Tornidovirineae* (tobaniviruses) [129]. Included within this taxonomic expansion is a distinct clade of nidoviruses that began with the discovery of nidoviruses in pythons, marking the first example of nidoviruses in reptilian hosts [9,111,112]. These reptilian nidoviruses are now classified as belonging to the suborder *Tornidovirineae* family *Tobaniviridae*. Since this initial discovery in pythons, related tobaniviruses have been discovered in additional snake species and lizards (subfamily *Serpentovirinae*), turtles (currently unclassified), and cattle (subfamily *Remotovirinae*) [130,131,57,132,133,56,134,78]. Several of these viruses have been associated with significant disease in the host, highlighting this group as a source of potential emerging pathogens that warrant additional investigation [9,111,112,130,131,133,134].

The first descriptions of nidovirus-associated disease in reptiles were found in ball pythons (*Python regius*) and Indian pythons (*Python molurus*), shortly followed by green tree pythons (*Morelia viridis*) [9,111,112,133]. In these cases, snakes were dying of interstitial proliferative and mucinous pneumonia, tracheitis, and esophagitis, and a novel serpentovirus was discovered by metagenomic sequencing in diseased samples. Serpentovirus quantification in multiple organs revealed tropism for the respiratory and gastrointestinal tracts. Genomic characterization of the viruses revealed similar characteristics to other nidoviruses: two large overlapping 5' ORFs, with a ribosomal frameshift signal (-1; AAAAAC), encoding a large polyprotein of non-structural proteins; a spike protein (ORF2); and five 3' ORFs encoding structural proteins (transmembrane glycoproteins, matrix protein, and nucleocapsid protein) with subgenomic RNA

expression [9,111–113,116,118,121,133]. The 33 kb genomes were the largest RNA genomes at the time of discovery (since surpassed by planarian nidovirus at 41 kb) [9,111,112,123,133]. Transmission electron microscopy (TEM) of infected ball pythons identified serpentoviruses in cytoplasmic vacuoles of respiratory epithelial cells (ciliated, mucous, and alveolar type II cells) [9]. Mature virions were bacilliform (180 x 50 nm) with a lipid membrane containing surface spikes and internal nucleocapsids [9]. TEM on serpentoviruses isolated in cell culture from green tree pythons were similar with bacilliform and curved rod-shaped particles 120 nm in length [133]. Intracytoplasmic viral RNA was also detected in snake tissues by RNA in-situ hybridization, further confirming localization to areas of disease [111,133].

Included in the initial studies of reptilian serpentoviruses was an examination of the underlying pathogenesis. In snakes, serpentovirus infection was associated with cytopathic effects and proliferative activity in epithelial cells of the respiratory tract [9,111,133]. Furthermore, cell proliferation resulted in significant increases in the number of mucus producing and secreting epithelial cells [133]. Increased cell turnover with epithelial proliferation and epithelial cell apoptosis have also been described for coronaviruses and toroviruses [135–138], indicating possible shared mechanisms of pathogenesis.

Recently, a related serpentovirus to those found in snakes was discovered in wild shingleback lizards (*Tiliqua rugose*) associated with respiratory disease [131]. Furthermore, a mass die-off of freshwater snapping turtles exhibiting conjunctivitis, dermatitis, splenitis, and nephritis (*Myuchelys georgesi*) was associated with a related serpentovirus [134]. These findings indicate that serpentoviruses of reptiles are prevalent in a diverse range of species and can be associated with significant mortality.

The genome organization, ultrastructural morphology, tissue tropism, and the pathogenic changes within targeted tissues for these novel reptilian serpentoviruses are similar to those of other pathogenic nidoviruses. The likeness to other significant pathogens is an important indicator that serpentoviruses represent a group of probable emerging pathogens of unknown, and possibly underestimated, significance in veterinary medicine.

CHAPTER 2: METAGENOMIC SEQUENCING AS A TOOL FOR PATHOGEN DISCOVERY

2.1: Rationale for Included Metagenomic Studies

Included in this chapter are three metagenomic-based studies of pathogen discovery. In each study, we investigate diseases suspected of infectious origin but for which conventional diagnostics failed to identify a causative agent. By means of example, the basic principles and methods of pathogen discovery are presented. Furthermore, each study demonstrates a different possible outcome, thereby highlighting the strengths and weaknesses of metagenomics for pathogen discovery. First, the failure to detect an infectious agent provides further evidence of a non-infectious cause (section 2.2); second, the detection of a known virus in a new host expands our knowledge of disease susceptibility (section 2.3); and third, the discovery of a novel virus during a fatal disease outbreak, but with only tenuous connections to disease causality, emphasizes the need for follow-up experimentation as a means of providing biological relevance (section 2.4).

2.2: Metagenomic Investigation of Idiopathic Meningoencephalomyelitis in Dogs (*Canis lupus familiaris*) [139]

2.2.1: Introduction

Meningoencephalomyelitis of unknown origin (MUO) is a common canine neuroinflammatory disease suspected to be caused by an underlying immune-mediated process. The classification of MUO includes several inflammatory diseases differentiated histopathologically, including necrotizing meningoencephalitis (NME), necrotizing leukoencephalitis (NLE), and granulomatous meningoencephalomyelitis (GME) [140]. All of these diseases predominately affect small breed dogs, but other breeds have been documented [140–147]. These diseases are histologically distinct, but without histological confirmation of disease, NME, NLE and GME tend to be collectively referred to as MUO.

MUO is thought to account for up to 25% of canine inflammatory CNS disease [148]. The prognosis of untreated MUO is poor, but treatment with immunosuppressant drugs such as corticosteroids can alleviate clinical signs and delay disease progression. This suggests that MUO is an immune-mediated disease. However, a study targeting the inflammatory components of GME found a predominance of MHC Class II and CD3⁺ T cells, which may be the result of a delayed hypersensitivity reaction [149]. Therefore, whether the immune response is targeting an infection is a critical open question that this study sought to answer.

Currently the etiology of MUO remains unknown. Studies searching for an infectious etiology have failed to reveal a consistent infectious agent [148,150–152]. Prior studies have utilized polymerase chain reaction (PCR), serology, culture and/or immunohistochemistry to investigate viruses commonly implicated in CNS disease, including herpesviruses, adenoviruses, parvoviruses, canine parainfluenza virus, encephalomyocarditis virus, bunyaviruses, coronaviruses, enteroviruses, flaviviruses, paramyxoviruses, and parechoviruses [151–153]. Although the overwhelming majority of these studies have been negative or inconclusive, they have been limited by targeted testing for specific agents. In response, we have utilized the unbiased approach of metagenomic sequencing to investigate possible infectious agents, a technique that has proved useful for pathogen discovery in other neurologic diseases [58,59,63,109,154,155].

2.2.2: Materials and Methods

2.2.2.1: Inclusion Criteria

To be included in the diseased group for this study, patients had to be greater than six months of age with a neurologic examination consistent with focal or multifocal neurological dysfunction. Additional inclusion criteria included negative PCR tests on whole blood and/or cerebrospinal fluid for the infectious agents caused by members of the species or genera *Toxoplasma gondii*, *Neospora caninum*, *Ehrlichia canis*, *Ehrlichia ewingii*, *Anaplasma*, *Neorickettsia*, *Bartonella* and *Rickettsia*; the presence of multifocal T2-

weighted hyperintense lesions on MRI; and CSF pleocytosis with a nucleated cell count of greater than 5 cells/ μ L with greater than 50% mononuclear cells and a red blood cell count of less than 4000 cells/ μ l [140]. For cases in which a necropsy was performed, histopathologic confirmation of disease was accepted in the absence of infectious disease testing, MRI and CSF. Due to the inflammatory nature of MUO, any potential subject to whom glucocorticoids were administered within two weeks of CSF or antemortem brain collection were excluded from this study; however, this criterion was not used for postmortem brain samples. Three animals in the diseased group and one animal in the control group received antimicrobials within several days of sample collection, which could have altered the results of the infectious disease testing. Animals in the control (non-MUO) group were subject to the same age criteria as the diseased group (MUO). The control cases had a low index of suspicion of inflammatory disease based on a non-inflammatory CSF analysis, inconsistent MRI findings, and/or histologically confirmed non-MUO disease processes (5 of 11).

2.2.2.2: Case Diagnostics

All animals in both the diseased (MUO) and control (non-MUO) groups received a physical and neurologic examination. The diagnostics performed for each group are summarized in Table 2.1. Of the animals in the MUO group, 4/11 were euthanized, 2/11 died as a result of their disease, 1/11 is currently stable, and 4/11 have been lost to follow up. Of the animals in the non-MUO group 7/11 were euthanized, 1/11 is currently stable and 3/11 were lost to follow up.

Table 2.1: MUO Case Summary. Diseased cases (11/22) represent animals diagnosed with MUO based on clinical presentation and antemortem diagnostics, with or without postmortem assessment. Antemortem diagnosis could not be further classified into the MUO subtypes. Postmortem diagnosis was made in 4/11 cases, two of which were diagnosed as either NME or GME and two of which had meningoencephalitis but lesions were not specific for any subset of MUO (see discussion). Control cases (11/22) are animals with non-inflammatory CSF and either a definitive non-MUO diagnosis or additional clinical findings inconsistent with MUO. For "Diagnostics" and "Sample Used," if a fraction is not specified, then it applies to all in the group. MUO, meningoencephalomyelitis of unknown origin; ME, meningoencephalitis; NME, necrotizing meningoencephalitis; GME, granulomatous meningoencephalomyelitis; YT, Yorkshire Terrier; Mix, mixed breed; Chi, Chihuahua; MP, Miniature Pinscher; IG, Italian Greyhound; Malt, Maltese; Col, Collie; MS, Miniature Schnauzer; MD, Miniature Dachshund; BM, Belgian Malinois; Box, Boxer; WC, Welsh Corgi; DP, Doberman Pinscher; GSD, German Shepherd; Wei, Weimaraner; SP, Standard Poodle; CSF, cerebrospinal fluid; NIDP, negative infectious disease profile; MRI, magnetic resonance imaging; HP, histopathology; AM, antemortem; PM, postmortem.

	Diagnosis	# of Cases	Avg. age (years)	Breeds Included	Diagnostics Performed	Sample Used
Diseased	Antemortem					
	MUO	7	5.3	YT, Mix, Chi, MP, IG, Pug	CSF, NIDP, MRI	CSF
	Postmortem					
	NME	1	2	Pug	CSF, HP (PM)	CSF
	GME	1	4	Malt	CSF, NIDP, MRI, HP-AM-PM	Brain (AM)
	ME (unspecified)	2	2	Col, MS	CSF, NIDP, MRI (1/2); HP-PM (2/2)	Brain (PM) and CSF
	Total	11				
Control	Diagnosis	# of Cases	Avg. age (years)	Breeds Included	Diagnostics Performed	Sample Used
	Neoplasia	5	8	Malt, MD, Mix, Box, WC	CSF, MRI (4/5); NIDP (3/5); HP-AM (2/5); HP-PM (4/5)	CSF (5/5) and Brain (PM) (2/5)
	Degenerative	4	4	BM, Mix, DP, GSD	CSF, MRI (4/4); NIDP (3/4); HP-PM (1/4)	CSF
	Trauma	1	6	Wei	CSF, MRI	CSF
	Epilepsy	1	10	SP	CSF, NIDP, MRI	CSF
		Total	11			

2.2.2.3: Sequencing Library Preparation

Total RNA was extracted from 26 fresh-frozen CSF and brain samples from 22 dogs (*Canis familiaris*) that fit the inclusion or control criteria described above. These samples were blinded as to their case or control origin before processing. Additionally, RNA was extracted from postmortem brain samples from a green tree python (*Morelia viridis*), American crow (*Corvus brachyrhynchos*), and American robin (*Turdus migratorius*), all of which had previously been tested by PCR and/or metagenomic sequencing and were found to be infected with specific known infectious agents. These were used as positive controls [9,156]. RNA was extracted using a combination of TRIzol (tissue; Ambion Life Technologies) or TRIzol LS (body fluid; Ambion Life Technologies) with RNA clean and concentrator columns (CC-5; Zymo Research). Approximately 100 mg of brain tissue was added to 1 ml of TRIzol and 250 μ l of body fluid (CSF, serum, or blood) was added to 750 μ l of TRIzol LS and incubated at room temperature (RT) for 5 minutes. Tissue samples were macerated using a single sterile metal BB shaken in a TissueLyzer (Qiagen) at 30 Hz for 3 minutes. Then, 200 μ l of chloroform (Sigma-Aldrich) was added, shaken for 15 seconds by hand, and incubated at RT for 2 minutes. Samples were spun at 12,000 RPM for 10 minutes at RT. The aqueous phase was removed (approximately 450 μ l) and was added to a mixture of 450 μ l of RNA binding buffer (CC-5; Zymo Research) and 450 μ l of 100% ethanol (EtOH). This was added to an RNA clean and concentrator column (CC-5; Zymo Research). The interphase and organic phase were set aside for DNA extraction (see below). The RNA column was washed with 400 μ l RNA wash buffer and then incubated with 6 U DNase enzyme (NEB), 1x DNase buffer (NEB), and RNA wash buffer for 15 minutes. The column was spun to remove DNase mixture and then washed with 400 μ l RNA prep buffer. Additional washes with 800 μ l and 400 μ l RNA wash buffer were performed, the column was dried with a 1 minute high-speed spin, and then RNA samples were eluted in 30 μ l of RNase-free water.

All CSF samples had undetectable concentrations of RNA by fluorometric quantification. These samples, along with a no template control, were reverse transcribed, the second DNA strand synthesized,

and total DNA amplified using the Ovation RNA Amplification System V2 (NuGEN) according to the manufacturer's protocol.

Reverse transcribed DNA from CSF samples was then amplified to generate detectable levels of DNA for fluorometric quantification. This was performed using Phi29 isothermal strand displacement amplification. Five μ l of template, including a no template control, was added to 50 μ M of random hexamer primer and incubated at 95°C for 3 minutes and then placed directly on ice. Template and primers were then added to a mixture containing 1x Phi29 buffer (NEB), 1x bovine serum albumin (NEB), 2.5 mM each dNTPs, 4 mM dithiothreitol (Invitrogen), and 5 U Phi29 DNA polymerase (NEB). Samples were incubated at 30°C for 2 hours then 65°C for 10 minutes.

For extracted RNA of brain samples, approximately 1000 nanograms of RNA was added to 200 pmol of a random pentadecamer oligonucleotide (5'-NNNNNNNNNNNNNNNN; MDS-286) and incubated for 5 minutes at 37°C; a separate no template control was also used for these samples. Reverse transcription reaction mixture containing 1x SuperScript III FS reaction buffer (Invitrogen), 5 mM dithiothreitol (Invitrogen), 1 mM each deoxynucleoside triphosphates (dNTPs), and 100 U SuperScript III reverse transcriptase enzyme (Invitrogen) was added to the RNA-oligomer mix (12 μ l total reaction volume) and incubated for 30 minutes at 42°C, then 30 minutes at 50°C, then 15 minutes at 70°C. Then, 1 U RNase H (NEB) diluted in 5 μ l 1x SuperScript III FS reaction buffer and 160 pmol MDS-286 was added to the reaction mixtures, which were incubated at 37°C for 20 minutes followed by 94°C for 2 minutes. Then, single-stranded cDNA was converted to double-stranded DNA by adding 2.5 U Klenow DNA polymerase (3' to 5' exo- NEB) in 5 μ l 1x SuperScript III FS reaction buffer and 2mM each dNTPs and incubated at 37°C for 15 minutes. DNA was purified using Sera-Mag Speed Beads at a 1.4:1 bead/DNA volume ratio according to the manufacturer's protocol. DNA was eluted in 20 μ l molecular grade water (Sigma-Aldrich).

The interphase and organic phase from the TRIzol extraction described above were used for DNA extraction according to the manufacturer's protocol (Invitrogen) with minor alterations. Briefly, 300 μ l of 100% EtOH per 1 ml TRIzol was added to the interphase and organic phase, gently mixed, and incubated

for 2 minutes at RT. Samples were centrifuged for 5 minutes at RT and the supernatant was removed and discarded. The DNA pellet was washed twice in 1 ml of 0.1 M sodium citrate in 10% EtOH pH 8.5 (per 1 ml TRIzol), with a 30 minute RT incubation, 5-minute centrifugation, and removal of the supernatant. The DNA pellet was then resuspended in 75% EtOH, gently mixed, and incubated for 20 minutes at RT. The samples were then centrifuged for 5 minutes, the supernatant discarded, and the pellet air-dried for 5 minutes. The DNA pellet was then resuspended in 100 μ l molecular grade water (Sigma-Aldrich), heated to 55°C for 10 minutes, and then centrifuged for 10 minutes at 4°C. The supernatant containing DNA was then transferred to a 1.5 ml conical new tube and purified using Sera-Mag Speed Beads as previously described.

The DNA concentration from each sample (both RNA and DNA derived samples) was measured fluorometrically and 10 ng was used as a template in 6.5 μ l of 1x Tagment DNA buffer and 0.5 μ l Tagment DNA enzyme (Illumina). The mixture was incubated at 55°C for 10 minutes and then placed directly on ice. Tagmented DNA was cleaned with Sera-Mag Speed Beads as previously described and used as a template (5.8 μ l) in the addition of full-length adaptors with unique bar-code combinations by PCR. The 25 μ l PCR reaction contained 1x Kapa real-time library amplification master mix (Kapa Biosystems), 0.33 μ M (each) MDS-143 and MDS-445 primers (5'CAAGCAGAAGACGGCATAACG3' and 5'AATGATACGGCGACCACCGA3', respectively), and 0.020 μ M each of adapter 1 and 2 bar-coded primers [157]. Thermocycling conditions in consecutive order were 72°C for 3 minutes, 98°C for 30 seconds, and 8 cycles of 98°C for 10 seconds, 63°C for 30 seconds, and 72°C for 3 minutes. Relative concentrations of libraries were measured in quantitative PCR (qPCR) reactions containing home-made 1x qPCR master mix (10 mM Tris-HCl pH 8.6, 50 mM KCl, 1.5 mM MgCl₂, 0.2 mM of each dNTP, 5% glycerol, 0.08% NP-40, 0.05% Tween-20, 1x Sybr green (Life Technologies) and 0.5 U Taq polymerase) and 0.5 μ M MDS-143 and MDS-445 primers. Equivalent amounts of DNA from each sample were pooled and then cleaned using Sera-Mag Speed Beads as previously described. The pooled libraries were run on a 2% agarose gel and size selected (400-500 nucleotides) by gel extraction with a gel DNA recovery kit

(Zymo) according to the manufacturer's protocol. Size-selected pooled libraries were amplified once more in a PCR mixture containing 1x Kapa real-time library amplification mix, 500 pmol of MDS-143 and -445 each, and 5 µl of library template in a 50 µl total reaction volume. This PCR also included single reactions of 4 separate fluorometric standards (Kapa). Thermocycler conditions were 98°C for 45 seconds and 8 cycles of 98°C for 10 seconds, 63°C for 30 seconds, and 72°C for 2 minutes, which was when the sample curve passed standard 1. DNA was purified using Sera-Mag Speed Beads as previously described. Library quantification was performed with the Illumina library quantification kit (Kapa Biosystems) according to the manufacturers protocol. Sequencing was performed on an Illumina NextSeq 500 instrument with a NextSeq 500/550 High Output Kit v2 (150 cycles).

2.2.2.4: Sequence Analysis

Sequences were trimmed using Cutadapt (version 1.9.1) in order to trim adaptor sequences and low-quality bases, and remove trimmed sequences that were less than a designated length (80 nucleotides) [158]. Base quality encoding was set to Phred+33 (default), and quality cutoff was set to 30 for the 5' and 3' ends. The first base of each sequence was also trimmed. The CD-HIT-DUP sequence clustering tool was then used to collapse reads with 99% global pairwise identity, leaving only unique reads remaining [159]. Host-derived sequences were then filtered using the Bowtie2 alignment tool (version 2.2.5) [160]. First, a bowtie index was generated from the host genomic sequence (assembly CanFam3.1 for dogs, assembly *Python_molurus_bivittatus*-5.0.2 for the green tree python, assembly ASM69197v1 for American crow, and all available assemblies in the NCBI Assembly database in the order *Passeriformes* for the robin [ASM128173v1, GWvir1.0, GWplu1.0, *Passer_domesticus*-1.0, *Taeniopygia_guttata*-3.2.4, FicAlb1.5, GeoFor_1.0, PseHum1.0, *Zonotrichia_albicollis*-1.0.1, SCA1, ASM69197v1, ASM69201v2, ASM69581v1, Hooded_Crow_genome, *Sturnus_vulgaris*-1.0, *Parus_major*1.0.3, *Lepidothrix_coronata*-1.0]) and then sequences aligning with a -local mode alignment score greater than 60 were removed. SPAdes genome assembler (version 3.5.0) was used to generate contiguous sequences (contigs) [161]. Then, to taxonomically categorize sequences, the NCBI nucleotide database was queried with all contigs

greater than 150 nucleotides using the BLASTn alignment tool (version 2.2.30+) [162,163]. Any hit with an expect value less than 10^{-8} was assigned taxonomically according to the sequence with the highest alignment score [162,164]. Additionally, to attempt to categorize contigs that were too divergent to produce a high scoring nucleotide alignment, the NCBI nr database was queried in a RAPSearch2 (version 2.23) with a minimum length of 20 amino acids and an expect value of 0.01 [165]. The same process was performed using all the reads that did not form contiguous sequences from SPAdes genomic assembly, except GSNAP alignment tool (version 2016-11-07) was used instead of BLASTn [166]. Raw sequence data was deposited in the NCBI Short Read Archive database (accession SRP118690).

We then looked for taxa that were specifically associated with cases and not controls. Samples were unblinded, and datasets were identified as either MUO or non-MUO (NM). All taxonomic identifications (TAXIDs) present within MUO samples that were also present in NM samples were removed from further analysis. Next, remaining TAXIDs were compared between MUO samples. A fraction was generated for each TAXID to determine the number of MUO samples that had alignments to the specific TAXID over the total number of samples evaluated. If a TAXID occurred in two MUO samples or more, the sequences associated with the TAXID were manually inspected by again querying NCBI BLASTn and BLASTx to corroborate initial taxonomic assessment [167,168]. This was performed four times for each sample using the different sequencing outputs: SPAdes generated contiguous sequences queried to 1) BLASTn and 2) RAPSearch2 and individual reads queried to 3) GSNAP and 4) RAPSearch2.

2.2.3: Results

2.2.3.1: Canine Meningoencephalitis Sequencing Results

RNA and DNA were extracted from CSF and/or brain samples from 11 MUO dogs and 11 non-MUO dogs as well as multiple positive controls samples. Nucleic acids were then converted into sequencing libraries and sequenced on an Illumina NextSeq 500 instrument. The datasets contained on average 1.16×10^7 , 150-nucleotide sequences per sample. A stepwise data analysis pipeline was used to remove adapter

sequences and low-quality reads, collapse sequences to unique reads, and filter out dog-derived sequences. Approximately 2% of sequences remained in each sample after filtering (Supplemental Table 2.1). Remaining sequences were assembled into longer contiguous sequences (contigs), which were queried against databases of nucleotide and protein sequences to identify possible pathogen-derived sequences. Sequences from no single organism were found in more than 3 MUO samples (out of 11) and organisms were inconsistent between DNA and RNA from the same tissue as well as brain and CSF collected from the same animal. A majority of sequences lacked specificity to any single organism based on nucleotide and protein sequence analysis. This was due to either poor quality of the read, or sequences that were low complexity or highly conserved, and thus taxonomically ambiguous. This was the case for all eukaryotic organisms detected. Bacterial-aligning reads were also detected, however, due to the range of bacterial species and the inconsistency of any given organism amongst samples, these were deemed environmental contaminants. The most common bacteria detected were *Pseudomonas*, *Streptococcus*, and *Staphylococcus* species. A low number of viral species were detected, but all that were present solely within MUO samples were bacteriophages, and therefore unlikely to be associated with disease. Overall, a consistent and specific candidate etiological candidate was not detected.

2.2.3.2: Positive Control Cases

We sequenced and analyzed in parallel known positive samples to validate our approach and to establish limits of detection. These included 1) brain from a captive green tree python positive for python serpentovirus [9]; 2) brain from a wild-caught American robin experimentally infected with West Nile virus (WNV) [156]; and 3) brain from a wild-caught American crow experimentally infected with WNV [156]. These samples had previously tested positive by metagenomic (green tree python) or targeted next generation sequencing (crow and robin). We used an identical analysis pipeline for positive control samples, except we used different, appropriate genome assemblies for filtering host sequences. As expected, we detected python serpentovirus and WNV in the green tree python and crow, respectively using our metagenomic sequencing approach (Supplemental Table 2.2). We did not detect WNV in the

experimentally infected robin brain but confirmed that the sample was positive for WNV RNA by qRT-PCR [169]. We quantified the WNV copy number in the bird brain samples at 168 genome copies/ μ l RNA in the robin and 8.82×10^4 genome copies/ μ l RNA in the crow [169].

2.2.4: Discussion

MUO is an idiopathic inflammatory neurologic disease, including GME and the necrotizing encephalidites (NME and NLE), for which the pathogenesis remains unknown. Similar to previous targeted diagnostic studies reported to date [148,150–153], our study using an unbiased approach failed to detect any infectious agents that were consistently associated with canine MUO cases. There are several possible biological and technical explanations for our study's inability to identify a candidate etiologic agent for MUO, including the underlying pathogenesis of the disease, sample type and collection methods, case inclusion criteria, sensitivity of diagnostics, and database limitations.

First, it is possible that the inflammation observed in MUO does not have an infectious etiology. In this case, the failure to detect an infectious agent might support the hypothesis that MUO is a primary autoimmune disorder.

Second, it may be that MUO has an infectious cause, but that we are sampling at a point in the natural history of the disease when the initiating pathogen is no longer present in detectable amounts. This possibility could be investigated by the development of a comprehensive serological panel for canine pathogens that would enable retrospective sampling of dogs with and without MUO [170].

Third, CNS lesions could be secondary to a primary infection elsewhere in the body, resulting in a systemic response that manifests as meningoencephalitis. The evaluation of multiple tissue types in dogs diagnosed with MUO, beyond CNS samples, could help assess this possibility.

Fourth, it might be that we sampled the wrong regions of the CNS. MUO, like many other neurologic diseases, can be focally or multifocally distributed. This limitation is likely to apply more to biopsy/postmortem samples than to pathogen detection in CSF. However, low or inconsistent shedding of

organisms into the CSF could reduce the likelihood of detection. Future studies could benefit from more consistent use of antemortem image-guided biopsies (only 1/11 of our MUO cases) and sampling of multiple sections of the CNS postmortem (only 4/11 MUO cases), as well as multiple time-separated CSF sample collections. Furthermore, although eleven cases in total were clinically diagnosed with MUO, only 4 had histopathology and only 2 of these cases yielded a definitive diagnosis of GME or NME. Although the inclusion/exclusion criteria were rigorous, the use of a greater number of cases with histologic confirmation could have strengthened the diagnostic certainty of each case and allowed for a more specific investigation of MUO based on histologic type.

Furthermore, although four of the diseased cases were histologically confirmed as having inflammatory brain disease, seven cases were presumptively diagnosed with MUO. Strict inclusion criteria were used for antemortem diagnosis in this study. However, the lack of histopathology does not definitively rule out other disease processes, such as lymphoma. Therefore, it is possible that not all the presumptively diagnosed MUO cases were GME, NME or NLE. Additionally, only 2 out of the 4 cases evaluated by histopathology yielded a definitive diagnosis of GME or NME, whereas the other 2 were diagnosed as meningoencephalitis of undertermined subtype. The use of a greater number of cases with histologic confirmation could have strengthened the diagnostic certainty of each case and allowed for a more specific investigation of MUO based on histologic type.

There are also several possible technical reasons that could have prevented us from identifying an infectious agent underlying MUO. First, it might be that we lacked the necessary sensitivity. Although metagenomic sequencing can detect any nucleic acid-based pathogen, it is generally less sensitive than targeted methods such as PCR. The sensitivity of PCR is typically defined in absolute units (e.g. 100 genome copies in a quantitative PCR reaction), but the sensitivity of metagenomic sequencing is limited by read depth and the relative pathogen concentration. For example, if a metagenomic dataset contains 1 million unique sequences and if a pathogen's nucleic acid is present at a concentration lower than 1 part per million host nucleic acid molecules, then it is unlikely to be detected. The development and use of methods to deplete mammalian nucleic acids could have improved the sensitivity of our study by

eliminating dog sequences and enriching for microorganismal nucleic acids. Our analysis of bird brain samples with high and low WNV copy numbers illustrates this sensitivity threshold. We detected WNV by sequencing in the crow brain, which had 8.82×10^4 viral RNA copies per microliter of RNA but did not detect WNV in the robin brain, which had 1.68×10^2 genome copies per microliter of RNA. It can, therefore, be deduced that our limit of detection lies somewhere between these values. This range is large, and the use of WNV-positive samples with intermediate copy numbers could have allowed us to narrow this empirically determined limit of detection. Additionally, CSF has inherently low nucleic acid content due to the low number of nucleated cells present when compared to tissue. Therefore, DNA and RNA extraction generally have a low yield and further amplification is required for library preparation in these samples. Amplification can introduce base-composition bias and increases the number of non-unique reads, contributing to reduced sequencing quality and read depth. Finally, it is also possible that the cause of MUO is an infectious agent so divergent from known pathogens that its sequence was unrecognizable. This is not likely, however. Eukaryotic and bacterial pathogens typically have characteristic conserved sequences that are easily recognizable (e.g. ribosomal RNA sequences), and viruses can typically be recognized by viral polymerase sequences, especially when compared at the protein level, as we did.

In summary, we applied the best available molecular methods to continue to the search for an MUO etiology and did not find a candidate agent. There are several technical and biological reasons that could have prevented us from doing so. However, the thoroughness of our approach, our inclusion of internal positive controls, similar negative results from previous studies, and the clinical responsiveness to immunosuppressant therapy all provide support for the hypothesis that MUO is a primary autoimmune disease.

2.3: Metagenomic Investigation of Meningoencephalitis of Unknown Origin in Free-Ranging Mule Deer (*Odocoileus hemionus*)

2.3.1: Introduction

In 2015, a free-range adult male mule deer (*Odocoileus hemionus*) in El Paso County, Colorado was found emaciated with bulging eyes and flaccid ears. The deer eventually fell and began convulsing and foaming at the mouth. The deer was euthanized and the carcass was submitted to Colorado Parks and Wildlife for postmortem examination. Gross and histologic evaluation revealed severe lymphocytic meningoencephalitis with cerebral swelling and cerebellar herniation. The right eye was also bulging and had severe intraocular hemorrhage. Based on histologic lesions that most resembled malignant catarrhal fever, a viral disease was suspected. Fresh-frozen tissues were submitted to Colorado State University Veterinary Diagnostic Lab (CSU VDL) for rabies virus fluorescent antibody test (brain), West Nile virus PCR (brain), bovine herpesvirus-1 PCR (brain), chronic wasting disease ELISA (lymph node), ovine herpesvirus-2 PCR (spleen), bluetongue virus PCR (spleen), and epizootic hemorrhagic disease virus PCR (spleen). Fresh-frozen brain was also submitted to the Wyoming State Veterinary Laboratory for *Odocoileus* adenovirus-1 PCR and the National Veterinary Services Laboratory for Eastern and Western equine encephalitis virus PCR. All tests were negative.

A similar case was found in 2018 in a free-range adult male mule deer in Jefferson County, Colorado. This deer was found to be acting blind with cloudy eyes and sluggish movements. The deer was euthanized. Gross and histologic evaluation revealed severe lymphocytic meningoencephalitis with necrotizing vasculitis, severe lymphoproliferative panuveitis, severe multifocal to coalescing necrotizing lymphadenitis, and severe interstitial lymphoplasmacytic orchitis with necrotizing arteritis. Fresh frozen tissues were submitted to the CSU VDL for chronic wasting disease ELISA (lymph node), ovine herpesvirus-2 PCR (lymph node), and aerobic culture of the cornea. Fresh-frozen spleen was also submitted to the Texas A&M Veterinary Medical Diagnostic Laboratory for bluetongue virus and epizootic

hemorrhagic disease virus PCR. All tests were negative except the aerobic culture, which yielded light growth of *Pasteurella multocida*, *Trueperella pyogenes*, and *Staphylococcus* species (coagulase negative).

In both cases a viral etiology was suspected but targeted diagnostics failed to identify a potential cause. Fresh-frozen tissues were submitted to the Stenglein laboratory for metagenomic sequencing and possible pathogen identification.

2.3.2: Materials and Methods

2.3.2.1: Metagenomic Sequencing

Methods can be referenced in sections 2.2.2.3 and 2.2.2.4 Total RNA and DNA were extracted from fresh-frozen brain (case 1 only), spleen, and retropharyngeal lymph node (RPLN). Sequencing libraries were generated from RNA and DNA from the brain of case 1 and RNA from the RPLN of case 2. The case 1 RNA library was sequenced (RNA-seq) using dual indexed, paired end, 2x150 methods on an Illumina NextSeq 500 instrument with a NextSeq 500/550 High Output Kit v2 (150 cycles). The case 1 DNA-seq and case 2 RNA-seq were performed using dual indexed, single end, 1x150 methods on the same platform. Data analysis was performed as previously described; host filtration was performed using *Bos taurus* genome (Bos_taurus_UMD_3.1.1).

2.3.2.2: Caprine Herpesvirus-2 PCR

Extracted RNA was reverse transcribed to complementary DNA (cDNA) as described above (2.2.2.3). PCR for caprine herpesvirus-2 (CpHV-2) was performed as previously described [171]. Briefly, a degenerate heminested primer set was used for the primary (Forward: CON-EX 5'to 3' CAYAAAYCTRTGCTACTCCAC; Reverse: GOT 5'to 3' CCGTAATAGAGGGGTCCT) and secondary reactions (Forward: 5'to 3'CONS TGGCCTCGGGCATGCTGC; Reverse: GOT 5' to 3'CCGTAATAGAGGGGTCCT). PCR was performed using 1x HOT FIREPol DNA Polymerase (Solis BioDyne), 3 µM of each primer, and 5 µl of diluted (1:10) cDNA or DNA in a 30 µl reaction. For the

second PCR reaction, the PCR product from the first reaction was diluted 1:10 and used as template. Both reactions were run on a thermocycler (Applied Biosystems) with the following cycle parameters: 94°C for 5 minutes; 94°C for 30 seconds, 51°C for 30 seconds, and 72°C for 30 seconds for 45 cycles; and 72°C for 7 minutes. Reaction products were evaluated by gel electrophoresis on a 1.5% agarose gel with ethidium bromide. DNA bands of the appropriate size were gel extracted (Zymo Gel DNA Recovery Kit) according to the manufacturer’s instructions. Bands were Sanger sequenced by GENEWIZ (San Diego, CA) using the forward primer (CON-EX).

2.3.3: Results

RNA-seq and DNA-seq were performed on tissues of two diseased mule deer with a suspected viral infection. The datasets contained ~4 to 11 million sequences per sample (Table 2.2). A stepwise data analysis pipeline was used to filter low quality, duplicated, and host-derived sequences. Remaining sequences were queried against databases of nucleotide and protein sequences to identify possible pathogen-derived sequences (Table 2.2).

Table 2.2. Average reads per deer sample and sequencing analysis summary. The average number of sequences generated per sample was calculated for the RNA-derived and DNA-derived libraries from each case. A) Average number of initial reads. B) Average number of reads remaining after removing low quality sequences. C) Average number of reads remaining after collapsing non-unique sequences into a single read. D) Average number of reads remaining after removing host-derived sequences. E) Total number of reads detected that aligned to a gammaherpesvirus (OvHV-2, AIHV-1, or CpHV-2).

Case	Nucleic Acid	Total Reads (A)	Remove low quality reads (B)	Collapse to unique reads (C)	Host filter (D)	Gamma-herpesvirus reads (E)
1	RNA	6.7 x 10 ⁶	4.2 x 10 ⁶ (63%)	5.8 x 10 ⁵ (9%)	4.3 x 10 ⁴ (0.6%)	1
1	DNA	4.2 x 10 ⁶	4 x 10 ⁶ (95%)	3.6 x 10 ⁶ (85%)	1.3 x 10 ⁶ (30%)	22
2	RNA	11 x 10 ⁶	8.9 x 10 ⁶ (82%)	2.3 x 10 ⁶ (22%)	2.2 x 10 ⁴ (2%)	0

RNA-seq of case 1 (brain tissue) generated a single paired read aligning to ovine herpesvirus-2 (OvHV-2; GenBank accession: NC_007646.1). Alignments of the ~300 bp sequence in BLASTn and BLASTx revealed sequence similarity to the ribonucleotide-reductase large subunit-like gene/protein of OvHV-2 with ~82% nucleotide identity and ~90% amino acid identity. RNA-seq from case 2 (RPLN) did not yield any reads aligning to gammaherpesviruses.

DNA-seq from the case 1 generated 22 single-end reads. One read (150 bp) aligned to CpHV-2 genome (GenBank accession: AF283477.2) with 100% nucleotide and amino acid identity. The available nucleotide sequence for CpHV-2 in GenBank spans 3,623 bp (partial cds of the glycoprotein B and DNA polymerase genes) of the estimated 135 kb genome. The remaining 21 reads aligned to the OvHV-2 genome or alcelaphine herpesvirus-1 (AIHV-1) genome (NC_002531.1) outside the region covered by the partial CpHV-2 sequence. These reads aligned with 67-90% nucleotide identity and 61-90% amino acid identity.

Heminested PCR of the brain, spleen, and RPLN was performed on DNA (case 1 and 2) and RNA (converted to cDNA; case 2). All DNA samples yielded amplicons of 433 bp (reaction 1) and 144 bp (reaction 2) for each tissue tested (Figure 2.1). Products from reaction 1 were pooled for each case and Sanger sequenced. Sequences aligned to CpHV-2 with 100% nucleotide and amino acid identity. The RNA samples from case 2 were negative in reaction 1 (spleen and RPLN). The spleen was also negative in reaction 2, but PCR amplification was detectable in the RPLN.

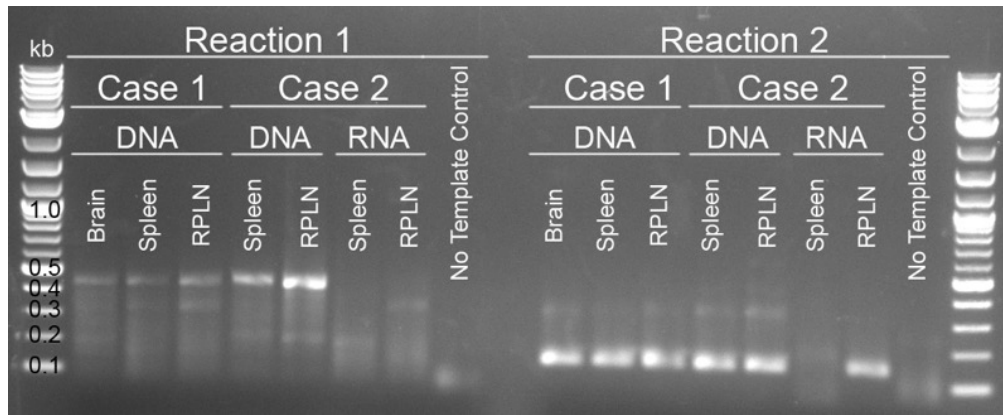


Figure 2.1. CpHV-2 detected by PCR in brain, spleen, and RPLN of two mule deer. CpHV-2 heminested PCR results from case 1 and case 2 mule deer following extraction of DNA or RNA. Reaction 1 had an expected 433 bp amplicon; reaction 2 had an expected 144 bp amplicon. The no template control contained no nucleic acid input (negative control). RPLN, retropharyngeal lymphnode. Kb, kilobase ladder.

2.3.4: Discussion

The rhadinoviruses are a genus of double stranded DNA viruses within the *Gammaherpesvirinae* subfamily, several of which are known to cause significant disease in humans and animals, including malignant catarrhal fever (MCF) [122]. MCF is a systemic viral disease of domestic and wild ruminants that can have fatal consequences in susceptible species. There are currently six known rhadinoviruses associated with MCF (MCFVs): AIHV-1 [172], AIHV-2 [173], OvHV-2 [174], CpHV-2 [171], MCFV of white-tailed deer (MCFV-WTD; also known as CpHV-3) [175,176], and ibex MCFV [177,178]. These viruses occur in carrier species (wildebeests, Jackson’s hartebeests, sheep, goats, and ibex, respectively) with asymptomatic infection. When viruses are transmitted from these hosts to a susceptible species such as cattle or deer, MCF is the result [175].

CpHV-2 occurs at a high prevalence in goats of North America [171]. MCF has been associated with CpHV-2 infection in captive white-tailed deer (*Odocoileus virginianus*; USA), sika deer (*Cervus nippon*; USA and China), and water buffalo (*Bubalus bubalis*; Switzerland), and free-ranging moose [*Alces alces*], roe deer [*Capreolus capreolus*], and red deer (*Cervus elaphus*; Norway) [179–185]. Previously, cases of MCF in both captive and free-ranging mule deer have been associated with OHV-2 infection [186,187]. However, this is the first case series of goat-associated MCF in mule deer. These findings

indicate that CpHV-2 should be on the list of differentials for mule deer with MCF-like disease, especially those negative for other viral agents.

Despite the severity of the histologic lesions in these cases, the detection of herpesvirus proved difficult. RNA is often used as the starting material for library preparation in pathogen discovery projects. In theory, RNA virus RNA, the messenger RNA transcripts of DNA viruses, and transcripts of prokaryotes and eukaryotes can be detected by total RNA. However, in this study we found RNA to be a poor starting material for the detection of CpHV-2. Total RNA-seq yielded 1 or no reads aligning to gammaherpesviruses. These data sets also generated a greater number of duplicated sequences during library preparation (Table 2.2), resulting in fewer non-host derived sequences available for pathogen detection. Furthermore, PCR using reverse transcribed RNA yielded mostly negative results with amplification only occurring after the second round of PCR in the RPLN of one deer. These findings indicate that RNA-seq may not be as reliable for total pathogen detection as previously anticipated. The extraction of DNA provided better starting material for the detection of CpHV-2 by metagenomic sequencing and PCR. Therefore, future pathogen discovery projects that yield negative results with RNA-seq may benefit from also performing DNA-seq.

2.4: Metagenomic Investigation of Granulomatous Nephritis of Unknown Origin in Lined Seahorses (*Hippocampus erectus*)

2.4.1: Introduction

In 2010, a collection of lined seahorses (*Hippocampus erectus*) began experiencing mass mortalities from an unidentified disease. Clinical signs of affected seahorses included lying in lateral recumbency, spending long periods of time at the bottom of the tank, gilling (heaving breathing), or moribund presentation. Quarantine combined with antibiotic and antiparasitic therapy were attempted, but animals responded poorly. Animals either died or were euthanized and necropsies were performed. Gross findings included thin body condition, pinpoint to large (up to 3 mm) multifocal white masses within the kidneys that were occasionally observed in the gill or coelomic cavity, edema and/or ulceration of the tail,

pouch emphysema with petechiation, and yellow liver (fatty liver). Histologic assessment of a subset of affected seahorses included severe necrotizing and granulomatous nephritis, mild to moderate necrotizing and granulomatous branchitis, mild necrotizing myositis, proliferative and ulcerative colitis, and diffuse meningeal edema. Seahorses continued to succumb to similar disease and by 2013 the entire collection was lost.

Attempts at identifying a possible underlying cause included bacterial and fungal culture, gram and acid-fast stains of coelomic swabs, and electron microscopy (EM) of fixed tissues. Possible organisms were identified by EM and suspected to be a *Ureaplasma* or *Mycoplasma* species, but follow-up testing for these agents were negative. Kidney samples were then submitted to the Stenglein laboratory for metagenomic sequencing in attempt to identify a potential causative agent.

2.4.2: Materials and Methods

2.4.2.1: Metagenomic Sequencing

A total of 19 kidney samples that had been fresh-frozen and maintained at -70°C were shipped on dry ice overnight to the Stenglein laboratory. Samples belonged to three groups of seahorses: 1) nephritis cases confirmed by gross and histopathologic examination (CN), 2) probable nephritis cases based on gross findings (PN), and 3) cases where nephritis was deemed absent by gross and histopathologic examination (non-nephritis group; NN). In the third group, seahorses died with other disease processes including disturbed osmoregulation, poor nutritional status, gas bubble disease, and cardiac algal infection. Samples were blinded for all steps prior to data analysis.

Methods can be referenced in sections 2.2.2.3 and 2.2.2.4. Total RNA was extracted from fresh-frozen kidneys. RNA-Sequencing libraries were generated and metagenomic sequencing was performed using a dual indexed, single end, 1x150 method on an Illumina NextSeq 500 instrument with a NextSeq 500/550 High Output Kit v2. Data analysis was performed as previously described; the complete

mitochondrial genome of the tiger tail seahorse (*Hippocampus comes*; H_comes_QL1_v1) was used for host filtration.

2.4.2.2: Seahorse Paramyxovirus PCR

Reads/contigs aligning to paramyxoviruses from seahorse A were used to generate a genome scaffold based on presumptive genome organization of other paramyxoviruses (salmon aquaparamyxovirus [GCF_000926395.1] and reptilian ferlavirus [GCF_000853985.1]). PCR primers were designed based on the generated scaffold to bridge sequence gaps (Supplemental Table 2.3). RNA from seahorse A was reverse transcribed to cDNA as previously described. PCR was performed using Luna Universal qPCR Master Mix. Twelve microliter reactions included a final concentration of 1x Luna Universal Master Mix and 0.3 μ M of each paramyxovirus primer mixed with 5 μ l of cDNA diluted 1:10 in water. Reaction mixtures were run with the following cycle parameters: 95°C for 1 minute; 95°C for 15 seconds and 60°C for 30 seconds to 3 minutes (depending on length of expected amplicon) with 45 cycles; and a melting curve. PCR products were run on a 1.5% agarose gel with ethidium bromide for confirmation of amplification and assessment of amplicon size. DNA bands were gel extracted (Zymo Gel DNA Recovery Kit) according to the manufacturer's instructions. Bands were Sanger sequenced by GENEWIZ (San Diego, CA) using the forward and reverse primers.

2.4.3: Results

RNA was extracted from seahorse kidney samples from 5 NN cases, 3 CN cases, and 11 PN cases and converted into sequencing libraries for metagenomic sequencing. The datasets contained ~1 to 13 million, 150-nucleotide sequences per sample (Table 2.3). A stepwise data analysis pipeline was used to filter low quality, duplicated, and host-derived sequences. Remaining sequences were queried against databases of nucleotide and protein sequences to identify possible pathogen-derived sequences.

No single organism was found in all nephritis (CN and PN) animals with absence in non-nephritis animals. In 6 seahorses (2 CN and 4 PN) a potential etiologic agent was not detected. In the remaining 13

seahorses (5 NN, 1 CN, and 7 PN), at least one of two novel viruses were identified: a paramyxovirus and parvovirus (Table 2.3).

Novel paramyxoviruses were detected in 12 out of 19 seahorses (5 NN, 1 CN, and 6 PN). A partial genome (8,495 bp) of the paramyxovirus from seahorse A was generated using a combination of metagenomics and PCR Sanger sequencing. BLASTn alignment of the partial genome revealed low nucleotide identity with paramyxoviruses from all genera (*Aquaparamyxovirus*, *Avulavirus*, *Ferlavirus*, *Henipavirus*, *Morbillivirus*, *Respirovirus*, and *Rubulavirus*). Nucleotide alignment was limited to the polymerase gene with up to 11% query coverage and 65% nucleotide identity in this short region.

Open reading frames were assessed using BLASTx and were found to include a presumptive matrix protein, fusion protein, hemagglutinin-neuraminidase protein, and 5' portion of the large polymerase protein. Nucleotide sequence for each of the proteins was used as the query sequence for BLASTx to assess amino acid identity to known paramyxoviruses. The matrix protein shared 28-33% amino acid identity with other paramyxoviruses; the fusion protein shared 31-39% amino acid identity; the hemagglutinin-neuraminidase protein shared 30-33% amino acid identity; and the large polymerase shared 45-47% amino acid identity. In all cases, the novel seahorse paramyxovirus aligned to paramyxoviruses from multiple genera, but reptilian ferlavirus and salmon aquaparamyxovirus typically generated the highest scoring alignments.

Paramyxovirus reads (150 bp each) from other seahorses (B-E, H-J, M, O, Q, S) were aligned to the partial genome from seahorse A. Nucleotide identity ranged from 80-100%, indicating more than one paramyxovirus genotype present within the seahorse population.

A novel parvovirus was also detected in 3 out of 19 seahorse kidneys (2 NN and 1 PN). In each seahorse, a 350-599 bp contig within the same region of the genome was identified that aligned to chapparvovirus species using BLASTn and BLASTx. In all three, BLASTn revealed an 83 bp alignment to porcine parvovirus 7 (NC_001718.1) with 75% nucleotide identity; BLASTx revealed ~40% amino acid identity over ~350 bp to the capsid protein of chapparvovirus species. Parvovirus contigs from each seahorse shared >95% nucleotide identity with one another.

Table 2.3. Infectious agents detected by metagenomic sequencing in seahorses with and without nephritis. NN seahorses were cases in which the lesions associated with disease were deemed absent by gross and histopathologic examination. CN seahorses were established cases of disease by gross and histologic examination. PN seahorses were cases consistent with disease based on gross examination only. The total read depth for the sample as well as the number of unique individual sequences that aligned to each infectious agent are provided within the table. N/A, not applicable.

Group	Seahorse ID	Total reads (depth)	Infectious Agent Detected	Number of Aligned Reads
Non-Nephritis (NN)	A	12.7 x 10 ⁶	Paramyxovirus	29
	B	6.7 x 10 ⁶	Paramyxovirus	41
	C	11 x 10 ⁶	Paramyxovirus	2
			Parvovirus	3
	D	10.5 x 10 ⁶	Paramyxovirus	2
Parvovirus			7	
E	6.1 x 10 ⁶	Paramyxovirus	18	
Confirmed Nephritis (CN)	F	10.2 x 10 ⁶	None	N/A
	G	11.8 x 10 ⁶	None	N/A
	H	9.8 x 10 ⁶	Paramyxovirus	13
Probable Nephritis (PN)	I	5.9 x 10 ⁶	Paramyxovirus	8
	J	11 x 10 ⁶	Paramyxovirus	61
	K	4.2 x 10 ⁶	None	N/A
	L	13.6 x 10 ⁶	Parvovirus	3
	M	8.5 x 10 ⁶	Paramyxovirus	76
	N	7.1 x 10 ⁶	None	N/A
	O	9 x 10 ⁵	Paramyxovirus	31
	P	6.4 x 10 ⁶	None	N/A
	Q	6.4 x 10 ⁶	Paramyxovirus	16
	R	7.3 x 10 ⁶	None	N/A
S	4.1 x 10 ⁶	Paramyxovirus	11	

2.4.4: Discussion

This study sought to identify a candidate etiologic agent for a fatal outbreak of granulomatous nephritis syndrome in a collection of seahorses. Two infectious agents were identified in both nephritis and non-nephritis groups: a novel paramyxovirus and a novel parvovirus. The presence of these viruses in both the case and control groups eliminates any overt disease association, however, this does not rule out these viruses as contributing to disease. Potential links between these viruses and disease as well as reasoning for the distribution of these viruses within the collection are discussed below.

Paramyxoviruses (family *Paramyxoviridae*) are a large and diverse group of negative-sense single-stranded RNA viruses known to cause significant disease in humans and animals [122]. This study is the

first to describe paramyxoviruses in seahorses. The only other classified paramyxovirus found in a non-mammalian aquatic species is the Atlantic salmon aquaparamyxovirus (ASPV) [188,189]. Unclassified paramyxoviruses of non-mammalian aquatic species have recently been identified, but only sequence data is available [56]. In our study, histologic lesions were most consistently observed in the urinary and respiratory tract (kidneys and gills, respectively); granulomatous nephritis was considered the main cause of morbidity and mortality. Some paramyxoviruses have been associated with renal disease in non-mammalian species, including Anaconda paramyxovirus and avian paramyxoviruses [190,191]. Paramyxoviruses have also been associated with respiratory disease in non-mammalian species, including ASPV, ferlavirus in vipers, and avian paramyxoviruses in birds [189,191,192]. These findings provide some credence for the association of seahorse paramyxoviruses with renal and respiratory disease.

Parvoviruses (family *Parvoviridae*) are a group of single stranded DNA viruses [122]. The sequences derived from the seahorse samples aligned to chapparvoviruses, a group of parvoviruses with a diverse host range [193]. Chapparvoviruses have recently been detected in aquatic species, including seahorses. Interestingly, a chapparvovirus sequence that was found in in a tiger tail seahorse (*Hippocampus comes*) was identified as an endogenous parvoviral element incorporated into the host genome [193]. In our study, 3 of the seahorses had short sequences (350-599 bp) from the same region of the viral genome that aligned to chapparvoviruses on a nucleotide (75% over 83 bp) and amino acid (~40% over ~351 bp) level. It is possible that these sequences represent endogenous parvoviral elements rather than active exogenous viral infection. This would explain the presence of viral sequences in both the nephritis and non-nephritis seahorse groups. On the other hand, these viruses have recently been associated with chronic kidney disease in laboratory mice, indicating a possible tissue tropism [194]. Beyond this single disease association, very little is known about this group of parvoviruses or their significance to health.

Paramyxoviruses and parvoviruses are both known to cause immunosuppression in some animals [195,196]. One hypothesis could be that infection of seahorses with these paramyxo- and/or parvoviruses results in an underlying immunosuppression that predisposes the host to additional infections and disease. Therefore, the virus(es) may have contributed to disease manifestation indirectly. This could also explain

viral infection in the non-nephritis group. One seahorse in this group died of an opportunistic algal infection, possibly indicating immunosuppression in some infected animals.

Finally, all seahorses from this study were derived from the same collection and were co-mingled. Therefore, it is possible that the non-nephritis group of seahorses did not represent a “non-infected” group but rather a group with a subclinical infection or an altered disease manifestation to those in the nephritis groups. This theory could be tested by the examination of a separate collection of lined seahorses free of this disease syndrome. If similar paramyxoviruses or parvoviruses are absent, this theory would be further supported. In contrast, these viruses may not play a role in disease but instead represent incidental findings in these species. Overall, the association of paramyxovirus and/or parvovirus infection in lined seahorses with granulomatous and necrotizing disease of the kidneys and gills remains unknown.

2.5: Conclusion

The study investigating canine MUO failed to detect a candidate etiologic agent. This is not an uncommon outcome in pathogen discovery projects. In some cases, negative results are attributed to biological or technical errors rather than true absence of a pathogen. However, as is presented in this case, the failure to detect an infectious agent may be an indication that the disease has a non-infectious etiology. Another example of this occurred in 2011 when a polar bear in Berlin died of encephalitis. Tissue samples were examined by metagenomic sequencing for the identification of an infectious cause but no pathogens were detected [197]. Subsequently, the bear was found to have died of an autoimmune disease, anti-NMDA receptor encephalitis [198]. These studies are examples of metagenomic studies in which negative results can point towards a non-infectious disease pathogenesis.

The second study established an association between CpHV-2 and MCF in mule deer. In this example, a known pathogen was identified in a new species. Targeted diagnostics are available for detection of CpHV-2, but as is the issue with targeted testing strategies, if the infectious agent isn't one for which diagnostics are routinely performed then the agent will go undetected. This study highlights an advantage

of metagenomic sequencing above targeted diagnostics: namely the ability to identify known but unexpected pathogens.

The final study identified two novel viruses in a collection of lined seahorses: a paramyxovirus and parvovirus. Seahorses in the collection had suffered a fatal outbreak of granulomatous nephritis, but viruses were found in seahorses with and without nephritis. Therefore, the association between infection and disease was questionable. This example describes an all-too-common issue with pathogen discovery projects: how to interpret the findings. The detection of an infectious agent does not, by itself, suggest disease association. As with any study, the careful selection of case and control samples is important for accurate interpretation, but even with appropriate sample selection results may not provide an obvious answer. Therefore, follow-up to these projects is essential for determining a probable or definitive causal relationship. Indeed, even in the best-case scenario of a perfect case-control association, sequencing alone cannot prove causality.

CHAPTER 3: RESPIRATORY DISEASE IN BALL PYTHONS (*PYTHON REGIUS*) EXPERIMENTALLY INFECTED WITH BALL PYTHON SERPENTOVIRUS [199]

3.1: Introduction

An introduction to serpentoviruses in reptiles is provided in Chapter 1. Below is a brief revisit of the salient topics of serpentovirus infection in snakes, as deemed applicable for the current chapter.

Snake-associated serpentoviruses have previously been described in ball pythons (*Python regius*), Indian pythons (*P. molurus*), and green tree pythons (*Morelia viridis*) in association with severe fatal respiratory disease [9,111,112,133]. In these studies, postmortem findings in sick pythons included stomatitis, sinusitis, pharyngitis, tracheitis, esophagitis, and proliferative pneumonia with significant mucus secretion in affected tissues; secondary bacterial infections were also noted in the respiratory tract or systemically in some snakes. These studies describing a disease association were based on metagenomic sequencing followed by TEM, histopathology, in-situ hybridization, and virus isolation in tissue culture. Revisiting Lipkin's 3 levels of certainty in disease causation, these reports of serpentovirus infection in snakes establish a probable causal relationship, but fall short of confirming disease association. As a follow-up, our study sought to definitively determine the role of serpentovirus in the respiratory disease of pythons through the fulfillment of Koch's postulates.

Furthermore, current studies have been limited to the examination of postmortem findings [9,111,112,133]. Therefore, the clinical signs associated with disease and the progression of symptoms over time is still unknown. Antemortem sampling and diagnosis have also been previously described using oral and cloacal swabs and whole blood, but have not been done in association with clinical assessment of disease nor have they been performed longitudinally [132]. Lastly, due to localization of virus within the respiratory tract, aerosolization or contact with respiratory secretions have been proposed as possible mechanisms of transmission, but investigation into transmission routes has not been done.

We performed experimental infections in ball pythons with a ball python-derived serpentovirus known as ball python nidovirus 1 (BPNV). The goal was to conclusively establish a causative relationship

between infection and respiratory disease as well as further characterize the clinical course of disease, describe useful diagnostic techniques, and to investigate possible routes of transmission.

3.2: Materials and Methods

3.2.1: Generation of a diamond python cell line

A non-immortalized cell line was generated from heart tissue collected from a diamond python (*Morelia spilota spilota*); DPHt cells. Multiple ~2 mm cubes of myocardium were collected from a diamond python directly following humane barbiturate overdose euthanasia for chronic vertebral disease. Tissues were collected within 2 hours of euthanasia and placed in 1.5 ml, ice-cold, sterile phosphate buffered saline (PBS) in 2 ml microcentrifuge tubes for transport to the laboratory. Tissue samples were individually transferred to a 6-well cell culture plate (Corning), washed three times with ice cold PBS, and manually minced with a sterile scalpel blade in 1.5 ml PBS with 0.25% trypsin (Gibco) and 1 mM ethylenediaminetetraacetic acid (EDTA). Samples were incubated at 37°C with gentle agitation every 20 minute (m) for a total of 60 m. Following incubation, 0.5 ml of the digested product was added per well of a 12-well cell culture plate (Corning) along with 2 ml of complete cell growth medium [Minimum Essential Medium with Earle's Balanced Salts, L-Glutamine, and Nonessential Amino Acids (MEM/EBSS; Hyclone); 10% irradiated fetal bovine serum (FBS; HyClone); 100 U penicillin; 100 µg streptomycin; 0.25 µg amphotericin B (Cellgro); and 50 µg gentamicin (Cellgro)] and placed at 30°C in a humidified 5% CO₂ atmosphere. Wells were monitored regularly for evidence of cell adherence and replication. Partial (~50%) medium changes were performed weekly. When cell monolayers reached ~70% confluence, monolayers were washed twice with room temperature sterile PBS, 1 ml enzyme free cell dissociation buffer (Gibco) was added to each well, and the samples were incubated for 5 m at 30°C. Cell monolayers were disrupted by gently pipetting samples up and down, and the cell/dissociation buffer mixture was transferred to a 60 mm tissue culture dish (Corning) with 7 ml of complete cell growth medium and returned to a 30°C,

humidified, 5% CO₂ atmosphere. The cells were monitored regularly for evidence of cellular replication with weekly, partial (~50%) medium changes. At ~70% confluence, monolayers were passed using 0.25% trypsin first into T25, and then into T75 tissue culture flasks (Corning). At 100% confluence, T75 flasks were trypsinized, washed in complete cell growth medium, and resuspended in 1 ml of complete cell culture medium with 20% irradiated FBS and 10% DMSO for storage in liquid nitrogen in 1.2 ml cryovials (Corning).

3.2.2: Isolation of BPNV

Oral swabs were collected from a ball python with upper respiratory disease that was part of a colony with a documented history of BPNV infections [111]. Swabs were placed in 1.5 ml of viral transport medium (MEM/EBSS, 0.5% bovine serum albumin, 200 U penicillin, 200 µg streptomycin, 0.25 µg fungizone, and 10 µg ciprofloxacin; Gibco) prior to inoculation on diamond python heart (DPHt) cells. Briefly, 1 ml of the swab extracts were added to DPHt cells in T25 culture flasks. After a 3 hour incubation at 30°C, monolayers were rinsed and cell growth medium added (MEM/EBSS, 10% irradiated FBS, 200 U penicillin, 200 µg streptomycin, 0.25 µg fungizone, and 10 µg ciprofloxacin; Gibco). Cultures were maintained at 30°C and monitored daily for cytopathic effects. At 7 days post inoculation cells were frozen at -70°C, thawed, and were re-inoculated onto new DPHt monolayers. The study challenge virus (deemed BPNV-148) was a passage 2 preparation.

3.2.3: Plaque assay

DPHt cells were incubated in complete cell medium [MEM/EBSS (HyClone), 10% irradiated FBS (HyClone), 10% Nu-Serum1 (Corning), and 2x penicillin-streptomycin solution (HyClone)] in a 6-well CELLSTAR cell culture plate (Greiner Bio-one) at 30°C in 5% CO₂ until 90% confluence was attained. BPNV-148 stock was diluted in serum-free MEM/EBSS to generate 5 dilutions of 1x10⁻² through 1x10⁻⁶. For cell inoculation, all medium was removed and 900 µl of each dilution was placed on cells, with serum-

free MEM/EBSS added to the last well as a negative control. Cells were incubated at 30°C in 5% CO₂ for 1 hour, after which the infected medium was removed and an agarose overlay was placed [complete cell medium with 0.8% UltraPure LMP Agarose (Invitrogen)]. Assays were incubated at 30°C in 5% CO₂ for 6 days, at which time 1 ml of 4% paraformaldehyde (EM grade; Electron Microscopy Sciences) in DPBS (Corning) was added to each well and incubated for an additional hour. The agarose overlay was removed, cells were rinsed with DPBS, and an additional 1 ml of paraformaldehyde mixture was added. Cells were placed at 4°C overnight. The formaldehyde was removed, cells were rinsed with sterile water, and 100 µl of crystal violet (0.5% crystal violet in 25% methanol and 75% sterile water) was added and incubated for 10 minutes at room temperature. Crystal violet was rinsed off with sterile water, assays were dried, and plaques were counted. Plaque assays were also performed using samples collected during experimental infection studies; the same protocol was utilized.

3.2.4: Experimental infection

Five captive-bred ball pythons (BP A-E; 4 males and one undetermined sex) were acquired, each approximately 6 weeks old and varying in size from 77-106 grams. All pythons were housed and treated according to the IACUC protocol ([15-6063A](#)) and Colorado State University Laboratory Animal Resources standards. Infected snakes were housed in a cubicle with separate HEPA-filtered air supply from control snakes and all snakes were housed in separate cages without direct contact. Uninfected snakes were always handled prior to infected snakes to prevent fomite transmission. Physical exams were performed and all snakes were deemed clinically healthy at the time of acquisition. Pre-infection choanal (CHS), oroesophageal (OES), and cloacal swabs (CLS) were collected and tested by qRT-PCR (see below) for BPNV. One week after arrival, three snakes were inoculated with BPNV infected DPHt cell culture supernatant discussed above (BP-A, B, and C) and two were sham inoculated (BP-D and E). Inoculation was performed both orally (200 µl) and intratracheally (100 µl) for each snake with 1.1×10^5 PFU in 300 µl for the infected snakes and a similar volume of uninfected cell culture medium for the control snakes.

Snakes were monitored daily, weights were taken weekly, and CHS, OES, and CLS were collected weekly from all snakes using PurFlock Ultra sterile flocked 6" plastic-handle swabs (Puritan Diagnostics). Swabs were placed in 2 ml Bacto brain-heart infusion medium (Becton, Dickinson and Company), incubated at room temperature (RT) for approximately 30 minutes, vortexed, and then stored at -80°C. BP-C was euthanized at 5 weeks post infection (PI) as a demonstration of early infection. BP-A was euthanized at 10 weeks PI and BP-B at 12 weeks PI based on clinical signs and established euthanasia criteria. Final CHS, OES, and CLS and culture swabs of the oral cavity (BBL CultureSwab plus Amies gel without charcoal; Becton, Dickinson and Company) were collected at the time of euthanasia. Sections of the glottis, nasal and oral cavity, cranial, middle, and caudal trachea and esophagus, lungs, heart, liver, kidneys, gallbladder, spleen, pancreas, stomach, small intestine, colon, feces, blood, urates, gonads, head and vertebrae with brain and spinal cord were saved fresh and/or placed in 10% neutral buffered formalin.

3.2.5: RNA Extraction

RNA from swabs and fresh-frozen tissues (lung, cranial trachea/esophagus, liver, kidney, heart, stomach, small intestine, colon, feces, urates) was extracted using a combination of TRIzol (tissue; Ambion Life Technologies) or TRIzol LS (swabs in BHI; Ambion Life Technologies) as previously described in section 2.2.2.3.

3.2.6: Viral RNA Detection

RNA extracted from swabs and fresh-frozen tissues was reverse transcribed into cDNA as previously described (section 2.2.2.3) Quantitative reverse transcription polymerase chain reaction (qRT-PCR) was performed using 1x HOT FIREPol DNA Polymerase (Solis BioDyne), 3 µM of each degenerate serpentovirus primer (MDS-918 and MDS-919; Table 3.1), and 5 µl of diluted (1:10) cDNA in a 30 µl reaction. Reaction mixtures were run in a Roche LightCycler 480 II with the following cycle parameters: 95°C for 15 minutes; 95°C for 10 seconds, 60°C for 12 seconds, and 72°C for 12 seconds with 40 cycles;

and a melting curve. All samples were run in duplicate, Ct values were averaged and standard deviations were calculated. The PCR reaction efficiency for each primer-pair was measured using a dilution series of positive samples (BP-B terminal OES for BPNV primers and BP-B trachea/esophagus for GAPDH primers); the dilution series samples were run in duplicate. Relative viral RNA for all CHS, OES, and CLS samples was determined by comparison of each sample Ct to the sample with the highest Ct (lowest viral RNA) at the first collection time point following inoculation (BP-B OES at week 1 PI). Relative viral RNA from tissues was determined by normalization to snake GAPDH within each sample (same qRT-PCR conditions with MDS-921 and MDS-923 primers; Table 3.1).

Table 3.1. List of oligonucleotides used during qRT-PCR for detection of BPNV or GAPDH and used for sequencing library generation. F, forward; R, reverse; N/A, not applicable.

Oligo Name	Target	Sequence (5'-3')	Direction (F/R)	Reference
MDS-143	Sequencing library adaptors	CAAGCAGAAGACGGCATAACG	F	[200]
MDS-445		AATGATACGGCGACCACCGA	R	
MDS-911	Random	NNNNNNNNNNNNNNNN	N/A	N/A
MDS-918	ORF1b BPNV	CAYAACATCGACATCGCACT	F	N/A
MDS-919		TCGATGAAGATYTCGGTGTT	R	
MDS-921	Python GAPDH gene	AATATCTGCCCATCAGCTG	R	[62]
MDS-923		GTTTTCCAAGAGCGTGATCC	F	

3.2.7: Antibody development

The predicted amino acid (aa) sequence for the ball python nidovirus 1 nucleocapsid protein (152 aa protein; GenBank: AIJ50569.1) and nucleocapsid protein sequences isolated from serpentoviruses of green tree pythons (unpublished data) were used by our lab to identify a relatively conserved peptide sequence with predicted high immunogenicity and epitope exposure. The peptide (aa 136-152 of the N

protein of a green tree python serpentovirus isolate: Cys-RAFIPLKHEGAETEEEV) was submitted to Pacific Immunology (Ramona, CA) for synthesis and polyclonal anti-nidoviral nucleocapsid antisera (NdvNcAb) was developed in two rabbits.

3.2.8: Histopathology and Immunohistochemistry

Formalin-fixed tissue was paraffin-embedded and 5 µm sections were stained by hematoxylin and eosin (H&E), Gram, periodic acid-Schiff (PAS), and Ziehl-Neelsen acid fast for light microscopy (performed by Colorado State University Veterinary Diagnostic Laboratory; CSUVDL). Immunohistochemistry was also performed by CSUVDL using the Bond Polymer Redefine Red Detection kit (Leica) and a 10-minute incubation with Epitope Retrieval Solution 1 (Leica). NdvNcAb (0.32 µg/ml) was used as the primary antibody and the slides were counter stained with hematoxylin. Lung tissue from a green tree python that was serpentovirus positive (PCR and virus isolation) and that died of respiratory disease was used as a positive control (data not shown).

3.2.9: Virus isolation and immunofluorescence

Oroesophageal swabs collected at the time of euthanasia from all infected and uninfected snakes were filtered (Merck Millipore UltraFree-MC 0.22 µm centrifugal filters) and 40µl was inoculated onto DPHt cells at 80% confluence in 35 mm diameter glass-bottom plates (MatTek corporation). Cells were maintained in 2 ml of complete cell medium and incubated at 30°C with 5% CO₂; medium was refreshed every other day. Cells infected with BP-A OES were formalin-fixed as previously described at 1, 12, 24, 48, 96, 144, and 192 hours PI; all other OES-infected cells (BP-B, C, D, and E) were formalin-fixed at 4 days PI. Approximately 50 mg of lung or feces from infected and uninfected pythons was homogenized in 500 µl of DPBS, clarified, and then filtered (0.22 µm). Infection of cell culture was as previously described. Lung-infected cells were formalin-fixed at 10 days PI and fecal-infected cells at 3 days PI.

Fixed cells were washed 3 times with 1 ml of PBS. Cells were permeabilized in 0.1% Triton X-100 (reagent grade; Amresco) in PBS for 5 minutes. Washes were repeated and then cells were incubated in blocking buffer (1% bovine serum albumin (Fisher Scientific) in PBS) for 1 hour. A 1:2000 dilution of NdvNcAb rabbit serum (primary antibody) was added to the blocking buffer and incubated for an additional hour. Wash steps were repeated and then new blocking buffer with 5 µg/ml of secondary antibody (Alexa Fluor 488 goat anti-rabbit IgG antibodies; A11008 Life Technologies) was added and incubated for 1 hour. Wash steps were repeated and then cells were stained with Hoechst 33342 (1 µg/ml final concentration; Life Technologies) to stain DNA. Cells were imaged on an Olympus IX81 motorized inverted system confocal microscope with FluoView 4.2 software. Images were processed in Adobe Photoshop CC (2017) and both infected and uninfected were processed equally.

3.2.10: Western blot

DPHt cells inoculated with OES from all infected and uninfected snakes, as previously described, as well as a sham inoculated control (BHI only) were harvested at 4 days PI. Cells were lysed using equal volumes of sample and SDS-based tissue lysis buffer (40mM TrisCl pH 7.6, 120mM NaCl, 0.5% Triton X-100, 0.3% SDS, Roche complete protease inhibitor cocktail tablet), mixed for 30 minutes at 4°C, and clarified by centrifugation at 4°C for 10 minutes at 10,000 rpm. Twelve microliters of sample or 4 µl of ladder with 8 µl of PBS (precision plus protein western C; BioRad) were combined with 1x NuPage LDS sample buffer (Life Technologies) and separated using a 4-12% polyacrylamide gel (Invitrogen). Protein was transferred to a nitrocellulose membrane using a Trans-Blot turbo (low molecular weight protein transfer; Bio-Rad). A 1 hour incubation of the membrane in blocking buffer [1x PBS, 0.05% Tween20, 1% Carnation nonfat dry milk, and 1:1000 Kathon CG/ICP preservative (Dow Chemical)] was followed by a 1 hour incubation with 1.6 µg/ml NdvNcAb in blocking buffer. The membrane was washed (1x PBS and 0.05% Tween20) 3 times for 5 minutes each followed by a 1 hour incubation with a 1:50,000 dilution of goat anti-rabbit IgG antibody conjugated to horseradish peroxidase (HrP; Pierce 31460 Invitrogen) and

1:4000 dilution of streptactin-HrP (ladder) in blocking buffer. A second wash was performed and the blot was developed using a 5 minute incubation with clarity western ECL substrate (BioRad). Imaging was via chemiluminescence for 60 seconds (BioRad Gel Doc).

3.2.11: Metagenomic sequencing

Shotgun libraries were generated from total RNA extracted from BP-A, B, C, D, and E lung and cranial trachea/esophagus and BPNV-148 inoculum. Library preparation and sequence analysis were performed similar to that previously described (section 2.2.2.3 and 2.2.2.4). Exceptions included host genomic sequence filtration with *Python bivittatus* (Burmese python) genome (NC_021479.1) and query of the protein database (NCBI nr) with contigs and reads was performed using Diamond (version 0.9.9.110) with an expect value of 0.001 [201]. A bowtie index was generated from ball python nidovirus 1 (NC_024709.1) and sequences aligning with a –local mode alignment score greater than 60 were evaluated in Geneious (version 9.0.5) for percent identity. The inoculum sequence was deposited in Genbank (MG752895.1) and raw sequence data was deposited in the NCBI Short Read Archive database (accession SRP118506).

3.2.12: Bacteriology

Oral swabs collected in agar medium (see “Experimental infection”) were submitted to the Colorado State University Veterinary Diagnostic Lab for aerobic bacterial culture.

3.3: Results

3.3.1: Antemortem clinical findings

Choanal, cloacal, and oroesophageal swabs tested negative for BPNV by qRT-PCR in all snakes prior to inoculation. Clinical signs in infected snakes (BP-A, B, and C) began at 4 weeks PI and progressed over time. Initial clinical signs were moderate reddening of the choanal and oral mucosa and excessive oral

mucus secretion. With progression, oral reddening and mucus secretions became more severe resulting in excessive swallowing and ventral oral swelling. This was accompanied by small mucosal hemorrhages (petechiations), increased respiratory effort and rate, open-mouthed breathing, and anorexia by weeks 10-12 (Figure 3.1).



Figure 3.1. Antemortem findings in ball pythons infected with BPNV. Clinical signs in infected snakes (BP-A, B, and C) began at 4 weeks PI and included moderate reddening of choanal and oral mucosa and abundant oral mucus secretion (A). This progressed to excessive swallowing, ventral oral swelling, mucosal petechiations, increased respiratory effort and rate, open-mouthed breathing (B), and anorexia by weeks 10-12. Control snakes were clinically normal throughout the experiment.

3.3.2: Postmortem gross and histologic findings

BP-C displayed mild clinical signs (mucinous exudate in the oral cavity) at 5 weeks PI and was euthanized to assess lesions of early infection. Grossly, the oral mucosa was diffusely and mildly reddened with moderate mucinous secretions in the oral cavity and cranial esophagus. Histologically, there was moderate chronic-active mucinous rhinitis, stomatitis, glossitis, tracheitis, and cranial esophagitis with variable epithelial proliferation. Inflammatory infiltrates were mixed with moderate numbers of lymphocytes, plasma cells, heterophils and macrophages. There was mild faveolar pneumocyte hyperplasia regionally with the accumulation of luminal proteinaceous material. The caudal esophagus was normal.

BP-A was euthanized at 10 weeks PI and BP-B was euthanized at 12 weeks PI, both due to anorexia, intermittent increased respiratory effort and open-mouthed breathing, following IACUC protocol euthanasia criteria. Grossly, oral cavities of each snake were similar to BP-C but with significantly more mucinous exudate. BP-A also had a focal ulceration of the glottis, the caudal esophagus adjacent to the lungs was markedly dilated with air and mucus, and the cranial 1/3 of the lungs were wet and red (Figure 3.2). BP-B lungs were slightly reddened and wet in the cranial portion but the caudal esophagus was grossly normal. Histologically, both snakes had similar but more severe lesions in the upper respiratory tract (URT) and cranial esophagus as compared to BP-C (Figure 3.3A and 3.3B). Additionally, there were regions of erosion and ulceration in areas of inflammation as well as individual epithelial cell necrosis and regions of marked epithelial proliferation. The caudal esophagus of BP-A also had similar inflammatory infiltrates to that in the cranial esophagus but these were significantly milder. Lumina of the URT, cranial esophagus, central lumen of the lung, and faveoli contained mucus, necrotic debris, heterophils, hemorrhage, and occasional colonies of short Gram-negative bacterial rods. Both snakes (BP-A greater than BP-B) had a minimal to mild interstitial pneumonia of the cranial lung field with pneumocyte proliferation (Figure 3.3C). Lesions were characterized by multifocal hyperplasia of respiratory epithelial cells lining the central lumen, hypertrophy and hyperplasia of faveolar pneumocytes (predominately in the luminal 1/3 of the faveoli), and expansion of the interstitium by edema and similar inflammatory cells to that in the URT.

Sham inoculated snakes (BP-D and E) did not show clinical signs nor have histologic lesions of the respiratory tract or esophagus (Figure 3.3D-F). Both the infected and control snakes had moderate to severe lymphoplasmacytic and heterophilic, non-ulcerative colitis of unknown origin and mild lymphohistiocytic to granulomatous embolic hepatitis, which are considered unrelated to the clinical and histologic signs found only in the infected snakes. Gram, PAS, and Ziehl-Neelsen acid fast stains did not elucidate an infectious agent associated with these lesions. Remaining tissues were histologically normal in control snakes (heart, kidneys, spleen, stomach, small intestine, pancreas, gall bladder, adrenal glands, gonads, brain, spinal cord, vertebral bone, bone marrow, skin, and skeletal muscle).

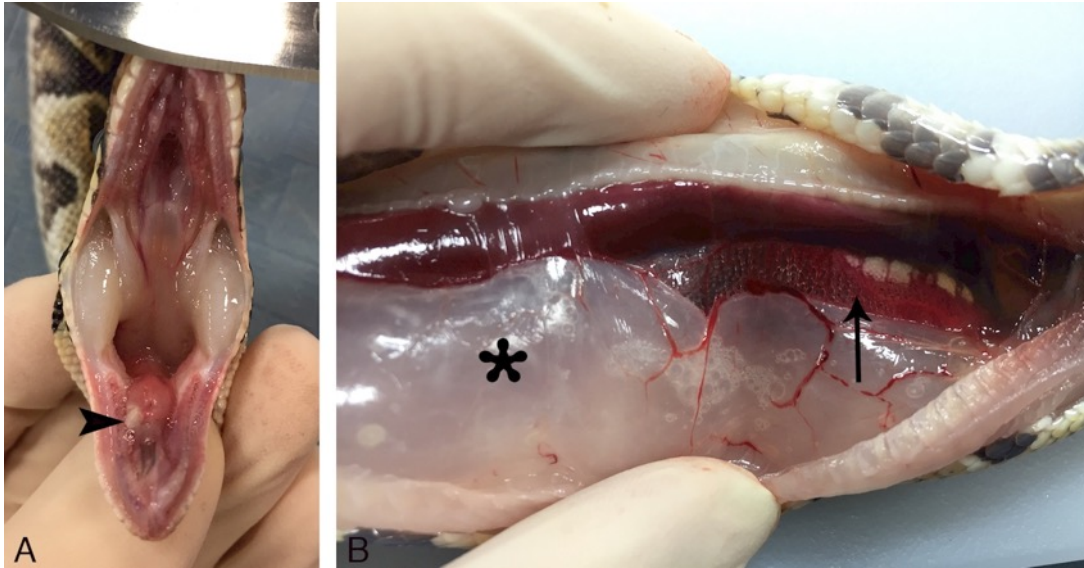


Figure 3.2. Postmortem findings in ball pythons infected with BPNV. Early lesions (BP-C) included diffuse reddening of the oral mucosa with moderate mucinous secretions in the oral cavity and cranial esophagus. Later lesions (BP-A and BP-B) included increased severity of early lesions with focal ulceration of the glottis in BP-A (A; arrowhead). The caudal esophagus adjacent to the lungs was markedly dilated with air and mucus (B; asterisk), and the cranial 1/3 of the lungs were wet and red in BP-A (B; arrow). Control snakes were normal.

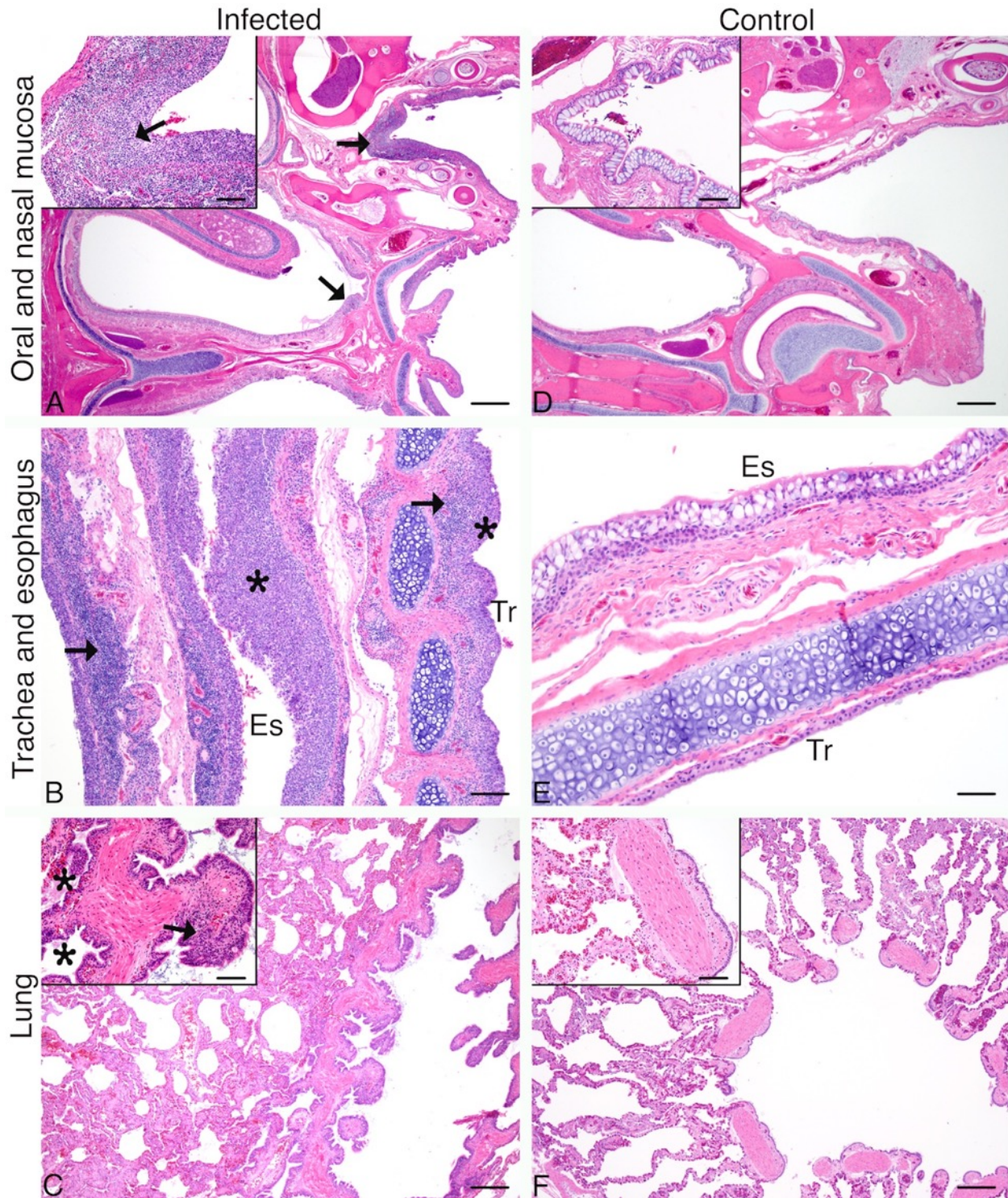


Figure 3.3. Histopathology of ball pythons infected with BPNV. Infected snakes had severe chronic-active mucinous rhinitis and stomatitis (A), tracheitis and esophagitis with epithelial proliferation (B), and interstitial proliferative pneumonia (C). Control snakes (D-F) were histologically normal. Arrows indicate inflammation; asterisks indicate epithelial proliferation. Hematoxylin and eosin. Boxes are represented in higher magnification in the insets (A, C, D, F). Scale bars: Inset scale 200 μm . (A) and (D) 1000 μm . (B) 200 μm . (E) 100 μm . (C) and (F) 500 μm . Es, Esophagus; Tr, Trachea.

3.3.3: Western blot

DPHt cells inoculated with oroesophageal swabs from both infected and uninfected snakes were analyzed by western blot using anti-nucleocapsid protein polyclonal antisera to determine antibody specificity. This polyclonal antibody was designed in our laboratory and developed in rabbits, and this is the first demonstration of its specificity. The predicted length and molecular mass of the BPNV nucleocapsid protein is 152 aa and 16.7 kDa (GenBank: AIJ50569.1) and a protein of approximately this size was detected in BP-A, B, and C (infected) but not BP-D or E (control; Figure 3.4).

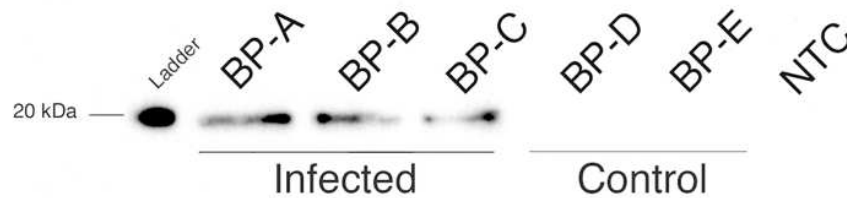


Figure 3.4. Western blot of BPNV nucleoprotein. Viral nucleocapsid protein (approximately 16.7 kDa) was detected in DPHt cells inoculated with OES from BP-A, B, and C (infected) but not BP-D or E (control).

3.3.4: Immunohistochemistry

Immunohistochemical staining of viral antigen (nucleocapsid protein) was present in all infected snakes within the epithelial surface of the oral mucosa, nasal mucosa, trachea, and esophagus (Figure 3.5A-C). Immunopositive staining was detected in the cytoplasm of presumed epithelial cells, predominately in regions of inflammation. Intact and degenerate cells containing viral antigen, or free viral antigen admixed with mucus was frequently present in the lumen of the URT and GI tract, or rarely faveoli (BP-A) (Figure 3.5D). Within the caudal esophagus, stomach, small intestine, and colon viral antigen was restricted to the luminal contents and not detected in epithelial cells. However, regions of mucosal-associated lymphoid tissue of the caudal esophagus, small intestine, and colon contained low to moderate numbers of immunopositive cells suspected to be associated with M-cell-like uptake and sampling of the luminal contents (Figure 3.6). Viral antigen was not detected in any other tissues in infected snakes (heart, kidneys,

spleen, pancreas, gall bladder, adrenal glands, gonads, brain, spinal cord, vertebral bone, bone marrow, skin, and skeletal muscle). No viral antigen was detected in the control snakes.

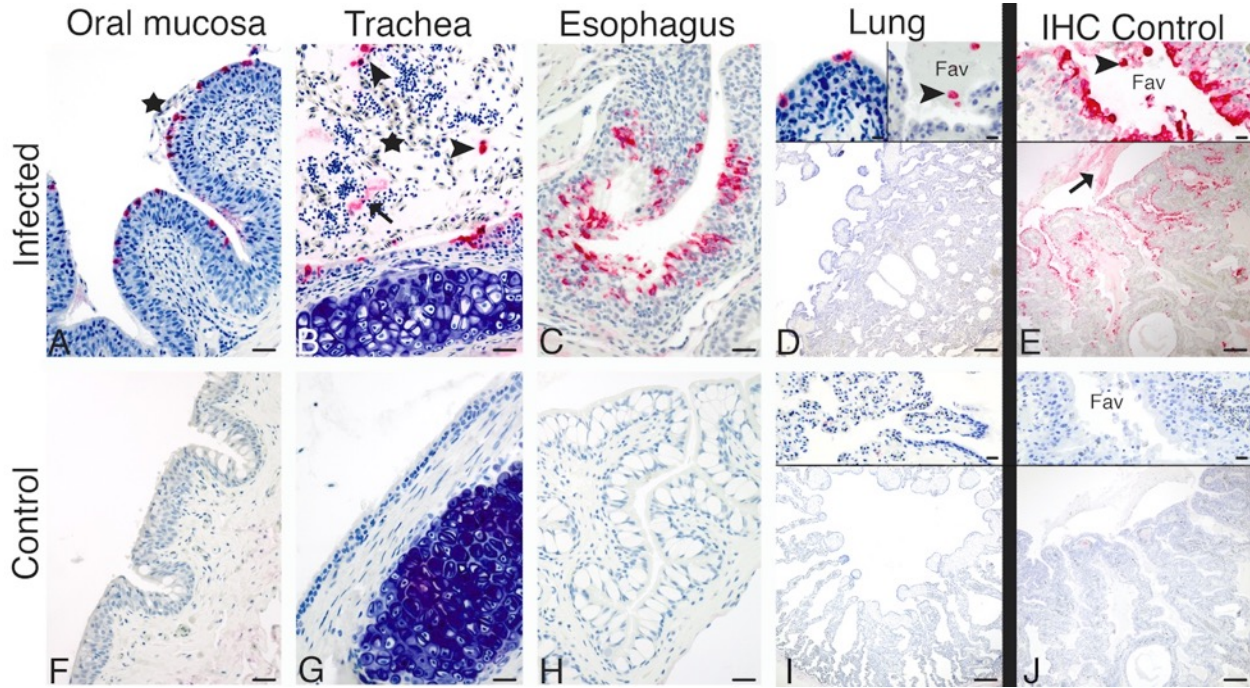


Figure 3.5. Immunohistochemistry of the respiratory tract and cranial esophagus in BPNV-infected ball pythons. Viral antigen (red staining) was prominent in the epithelial layer of the oral mucosa, trachea, and cranial esophagus of infected snakes (A-C). There were only rare positive cells within the pulmonary epithelium (D top left inset) and faveolar lumen (D top right inset) of one infected snake (BP-A), as compared with the positive IHC control from a serpentovirus-positive green tree python that died of respiratory disease (E, lung). Intact and degenerate cells that contained viral antigen were also found in the lumen of these tissues (arrowheads) admixed with cell-free viral antigen in mucus (arrow) and hemorrhage (star). No viral antigen was detected in the control snakes (F-I). The IHC negative control (J) was the same lung tissue as that used for the positive control, but lacking primary antibody application. Fav, faveolar lumen; IHC, immunohistochemistry. Primary antibody: polyclonal rabbit NdvNcAb. Counter stain: hematoxylin. Scale bars: A-C and F-H = 50 μ m; D-E and I-J lower = 500 μ m, upper (inset) = 20 μ m.

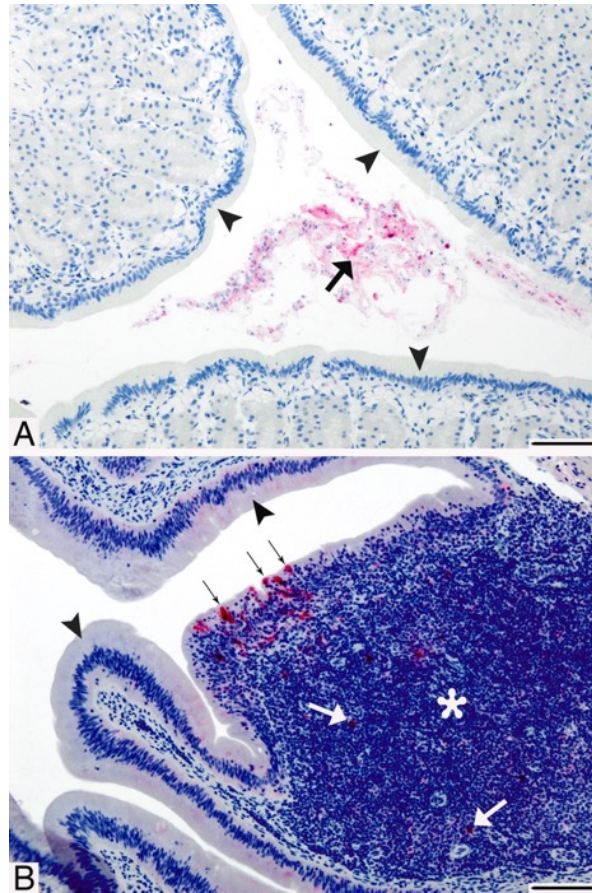


Figure 3.6. Immunohistochemistry of the gastrointestinal tract in BPNV-infected ball pythons. Representative images of the stomach (A) and small intestine (B) of infected snakes. Viral antigen (red staining) was detected in the lumen of the GI tract admixed with intact and degenerate cells and mucus (large black arrow). Epithelial cells (arrowheads) were immunonegative throughout the caudal esophagus and GI tract. However, viral antigen was detected in cells along the mucosal surface (small black arrows) overlying mucosal-associated lymphoid tissue (MALT; asterisk) of the esophagus, small intestine, and colon. Immunopositive cells extended into the center of MALT (white arrows). Primary antibody: polyclonal rabbit NdvNcAb. Counter stain: hematoxylin. Scale bars = 100 μ m.

3.3.5: Viral RNA Detection

Viral RNA was detectable in oroesophageal, choanal, and cloacal swabs by qRT-PCR beginning at 1 week PI in all infected snakes, with an increase noted at 4 weeks PI in choanal and oroesophageal swab samples, coinciding with the onset of clinical signs. Levels of viral RNA increased steadily over the course of the experiment and reached levels exceeding 1000x more than the initial sampling time point (Figure 3.7). Viral RNA was detected in multiple postmortem tissues from infected snakes, including trachea and

esophagus, liver, kidney, heart, stomach, and feces, the lung of BP-A, and the small intestine and colon of BP-A and BP-C (Figure 3.8). Respiratory and GI tract tissues and feces contained the highest viral RNA per host mRNA (GAPDH), with remaining organs having detectable but lower viral RNA levels. Viral RNA was not detected in any swabs or tissues from control snakes.

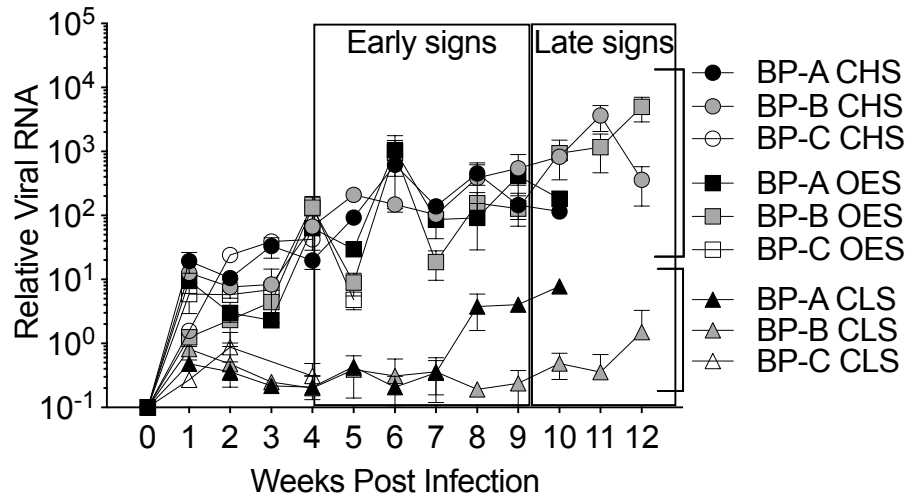


Figure 3.7. Relative viral RNA in antemortem swabs. Total RNA was extracted from choanal (CHS), oroesophageal (OES), and cloacal (CLS) swabs and was analyzed by qRT-PCR using primers targeting BPNV RNA. Relative viral RNA was determined by comparison of each sample Ct to the sample with the highest Ct (lowest viral RNA) at the first collection time point following inoculation (BP-B OES week 1 PI). All samples were run in duplicate and error bars indicate standard deviations. Viral RNA was detectable beginning at 1 week PI in all swabs of the infected snakes, with an increase noted at 4 weeks PI, correlating with the initiation of clinical signs. Viral RNA continued to increase over the course of the experiment, consistent with amplification in the host. Control snakes were negative throughout the experiment.

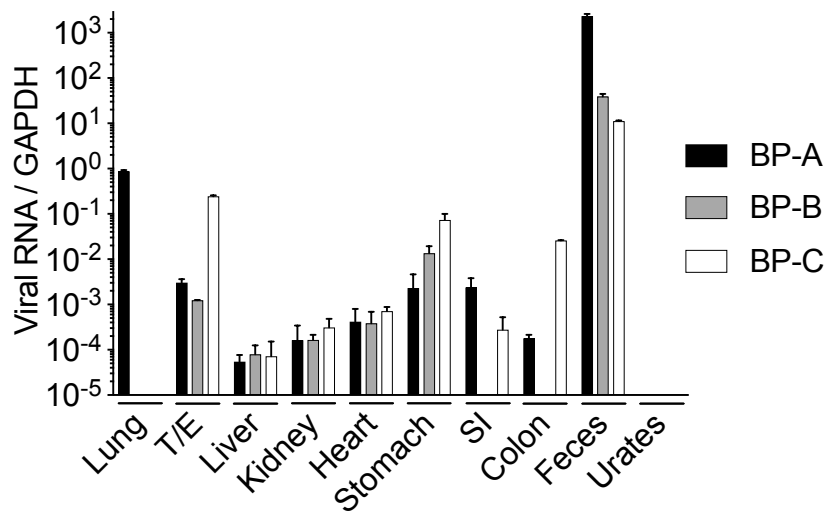


Figure 3.8. Relative viral RNA in postmortem tissues. Total RNA was extracted from fresh tissues and analyzed by qRT-PCR. Relative viral RNA was determined by normalization of BPNV Ct to GAPDH (a cellular mRNA) Ct within each sample. All samples were run in duplicate and standard deviation is represented by error bars. Viral RNA was detected in nearly all tissues of infected snakes (BP-A, B, and C). Control snakes were negative in all tissues. T/E, trachea/esophagus; SI, small intestine.

3.3.6: Virus isolation

The presence of infectious virus in collected swabs, tissues, and excreta was evaluated by virus isolation in cell culture. Inoculation of DPHT cells with terminal oroesophageal swabs from infected snakes (BP-A, B, and C) resulted in viral replication, as determined by immunofluorescence using antibodies targeting the BPNV nucleocapsid protein, and cytopathic effects (Figure 3.9). Speckled immunofluorescent staining was restricted to the cytoplasm of infected cells. Cytopathic effects included cell death and syncytial cell formation (Figure 2.9 2DPI HM panel). Viral infection of cells was detected as early as 12 hours PI with greater than 50% of cells infected by 2 days PI and significant cell death detected by day 4 PI. Plaque assay of the terminal oroesophageal swab from BP-A revealed a viral titer of 1.67×10^3 PFU/ml. Infectious virus was also isolated from feces of infected snakes, as determined by immunofluorescence of cell culture, but viral titers were not measured. Inoculation of DPHT cells with oral swabs and feces from control snakes (BP-D and E) did not produce detectable virus by immunofluorescence nor result in

cytopathic effects. Virus isolation attempts with post-mortem fresh lung samples from all snakes (infected and control) were negative.

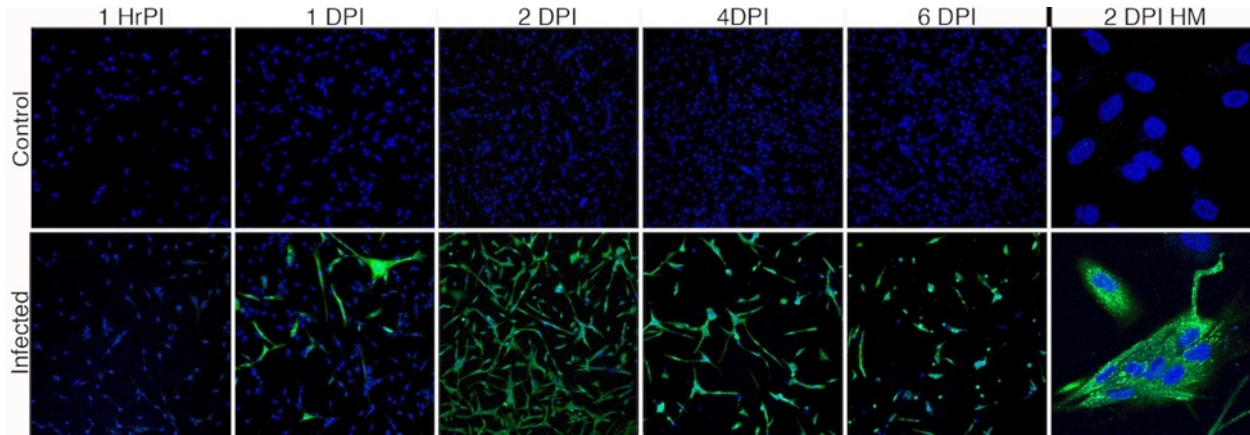


Figure 3.9. Immunofluorescence of DPHt cells inoculated with infectious swabs and tissues. DPHt cells were inoculated with filtered terminal oroesophageal swabs (OES) and feces from infected snakes (BP-A OES represented in the bottom panel) resulting in viral infection, amplification, and cytopathic effects (syncytial formation and cell death). Inoculation with lung homogenate from infected snakes yielded negative results. Swabs and tissues from control snakes also yielded negative results. The top panel represents uninfected DPHt cells. HrPI, hours post infection; DPI, days post infection; HM, high magnification. Magnification is 100x in all images, except HM (high magnification) which is 1000x. Fluorescence is Hoescht 33342 (blue) for nuclear staining and Alexa 488 (green) for the BPNV nucleocapsid protein detection using NdvNcAb. All images include overlay of both fluorescence filters.

3.3.7: Metagenomic sequencing

Metagenomic sequencing was used to validate the purity of the inoculum, to rule out other possible etiologic agents, and to evaluate genomic sequence of virus reisolated from infected snakes. The average number of read pairs per sample was 4.4×10^6 . On average, 93%, 11%, and 3.6% of sequences remained following adaptor and quality filtering, collapsing to unique reads, and filtration of python derived sequences, respectively. Remaining sequences were compared against nucleotide and protein databases for taxonomic assessment. Sequences aligning to ball python nidovirus 1 (NCBI taxonomy ID: 1986118) and *python nidovirus* (NCBI taxonomy ID: 1526652) were detected in the lung and trachea/esophagus of BP-A, B, and C (infected snakes) and BPNV-148 inoculum. Virus sequences were not detected in BP-D or E (control snakes). In addition to BPNV, BP-A lung had sequences aligning to *Pseudomonas* species. In all

samples, *Python molurus* and *curtus* endogenous retrovirus-like sequences were detected. Other sequences aligning to organisms in the queried databases were predominately non-specific alignments due to low complexity or taxonomically ambiguous sequences that span multiple taxa. Other than *Pseudomonas* reads found in BP-A lung, no other sequences specifically aligning to known primary pathogenic or opportunistic infectious agents were identified. We analyzed the sequences generated through bowtie alignment of the BPNV inoculum and the viruses re-isolated from infected snakes. The sequence of the virus in the inoculum was 96.2% identical to ball python nidovirus 1, and we obtained coverage across the complete genome. We did not obtain complete genome coverage for the recovered viruses, but the bowtie-mapped reads that did align to the BPNV inoculum sequence were 99.7-100% identical.

3.3.8: Bacteriology

Aerobic culture was performed on oral swabs from BP-A, B, D, and E. BP-A yielded heavy growth of *Pseudomonas aeruginosa* and *Stenotrophomonas maltophilia* and BP-B yielded moderate growth of *Bordatella* and *Pseudomonas* species. In the control snakes, BP-D yielded light growth of *Acinetobacter baumannii*, *Brevundimonas* species, *Delftia acidovorans*, and *Pseudomonas* species; BP-E yielded light growth of *Pseudomonas aeruginosa*.

3.4: Discussion

Novel serpentoviruses were recently found in multiple python species with respiratory disease, but a causal relationship between infection and disease has not been established [9,111,112,132,133]. Through the use of experimental infections, our study is the first to fulfill Koch's postulates and demonstrate a causal relationship between python serpentovirus infection and respiratory and esophageal disease in ball pythons. Our findings demonstrate that BPNV infection caused marked mucinous inflammation of the URT and cranial esophagus with progression towards proliferative interstitial pneumonia. These findings are consistent with previous reports of serpentovirus infection in multiple python species [9,111,112,133]. In our study, the clinical hallmark of this disease was excessive mucous production in the oral cavity, which

was accompanied histologically by marked inflammation and epithelial proliferation. Additionally, cranial esophagitis was a prominent lesion, similar to that in previous reports [111]. Mucous production and esophagitis are not characteristic findings with other respiratory viruses in snakes and, therefore, may be useful clinical and histologic features for differential diagnosis of serpentovirus infection in pythons. However, the overlap in clinical and histologic lesions with other viral agents (e.g. respiratory distress, anorexia, and proliferative pneumonia) could warrant the development of a multiplex PCR test to screen for multiple reptile respiratory viruses.

Viral antigen was detected in the mucosa of the oral and nasal cavity, trachea, and esophagus of all infected snakes, indicating a tropism for epithelial cells, especially ciliated cells of the respiratory tract and upper esophagus. Viral antigen was rarely detected in pulmonary epithelial cells, which may be due to the short time course of the experimental infections as discussed below. Viral antigen was not detected in the epithelium of the caudal esophagus or GI tract, but was present in the GI lumen by IHC and viral RNA was detected in these samples by qRT-PCR. This suggests that GI epithelium is not a site of viral replication, but the GI tract is a conduit for virus that is swallowed and passed in the feces. Additionally, viral antigen was detected in mucosal-associated lymphoid tissue of the caudal esophagus, small intestine, and colon. Sampling of the luminal contents by M-cell-like uptake could be a method for systemic spread, as indicated by viral RNA detection in non-respiratory/GI tissues.

Until recently, primary viral causes of pneumonia in pythons included paramyxovirus (ferlaviruses) and reovirus [105,192,202]. Other causes of proliferative pneumonia include chlamydophilosis, mycoplasmosis, chronic bacterial or parasitic infection, or toxin exposure [203–205]. Histopathology, bacterial culture, and next generation sequencing did not yield evidence of other primary infectious agents in the infected snakes or inoculum, consistent with BPNV as the principal cause of respiratory disease. The bacteria detected by oral aerobic culture and sequencing of the lung have been found as oral flora in clinically healthy snakes, [90–92] but the presence of moderate to heavy growth in the infected snakes is suspected to be secondary to viral infection and disruption of physical or immune barriers. Secondary bacterial infections are a common sequelae to viral disease in all types of animals and humans and have

been documented in previous cases of python serpentoviral infection [111,112]. The role of secondary infections and the progression of disease in pythons has yet to be determined and warrants further investigation.

In previous reports, the degree of pneumonia associated with serpentovirus infection was more advanced at the time of death when compared to our study [9,111,112,133]. This is highlighted by our immunohistochemistry control (Figure 3.5E) collected from a green tree python that had been serpentovirus positive for over 6 months and eventually died of respiratory disease. Had we allowed for a longer time course of infection in this study, it is likely that the infected snakes would have progressed to more severe disease.

Pythons have an overcapacity for oxygen consumption, and therefore rarely show clinical signs of respiratory disease until the oxygen exchange capacity is severely limited [206]. A recent report in green tree pythons demonstrated infection of respiratory and faveolar epithelial cells to be associated with apoptosis, proliferation, and high numbers of serous/mucous granules within the cytoplasm [133]. Respiratory epithelial proliferation and mucus production were postulated to result in mechanical and physiologic inhibition of gas exchange within the lungs, resulting in death. Our study ended at 12 weeks PI based on euthanasia criteria, however the degree of respiratory effort was greater than would be expected for the mild pneumonia in the infected snakes. It is thought that the excessive production of mucus in the oral cavity and upper airway contributed to respiratory difficulty through obstruction of the airway and glottis. Therefore, the obstructive mechanical effects of mucus could also play a role in the upper respiratory tract by affecting overall air intake, in addition to the effects in the lung on direct oxygen exchange [133].

Although the disease we observed closely resembles that seen in naturally infected snakes, there are several aspects of our study that may not have recapitulated natural infection. First, disease may be dose-dependent, and the 1.1×10^5 PFU administered may exceed a typical natural infectious dose. Second, the natural route(s) of transmission are unknown. Serpentovirus RNA has been detected in oral swabs [132] and respiratory/pulmonary epithelial cells of infected snakes [111,133], indicating the oral cavity and respiratory tract as regions of viral replication and possible routes of exposure. We inoculated snakes in the

oral cavity and upper trachea to mimic URT exposure and subsequently detected infectious virus in these regions indicating that virus is released in respiratory and oral secretions. Based on this finding, transmission may involve fomites or aerosolization. The presence of infectious virus in the feces indicates that fecal-oral transmission is also possible.

Other factors, including husbandry, age, sex, and immune status could modulate disease progression. Care of the snakes in this study followed best practices for ball python husbandry. Snakes were housed separately with appropriate enclosures and climate control and handled minimally to limit stress. Although all snakes in this study were juvenile males (one was of undetermined sex), reports have documented serpentovirus-associated respiratory disease in snakes of various sexes and ages [9,111,133].

We have definitively established serpentovirus as a cause of respiratory disease in pythons, but this is only the first step in disease characterization. Additional investigation is necessary to understand the factors that influence infection and disease and the snake species that are susceptible.

CHAPTER 4: EPIDEMIOLOGIC INVESTIGATION OF SERPENTOVIRUSES IN CAPTIVE SNAKE POPULATIONS [207]

4.1: Introduction

Snake-associated serpentoviruses were discovered in 2014 and were indirectly linked to respiratory disease in pythons [9,111,112,133]. Subsequent experimental infections of ball pythons confirmed a causal relationship between serpentovirus infection and respiratory disease, emphasizing the importance of these emerging viruses in veterinary medicine (Chapter 3) [199]. Since the initial discovery, related viruses have been detected in snake species spanning multiple families within the *Serpentes* suborder throughout North America, Europe, and Asia. These include *Pythonidae* species (ball python [*Python regius*], Indian python [*P. molurus*], Burmese python [*P. bivittatus*], green tree python [*Morelia viridis*], and carpet python [*M. spilota*]); *Boidae* species (boa constrictor [*Boa constrictor*]); *Colubridae* species (Pope's keelback [*Hebius popei*], red-banded snake [*Lycodon rufozonatus*], and Mandarin rat snake [*Euprepiophis mandarinus*]); and *Homalopsidae* species (Chinese water snake [*Myrrophis chinensis*]) [9,56,111,112,132,133,208].

Despite a growing list of susceptible snake hosts to serpentovirus infection, there is limited information regarding the biological relevance of serpentoviruses in non-python species. Those studies following outbreaks of natural infection have been limited to python species and have primarily focused on postmortem evaluation of snakes following mortality events [9,111,112,133]. Pythons also remain the only group of snakes in which serpentovirus-associated respiratory disease has been described or confirmed [9,111,112,208]. Only two studies have assessed serpentovirus infection in antemortem samples (oral/esophageal swabs, blood, cloacal swabs, and tracheobronchial lavages) [132,208]. One antemortem study was the first to test snakes within the *Boidae* family, identifying boa constrictors as an additional susceptible species to infection. In this case, disease status was not evaluated for infected snakes; therefore, the association of infection and disease could not be assessed [132]. In another study, metagenomics was used to identify RNA viruses in vertebrates [185]. Several novel serpento-like viruses (currently unclassified) were detected in colubrid and homalopsid snakes [56]. This marked the first identification of

these viruses in colubrid and homoalopsid species, but no information beyond the host species was provided, limiting interpretation of the significance of these viruses. Additionally, no published study has tested snakes in the families *Viperidae* or *Elapidae*, two large families that include a majority of the venomous snakes. Therefore, despite mounting evidence that serpentoviruses are common and potentially significant pathogens of snakes, the extent of species susceptibility to infection and correlation with disease remains poorly understood.

The purpose of this study was to evaluate the epidemiology of serpentovirus infection in captive snakes. Mixed captive snake collections with both known and unknown serpentovirus infection status were targeted. The collections included snakes from the major snake families: *Pythonidae*, *Boidae*, *Colubridae*, *Lamprophiidae*, *Viperidae*, and *Elapidae*. Data from individual snakes within each collection was collected to assess correlations between species, age, sex, and clinical signs with serpentovirus status. Furthermore, sequencing data was generated to investigate serpentovirus genetic diversity and whether strains clustered by collection, species, and disease state. Longitudinal sampling was performed to determine persistence and progression of infection within a collection and evaluate the potential for viral clearance and vertical transmission.

4.2: Materials and Methods

4.2.1: Snake collections/populations

Eleven collections (A-K) were tested, either in entirety (all the snakes were tested) or partially (a subset of snakes). A twelfth, catch-all group (L) included snakes from a variety of collections that were individually submitted by veterinarians or owners. One collection was sampled longitudinally (collection A) while the remaining collections were sampled once. Species, age, sex, clinical signs, and a respiratory score (see below) were recorded for each snake, when available. Snakes were recorded as either the species or subspecies depending on availability. If known, exact ages were recorded; in cases where only the age category was noted a standard age was provided (hatchling 0.1 year, juvenile 0.5 year, and adults were not

estimated). If an age or age category was not provided, these snakes were not included in analyses where age was a variable. Sex was recorded as male, female, or unknown. Following evaluation of snakes and discussion with owners, veterinarians or veterinary technicians provided a respiratory score based on a specific rubric: 0 – no respiratory signs; 1 – mild respiratory signs (e.g. increased mucus in the oral cavity and/or reddening of the oral mucosa but otherwise acting normal); 2 – moderate respiratory signs (e.g. wheezing, coughing); and 3 – severe respiratory signs (e.g. open-mouthed breathing, respiratory distress). Summary data for each collection can be found in Supplemental Table 4.1.

4.2.2: Longitudinal sampling

Collection A was tested longitudinally following an outbreak of serpentovirus-associated respiratory disease. The first pythons in this collection were tested by our laboratory in 2015 by PCR and metagenomic sequencing (see below), at which point serpentovirus was determined to be established in the collection, but an overt outbreak had not occurred. In December 2015, a group of green tree pythons were purchased from another state. The snakes were acquired from the seller in July 2016, by which time approximately 9 of the purchased snakes had died of undiagnosed disease. Upon acquisition, the remaining snakes were quarantined in a separate room of the house where the main collection resided and 2 weeks into the quarantine snakes began to show signs of respiratory disease; snakes began to die at 3 weeks into quarantine. Shortly after, pythons in the original collection also exhibited signs of respiratory disease. At this point, all pythons in the collection were sampled and any snakes found to be serpentovirus-positive, or had significant risk of exposure to serpentovirus were, separated from the main collection and placed in a separate building where quarantine and sterility measures were undertaken. These included separate tools and supplies that remained in quarantine, cleaning tools and surfaces with a quaternary ammonium compound, outer clothing and footwear specific for the quarantine area, only one designated caretaker for infected snakes, showering directly after exiting the quarantine area, and air filters placed on all vents leading out of the quarantine building. All pythons within the collection had continued testing over the course of 28 months at approximately 4-month intervals. In contrast to the sampling of the python species

within the collection, only a subset of venomous snakes (12 elapids and 13 vipers) were tested; these snakes were only tested once.

During the 28 months, a serpentovirus-positive male and female green tree python were bred in the quarantine area, resulting in a clutch of eggs. The eggs were removed from the parents and artificially incubated in the main collection area. Egg surfaces were cleaned by exposure to UV light (Zoo Med brand 5.0 light). Following hatching, eggs were frozen and egg shells/remaining contents were submitted for sampling, along with choanal swabs from the hatchlings. Hatchlings were sampled at approximately 4-month intervals for 20 months.

Similarly, a serpentovirus-positive male and female jungle carpet python (*Morelia spilota cheynei*) were bred, resulting in a clutch of eggs. The eggs were removed from the parents and artificially incubated in the quarantine area. Egg surfaces were briefly cleaned with a quaternary ammonium compound. Upon hatching, offspring were removed from quarantine and placed in a separate room away from both serpentovirus-positive snakes and the main collection. Eggs were tested following hatching and offspring were tested twice during a 6-month interval.

4.2.3: Postmortem Examination

A necropsy was performed on a subset of snakes from collection A, H, and L that died during the study. Fresh frozen and formalin-fixed tissues were collected. Formalin-fixed tissues were processed routinely and histopathology was performed on an a select few of these cases, as previously described [199].

4.2.4: Snake sampling

Swabs: All antemortem samples were collected by a veterinarian or certified veterinary technician. Swabs from the choana or oral cavity were collected from each individual snake using cotton- or rayon-tipped swabs (Figure 4.1). Dry swabs were then placed in either a 1.5 ml Eppendorf tube or 2 ml screw-cap conical tube and frozen at -20°C for 1-14 days. Samples were then shipped overnight on ice to the Stenglein

laboratory. At the time of arrival, swabs were suspended in 1 ml of brain heart infusion (BHI) broth (Becton Dickinson) and vortexed prior to storage at -80°C.

Tissues: Samples from post mortem analysis of collection A, H, and L (see above) were submitted as fresh-frozen tissues (-20°C or -80°C). Lung, trachea, and esophagus were pooled or submitted as individual samples. Additionally, to assess vertical transmission in Collection A, eggs collected post-hatching were submitted frozen (-20°C). Tissue/egg samples were stored at -80°C upon arrival to the Stenglein laboratory.



Figure 4.1. Oral (top) and choanal (bottom) swabbing of captive snakes. Usambara bush viper (*Atheris ceratophora*), top panel. Green tree python (*Morelia viridis*), bottom panel. Photos courtesy of Greg Lepara.

4.2.5: RNA extraction

Swabs: Viral RNA was extracted from swabs in BHI using Zymo Research viral RNA kit with either individual columns or in a 96-well plate. Approximately 200 µl of BHI was processed according to

the manufacturer's instructions. RNA was eluted in 30 μ l of RNase/DNase-free water. Extracted RNA was stored at -80°C .

Tissues: Total RNA was extracted from tissues and pooled eggs (shell and remaining contents; 4 eggs per pool) using a combination of TRIzol (Ambion Life Technologies) with RNA clean and concentrator columns (CC-5; Zymo Research) as previously described [199]. Extracted RNA was stored at -80°C .

4.2.6: Viral RNA detection

RNA extracted from snake samples was tested for serpentovirus RNA multiple times by independent methods. First, a hemi-nested polymerase chain reaction (PCR) was performed. Round 1, a reverse transcription quantitative PCR (RT-qPCR), was performed using Luna Universal One-Step RT-qPCR kit (New England BioLabs). Twelve μ l reactions included a final concentration of 1x Luna Universal One-Step Reaction Mix, 1x Luna WarmStart RT Enzyme Mix, and 0.3 μM of each degenerate serpentovirus primer (BarniPVTF and BarniGGTR; Table 4.1) mixed with 4 μ l of RNA template. Reaction mixtures were run in a Roche LightCycler 480 II with the following cycle parameters: 55°C for 10 minutes; 95°C for 1 minute; 95°C for 10 seconds and 60°C for 30 seconds with 45 cycles; and a melting curve (95°C for 5 seconds; 65°C for 1 minute; ramp to 97°C with a rate of $0.11^{\circ}\text{C}/\text{second}$; and 40°C for 30 seconds). A no-template water control and positive RNA control from previous experiments with serpentovirus positive snakes [199] were included with each plate. Round 2, a qPCR, was performed using Luna Universal qPCR Master Mix. Twelve microliter reactions included a final concentration of 1x Luna Universal Master Mix and 0.3 μM of each degenerate serpentovirus primer (BarniPVTF and BarniDYTR; Table 4.1) mixed with 5 μ l of PCR product from round 1 diluted 1:10 in water. Reaction mixtures were run with the following cycle parameters: 95°C for 1 minute; 95°C for 15 seconds and 60°C for 30 seconds with 45 cycles; and a melting curve. Both round 1 and round 2 PCR products were run on a 1.5% agarose gel with ethidium bromide for confirmation of amplification and assessment of amplicon size.

RNA from all positive samples from the first hemi-nested PCR was re-tested by a second PCR protocol to confirm results. Reverse transcription from RNA to complementary DNA (cDNA) was performed using random priming as previously described [199]. The hemi-nested PCR described above was then repeated using the same primers (round 1: Barni PVTF and BarniGGTR; round 2: BarniPVTF and BarniDYTR) but utilizing the Luna Universal qPCR Master Mix reaction parameters and cycle conditions for both rounds.

A subset of samples with inconclusive PCR results were selected for an additional PCR using the internal primer set (BarniPVTF and BarniDYTR) in a non-nested reaction; this primer set was found to provide increased sensitivity for more divergent serpentoviruses when used independently of the outer primer set. PCR was performed as described above, beginning with diluted cDNA as template. Cycle parameters were altered as follows: 95°C for 1 minute; 95°C for 15 seconds, 46°C for 20 seconds, and 60°C for 20 seconds with 45 cycles; and a melting curve.

To confirm previous positive results were not the outcome of PCR contamination during round 1 or round 2 of the hemi-nested reactions and to achieve a longer amplicon sequence for phylogenetic analysis, new primers were designed that flanked the previous hemi-nested set using partial or full-length ophidian serpentovirus sequences available in our laboratory from python hosts (MDS-1529 and MDS-1530; Table 4.1). Positive samples were tested as previously described using the new primers and beginning with random-primed cDNA as template. Cycle parameters were as follows: 95°C for 1 minute; 95°C for 15 seconds and 60°C for 30 seconds with 45 cycles; and a melting curve.

4.2.7: Sanger sequencing

Samples that were positive by qPCR and demonstrated the correct amplicon size by gel electrophoresis were Sanger sequenced. Samples were submitted to GENEWIZ (San Diego, California) as premixed samples with the appropriate forward primer (BarniPVTF or MDS-1529); sequencing reactions with the reverse primer were not performed.

Table 4.1. Primer sets targeting serpentoviruses. F, forward. R, reverse. RdRp, RNA-dependent RNA polymerase. ORF1b, open reading frame 1b. Bp, basepairs.

Primer	F/R	Sequence (5'-3')	Target	Pair	Amplicon (bp)
BarniPVTF (MDS-1222)	F	GAGCACTCCACAARCCAGTCAC	RdRp	BarniGGTR	353
				BarniDYTR	185
BarniGGTR (MDS-1224)	R	KGCATCRCCRCTACTTGTGCCTCC	-	-	-
BarniDYTR (MDS-1223)	R	RCTRCGGTTCGCATTTTCGTRTARTC	-	-	-
MDS-1529	F	GCAGCACCAGACAACCTTCAT	ORF1b/ RdRp	MDS-1530	536
				BarniDYTR	385
MDS-1530	R	TTGTACAGWGTGTTGGCGAA	-	-	-

4.2.8: Metagenomic sequencing

A subset of samples with inconclusive PCR results were targeted for shotgun metagenomic sequencing (Supplemental Table 4.2). RNA libraries were generated using the Kapa RNA HyperPrep Kit (Kapa Biosystems) according to the manufacturer's instructions with an input concentration of approximately 100 ng of RNA and 8 rounds of amplification. Kapa Dual-Indexed Adapter Kit Illumina Platform (Kapa Biosystems) was used for adapter ligation and barcoding. Equivalent masses of DNA from each sample were pooled and libraries were size selected (200-600 bp, including Illumina adapters) by gel electrophoresis on a 2% agarose gel. Gel extraction was performed using the Zymo Gel DNA Recovery Kit (Zymo Research) according the manufacturer's instructions. Library quantification was performed with the Kapa Biosystems Illumina library quantification kit according the manufacturer's instructions. Dual indexed, single-end 1 x 75 or 1 x 150 sequencing was performed on an Illumina NextSeq 500 instrument with a NextSeq 500/550 High Output Kit v2 (75 cycles) or Mid Output v2 (150 cycles), respectively. Sequencing analysis was performed as previously described [199].

4.2.9: Data analysis

Statistical analyses: Overall prevalence was assessed within each snake family (*Pythonidae*, *Boidae*, *Colubridae*, *Lamprophiidae*, *Elapidae*, *Viperidae*). Age was compared to infection status (positive or negative) by an unpaired t-test. Sex (male, female, or unknown) was compared to infection status by a chi-squared test. Age and sex were also independently compared to the respiratory score (0, 1, 2, 3) by a Kruskal-Wallis test.

Phylogenetic analyses: Sequences generated by either Sanger sequencing or metagenomic sequencing were utilized for phylogenetic analysis. Sequences spanning a 467 bp region of ORF1b, including the RNA-dependent RNA polymerase, were aligned using MAFFT software with default parameters (E-INS-i algorithm, 200PAM / k=2 scoring matrix, gap open penalty of 3, and offset value of 0) in Geneious 11.0.4 [209,210]. A phylogenetic tree was generated using PhyML in Geneious with Hasegawa-Kishino-Yano (HKY, nst=2) substitution model, with 1000 bootstrap replicates, an estimated transition/transversion rate, a fixed proportion of invariable sites (0), 4 substitution rate categories, and a fixed gamma distribution parameter (1) [211,212].

4.3: Results

4.3.1: Prevalence

Serpentovirus infection was detected in all snake collections except collection J, and prevalence within each serpentovirus-positive collection ranged from 5-100% (Supplemental Table 4.1). In total, 165 snakes out of 639 were found to be positive for serpentovirus (26%). Prevalence among pythons was markedly higher (38%) compared to boas (10%), colubrids (less than 1%), and lamprophiids, elapids, or vipers (all 0%) (Figure 4.2). Prevalence in individual species ranged from 0-100% (Table 4.2).

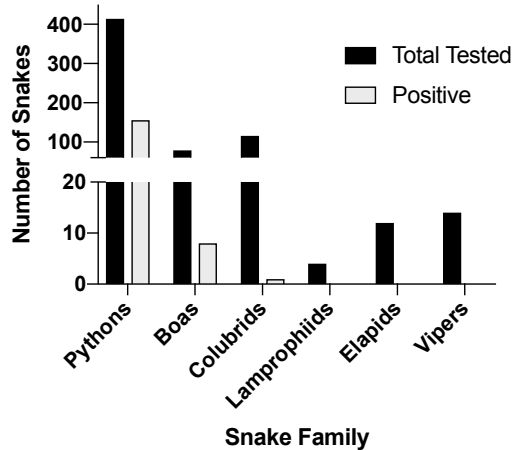


Figure 4.2. Captive pythons in some collections have a high prevalence of serpentovirus infection. Prevalence of serpentovirus in snakes of each family: Pythons 37.7% (156/414), Boas 10.1% (8/79), Colubrids 0.9% (1/116), Lamprophiids 0% (0/4), Elapids 0% (0/12), Vipers 0% (0/14).

In collections A and H, physical separation of infected snakes from the rest of the collection resulted in high prevalence of infection in quarantined snakes and low prevalence in the main collection. In collection A, quarantined snakes were kept in a separate building. The prevalence of serpentovirus in quarantined snakes (A1-9 and 13-36) was 94% (31/33) and prevalence within the primary collection remained near 0%: only 1 green-tree python became positive, see “Long-Term Sequential Sampling”. In collection H, snakes exhibiting respiratory signs (suspected infection) or snakes that were in contact with diseased animals were quarantined in a separate building. Prevalence in quarantined snakes (H118-154) was 68.4% (26/38) and prevalence in the main collection (H1-117) was 4.3% (5/117). The quarantine practices for all other collections were unknown or quarantine of infected snakes did not occur.

Table 4.2. Prevalence of serpentovirus by snake species, family, and total.

Pythons (<i>Pythonidae</i> family)				
Common Name		Total # Tested	# Positive	Positive (%)
Children's python	<i>Antaresia childreni</i>	1	0	0%
Spotted python	<i>Antaresia maculosa</i>	3	0	0%
Anthill python	<i>Antaresia perthensis</i>	2	1	50%
Stimson's python	<i>Antaresia stimsoni</i>	1	1	100%
Black-Headed python	<i>Aspidites melanocephalus</i>	2	0	0%
Woma python	<i>Aspidites ramsayi</i>	3	1	33%
Bismarck ring python	<i>Bothrochilus boa</i>	2	0	0%
Savu python	<i>Liasis mackloti</i>	4	0	0%
Olive python	<i>Liasis olivaceus</i>	3	0	0%
Reticulated python	<i>Malayopython reticulatus</i>	14	6	43%
Rough scaled python	<i>Morelia carinata</i>	2	2	100%
Carpet python	<i>Morelia spilota</i>	13	8	62%
Jungle carpet python	<i>Morelia spilota cheynei</i>	8	6	75%
Inland carpet python	<i>Morelia spilota metcalfei</i>	2	2	100%
Diamond python	<i>Morelia spilota spilota</i>	4	4	100%
Green tree python	<i>Morelia viridis</i>	120	91	76%
Angolan python	<i>Python anchietae</i>	6	1	17%
Burmese python	<i>Python bivittatus</i>	2	0	0%
Borneo python	<i>Python breitensteini</i>	20	2	10%
Blood python	<i>Python brongersmai</i>	45	16	36%
Sumatran python	<i>Python curtus</i>	20	7	35%
Indian rock python	<i>Python molurus</i>	1	1	100%
Ball python	<i>Python regius</i>	136	7	5%
TOTALS		414	156	37.7%

Boids (<i>Boidae</i> family)				
Common Name	Scientific Name	Total # Tested	# Positive	Positive (%)
Dumeril's boa	<i>Acrantophis dumerili</i>	2	1	50%
Boa constrictor	<i>Boa constrictor</i>	16	0	0%
Puerto Rican boa	<i>Chilabothrus inornatus</i>	1	1	100%
Emerald tree boa	<i>Corallus caninus</i>	29	5	17%
Amazon tree boa	<i>Corallus hortulanus</i>	2	1	50%
Brazilian rainbow boa	<i>Epicrates cenchria</i>	5	0	0%
Kenyan sand boa	<i>Gongylophis colubrinus</i>	11	0	0%
West African sand boa	<i>Gongylophis muelleri</i>	10	0	0%
Rosy boa	<i>Lichanura trivirgata</i>	3	0	0%
TOTALS		79	8	10.1%

Colubrids (<i>Colubridae</i> family)				
Common Name	Scientific Name	Total # Tested	# Positive	Positive (%)
Western hognose	<i>Heterodon nasicus</i>	7	0	0%
CA kingsnake	<i>Lampropeltis getula californiae</i>	16	0	0%
Nuevo Leon kingsnake	<i>Lampropeltis mexicana thayeri</i>	17	0	0%

AZ mountain kingsnake	<i>Lampropeltis pyromelana</i>	9	0	0%
Milksnake	<i>Lampropeltis triangulum</i>	1	0	0%
LA milksnake	<i>Lampropeltis t. amaura</i>	2	0	0%
Pueblan milksnake	<i>Lampropeltis t. campbelli</i>	3	0	0%
Honduran milksnake	<i>Lampropeltis t. hondurensis</i>	4	1	25%
Nelson's milksnake	<i>Lampropeltis t. nelsoni</i>	1	0	0%
Sinaloan milksnake	<i>Lampropeltis t. sinaloae</i>	6	0	0%
Baja CA mountain kingsnake	<i>Lampropeltis zonata algama</i>	3	0	0%
Tricolor hognose	<i>Lystrophis pulcher</i>	7	0	0%
Cornsnake	<i>Pantherophis guttatus</i>	34	0	0%
Bullsnake	<i>Pituophis catenifer sayi</i>	2	0	0%
Cape gopher snake	<i>Pituophis vertebralis</i>	4	0	0%
TOTALS		116	1	0.9%

Lamprophiids (<i>Lamprophiidae</i> family)				
Common Name	Scientific Name	Total # Tested	# Positive	Positive (%)
African house snake	<i>Boaedon filiginosus</i>	4	0	0%
TOTALS		4	0	0%

Elapids (<i>Elapidae</i> family)				
Common Name	Scientific Name	Total # Tested	# Positive	Positive (%)
Death adder	<i>Acanthophis rogosus</i>	1	0	0%
Angolan coral cobra	<i>Aspidelaps lubricus cowlesi</i>	1	0	0%
Shield-nosed cobra	<i>Aspidelaps scutatus</i>	1	0	0%
Blackbacked Jameson's mamba	<i>Dendroaspis jamesoni jamesoni</i>	3	0	0%
Black mamba	<i>Dendroaspis polylepis</i>	1	0	0%
Western green mamba	<i>Dendroaspis viridis</i>	3	0	0%
Eastern green mamba	<i>Dendroaspis angusticeps</i>	1	0	0%
Rinkhal's spitting cobra	<i>Hemachatus haemachatus</i>	1	0	0%
TOTALS		12	0	0%

Vipers (<i>Viperidae</i> family)				
Common Name	Scientific Name	Total # Tested	# Positive	Positive (%)
Usambara eyelash bush viper	<i>Atheris ceratophora</i>	3	0	0%
Mexican nomad viper	<i>Atropoides nummifer</i>	1	0	0%
Speckled forest pit viper	<i>Bothriopsis taeniata</i>	4	0	0%
Brazilian lance-head pit viper	<i>Bothrops moojeni</i>	2	0	0%
Sumatran pit viper	<i>Trimeresurus sumatranus</i>	1	0	0%
Sri Lankan palm pit viper	<i>Trimeresurus trigonocephalus</i>	3	0	0%
TOTALS		14	0	0

TOTALS		639	165	25.8%
---------------	--	------------	------------	--------------

4.3.2: Morbidity and Mortality

Clinical signs noted at the time of sampling included increased oral reddening and increased oral and nasal mucus (respiratory score 1; Figure 4.3), wheezing and/or audible breathing (respiratory score 2), open-mouthed breathing or difficulty breathing (respiratory score 3), and other non-specific signs such as anorexia, inappropriate shedding, difficulty perching (in arboreal snakes), and spectaculitis (inflammation of the spectacle of the eye). Respiratory scores were compared between snakes in each genus with at least one positive result (Figure 4.4). Scores ranged from 0 (absent disease) to 3 (severe disease) within snakes of the *Pythonidae* family, including within each genus. In contrast, only 1 out of 8 snakes within the *Boidae* family had a non-zero respiratory score. Only one snake from the *Colubridae* family was found to be positive and had a respiratory score of 0. Statistical comparisons were not performed due to the low number of snakes available in each genus other than *Morelia* and *Python*. Low numbers of snakes that were serpentovirus-negative also exhibited signs of respiratory disease (Supplemental Table 4.1).



Figure 4.3. Excessive oral and nasal mucus production in a serpentovirus-positive snake. Blood python; Collection H.

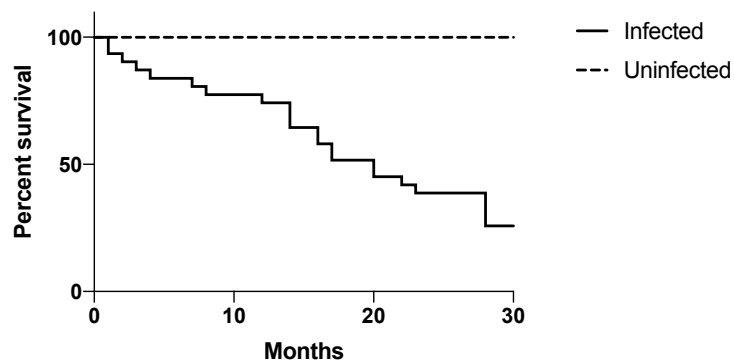


Figure 4.5. Infected snakes are statistically more likely to experience mortality than uninfected snakes. Longitudinal assessment of mortality between infected and uninfected snakes in collection A. Time is represented in months and begins at the onset of a serpentovirus outbreak (September 2016). Kaplan-Meier survival curve; p-value = <0.01.

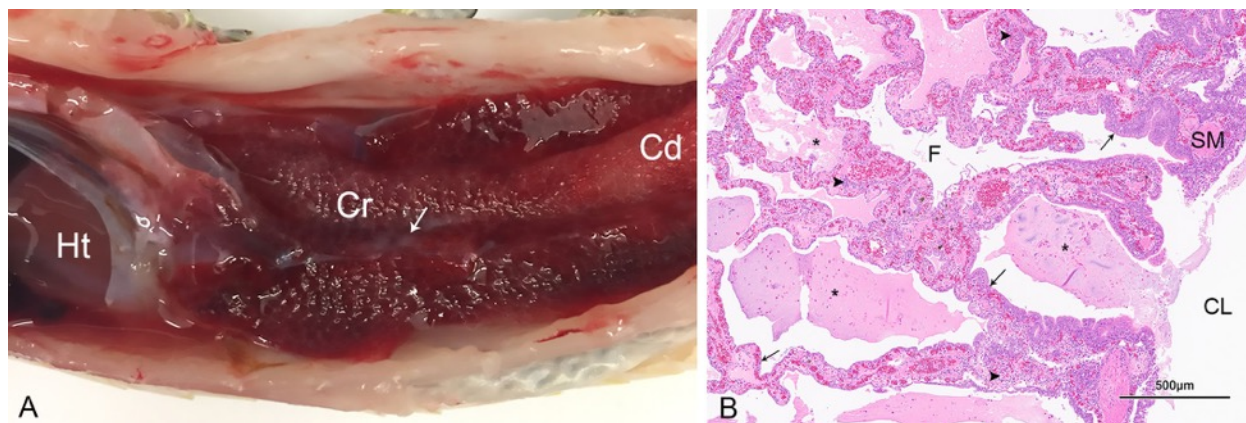


Figure 4.6. Gross and histologic pulmonary lesions in a serpentovirus-positive green tree python from collection A (snake A26). A) The lungs are markedly thickened and dark red, especially in the cranial (Cr) lung compared to the caudal (Cd) lung. There are small mucoid aggregates within the central lumen (arrow). The heart (Ht) is indicated for orientation. B) Histopathology of the lung revealing proliferative and interstitial mucinous pneumonia characterized by excessive mucus, edema, and necrotic debris (asterisks) within the central lumen (CL) and faveoli (F), marked epithelial hypertrophy and hyperplasia lining faveoli (arrows), and mixed chronic-active inflammation within thickened faveolar septa (arrowheads). These lesions are consistent with serpentovirus infection. SM, smooth muscle. Hematoxylin and Eosin. 40x magnification.

4.3.3: Age and Sex

Infection status was compared to age (range of 0.1 – 22 years) and sex (male, female, and unknown). A statistically significant higher mean age of positive snakes was found compared to negative snakes (P-value<0.001; Figure 4.7A). No difference was observed between the percentage of infected snakes by sex (P-value=0.42; Figure 4.7B). Neither age (Figure 4.7C) nor sex (Figure 4.7D) were statistically associated with respiratory score.

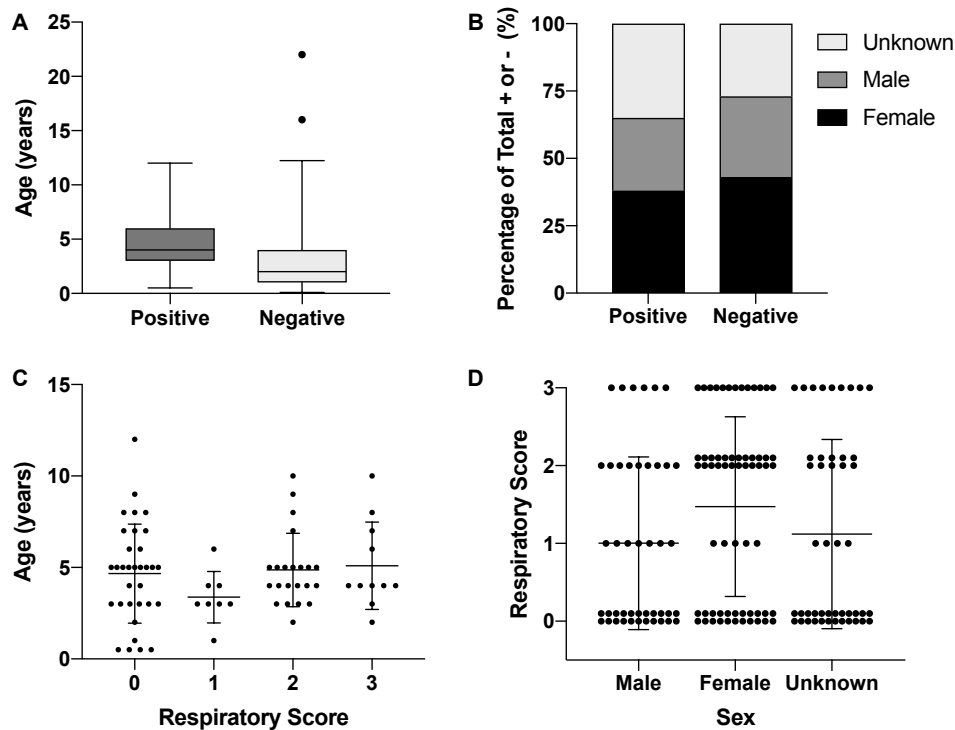


Figure 4.7. Serpentovirus infection is statistically associated with age but not with sex; Clinical signs are not statistically associated with age or sex. A) Comparison of ages between serpentovirus-positive and negative snakes. Average ages: 4.7 (positive) and 2.6 (negative). Unpaired t test; p-value = <0.01. Box and whisker plot 1-99 percentile. B) Comparison of the percentage of male, female, and snakes of unknown sex that are serpentovirus positive or negative. Chi-squared test; p-value = 0.42. C) Comparison of respiratory score to age in serpentovirus-positive snakes. Kruskal-Wallis test (one-way ANOVA on ranks, non-parametric); p-value = 0.32. Scatter dot plot mean with standard deviation. D) Comparison of respiratory score with sex in serpentovirus-positive snakes. Kruskal-Wallis test (one-way ANOVA on ranks, non-parametric); p-value = 0.13. Scatter dot plot mean with standard deviation.

4.3.4: Phylogenetic Analysis

Serpentovirus sequences were generated by metagenomic or Sanger sequencing. In 8 of 39 snakes, PCR results were negative or inconclusive but serpentovirus sequences were detectable by metagenomics (Supplemental Table 4.2). All instances occurred in boas (genera *Acrantophis*, *Corallus*, and *Chilabothrus* species) and a colubrid (genus *Lampropeltis*).

Viral sequences were phylogenetically analyzed to assess overall genetic diversity, to reconstruct possible transmission events, and to test for associations between viral genotypes and host species or disease (Figure 4.8).

Two serpentovirus groups were evident. One definitive clade, which accounted for most of the sequences generated in this study, contained sequences recovered from python species in the genera *Morelia*, *Python*, *Aspidites*, and *Antaresia* (**Figure 8**). This clade included the serpentoviruses previously associated with respiratory disease in pythons, such as ball python nidovirus (1–3,8,12). The sequences in this python-only clade shared >80% pairwise nucleotide identity in the aligned ORF1B region.

The other group contained sequences from boas (genera *Corallus* and *Chilabothrus*), a colubrid (genus *Lampropeltis*), and reticulated pythons (genus *Malayopython*) in addition to sequences that were identified by metagenomic surveys of colubrid and homalopsid snakes in China (9). This second group was less well supported phylogenetically and contained more overall genetic diversity than the python-only clade, with sequences sharing $\geq 57\%$ pairwise nucleotide identity. These sequences were identified using metagenomic sequencing of samples from snakes for which PCR results had been negative or inconclusive (**Supplemental Table S2**).

Although the virus phylogeny did not form well-supported monophyletic clades by host, viruses with more similar sequences were generally found in snakes of the same species or genus. Exceptions to this included closely related viruses that infected pythons of multiple genera in the same collection. For example, virtually identical viruses ($\geq 99.8\%$ pairwise identity in the region used to make the tree) were recovered from three snakes of different genera from collection G: G47 (*Morelia viridis*), G58 (*Antaresia perthensis*), and G59 (*Python regius*). Similar examples included the viruses from snakes G42, G50, and G61, and those from L14 and L23. Genetically distinct serpentovirus sequences were recovered from all positive collections, except collection I.

We also investigated the possibility that some viral genotypes were more pathogenic than others. In the python-only clade, respiratory score ranged from 0 to 3 and an overt association between viral genotype and clinical disease was not evident. In contrast, respiratory scores were 0 for all boas, colubrids, and reticulated pythons outside the python-only clade. The only boa in this study that was documented to have clinical disease (L22, Dumeril's boa; respiratory score of 2) was not included in this phylogeny due to sequence length limitations (155 bp available compared to 467 bp for sequences in the phylogeny). Alignment of the short Dumeril's boa sequence revealed it to be slightly more related to the viruses in the python-only clade, with which it shared $\sim 70\text{-}77\%$ nucleotide identity, in contrast to 49-62% identity to viruses derived from boas, colubrids, and reticulated pythons.

Partial or complete genome sequences derived from metagenomic sequencing were globally aligned to ball python nidovirus (BPNV; NC_024790.1) and percent nucleotide identity was assessed (**Supplemental Table S2**). Python serpentoviruses (A93-95, F17, H0-1, -2, L1, 3, 4, 8, 14) ranged from 62-94% nucleotide identity; boa serpentoviruses (C18-19) ranged from 31-43% nucleotide identity; the colubrid serpentovirus (L25) exhibited 30% nucleotide identity; the reticulated python serpentovirus (K48) exhibited 31% nucleotide identity. These new serpentovirus genomes had similar overall genome structures to that of BPNV at the 5' end: two large overlapping open reading frames, ORF1A and ORF1B, separated by a ribosomal frameshift signal (AAAAAC) that together encode a large polyprotein of non-structural proteins. These large ORFs were immediately followed by a spike protein gene (ORF2). The 3' end of the

genomes of the viruses in the python-only clade were similarly organized to BPNV with five predicted ORFs encoding: a transmembrane protein, matrix protein, nucleoprotein, and 2 additional predicted transmembrane proteins. The other serpentoviruses outside the python-only clade for which we obtained near-complete genomes had more variable 3' end gene content, but all had predicted matrix and nucleoprotein genes flanked by variable numbers of genes encoding proteins with predicted transmembrane domains.

4.3.5: Co-Infection

We detected serpentovirus co-infection in a blood python from collection H (snake H0). One complete coding genome (H0-1) and one nearly complete coding genome (H0-2) were generated from sequencing reads (Supplemental Table 4.2). These sequences shared approximately 71% global nucleotide identity. When a short nucleotide sequence from each H0 serpentovirus was compared to other snakes in the collection (Figure 4.8), H0-1 shared >99% nucleotide identity to H121 and only 90% to H0-2 and H104, respectively; H0-2 shared >99% identity to H104. Possible coinfections were also detected in three other snakes (H136 and L21) in which low numbers of unique serpentovirus reads detected by metagenomic sequencing did not align to the primary assembled serpentovirus genome.

4.3.6: Long-term Sequential Sampling of Collection A

Forty pythons in collection A were sampled longitudinally at approximately 4-month intervals over 28 months following an outbreak of serpentovirus that began in 2016. The infection status and clinical progression of individual snakes (Figure 4.9), and horizontal transmission (Figure 4.10) were assessed. Three snakes that were part of the original collection (introduced in 2008) were diagnosed with serpentovirus in 2015 and died (A93-95). Snakes A1-9, 30-31, and 33-36 were introduced between 2013-2015 and their infection status was unknown prior to the 2016 outbreak. Snakes A10-29 and 32 were purchased and introduced to the collection in 2016, after which the outbreak of serpentovirus-associated respiratory disease occurred. Snakes A98 and A99 were also purchased from the same seller and had contact

with A10-29 and 32 but died prior to introduction into collection A. Positive snakes (tested at 0 and 4 months into the outbreak; A1-9 and 13-34) were quarantined away from remainder of collection. Snakes A37-40 were purchased after the outbreak (2017) and were never directly exposed to serpentovirus-positive snakes in the collection.

Overall, positive snakes remained positive during the 28-month period (Figure 4.9); no snakes were seen to transition from consistently positive to consistently negative. Snakes A11-12 (green tree pythons) were serpentovirus-negative at initial sampling were housed with the main collection and remained negative. Only one snake in the main collection converted to positive (A66); see “Vertical Transmission.” Two snakes (A35-36, olive pythons) that were initially negative, but potentially exposed to serpentovirus, were housed in the quarantine area; these snakes remained negative throughout the study. In a subset of quarantined snakes (A13-18), intermittent negative results were obtained despite overall positivity. These negative results primarily occurred in snakes exhibiting lower respiratory scores (0-1). Sanger sequencing of PCR amplicons before and after time points with negative results yielded identical viral sequences.

Phylogenetic analysis of viral sequences from snakes in collection A was performed on 26 of 40 positive snakes; 5 viral genotype groups were detected, three of which were present in the 2016 outbreak (Figure 4.10). The first viral genotype group was found in one of the initial snakes diagnosed with serpentovirus (A95) and was also detected in other snakes from the original collection (A1-6, 8-9, 33) but not in any purchased snakes. The second and third viral genotypes were found in the purchased snakes that died before introduction into the collection (A98 and 99). These genotypes were also detected in the purchased snakes that were introduced (A21, 26, 27, 66) as well as snakes from the original collection (A7 and 34), consistent with transmission from the purchased snakes to the original collection. Longer viral sequences for phylogenetic analysis were not collected from all positive snakes in the collection; therefore, we cannot rule out the presence of other viral genotypes not represented in the phylogeny.

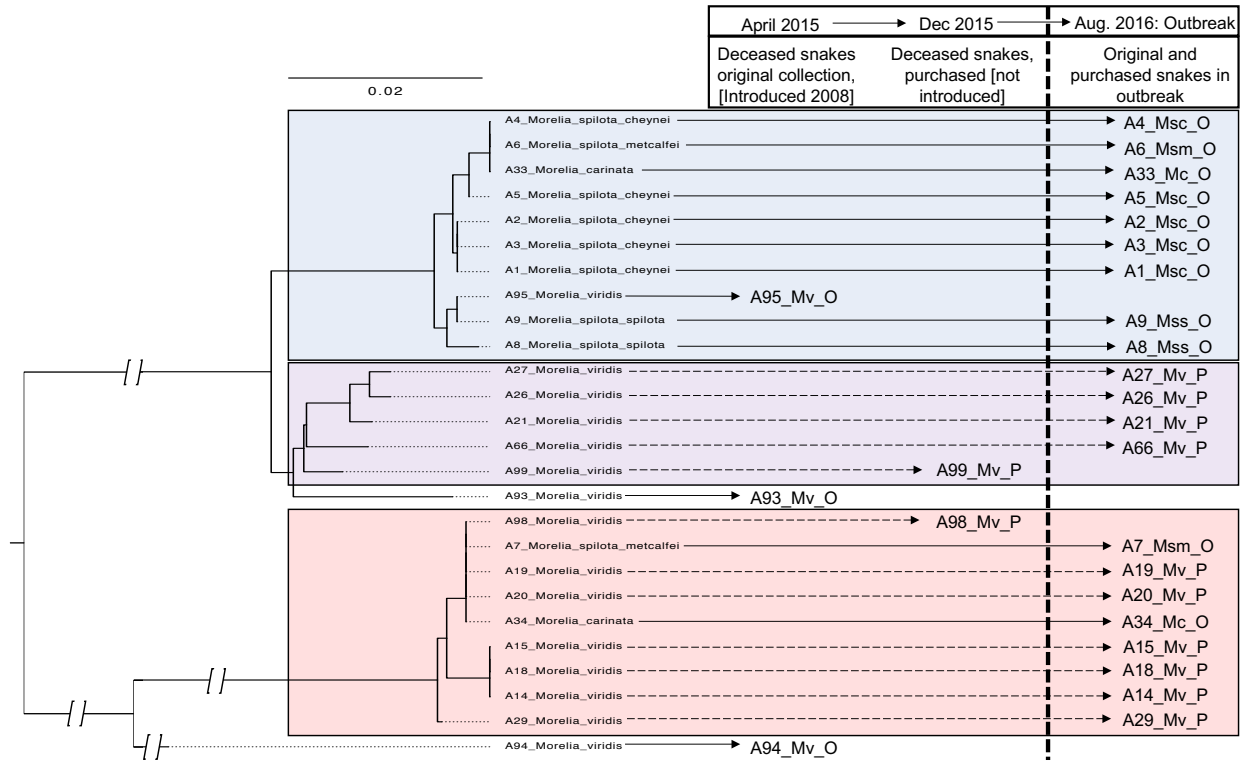


Figure 4.10. Phylogeny and proposed horizontal transmission in collection A. Nucleotide sequences (467 basepairs) aligned and analyzed with PhyML with HKY85 substitution model and 1000 bootstrap replicates; arbitrary rooting; discontinuous scale in branches closer to root indicated by branch breaks. Snake ID denoted by A and number; Mv, *Morelia viridis*; Msc, *Morelia spilota cheynei*; Msm, *Morelia spilota metcalfei*; Mc, *Morelia carinata*. O, original collection. P, purchased.

4.3.7: Vertical Transmission

During the longitudinal sampling of collection A, two separate serpentovirus-positive mating pairs (green tree pythons A27 and A29; jungle carpet pythons A1 and A3) were bred and resulted in a clutch of eggs. The green tree python mating pair resulted in 17 eggs and 16 viable hatchlings which were sampled orally at 4 month intervals for 20 months; 7 of these were only tested once due to death within the first 4 months. The egg shells and liquid contents (post hatching) were pooled (4 eggs per pool) and all were found to be serpentovirus RNA positive. All offspring were negative at each sampling time-point except one (A66) that became serpentovirus-positive between 8-12 months age. Sanger sequencing was performed on oral/choanal swabs from the adult male, female, and positive offspring, and the pooled egg shell/contents.

Viral sequences from the adult female and the egg shell/contents were >99% similar to each other but only 84% similar to the viral sequences detected in the adult male and offspring, which were >98% similar to each other. A second mating pair of jungle carpet pythons produced a clutch of 9 eggs and 2 viable offspring that were sampled twice during a 6-month period. Egg pools were again found to be positive but the offspring remained negative during the sampling period. It is suspected that the virus detected in/on eggs represented contamination from feces within the cloaca rather than infection of the embryo or egg contents and that low rates of viability were due to artificial incubation errors, but this cannot be confirmed.

4.4: Discussion

In this study we screened 639 snakes from 6 snake families, 28 genera, and 62 species for infection with ophidian serpentoviruses. Prevalence of infection was highest in pythons (nearly 40%) and we detected serpentovirus in pythons in the *Morelia*, *Python*, *Malayopython*, *Antaresia*, and *Aspidites* genera. This agrees with reports in the literature that many python species are susceptible to serpentovirus infection [9,111,112,132,133]. Most positive pythons in this study were *Morelia* species. For many years, the veterinary community has anecdotally regarded these pythons as being more predisposed to respiratory infection. It is possible that this anecdotal belief reflected an increased susceptibility and high prevalence of serpentovirus infection in captive *Morelia* species. It is important to note that 5 of the collections in our study were known to have serpentovirus infections, which biased our sample set and could have inappropriately increased prevalence measures. Nonetheless, these findings highlight the high rate of infection that can occur in collections in which serpentoviruses have been introduced (up to 100%).

In contrast to a high prevalence in pythons, serpentoviruses were detected at a significantly lower rate in snakes from the *Boidae* and *Colubridae* families and not detected in any snakes from the *Lamprophiidae*, *Elapidae*, or *Viperidae* families. These findings could indicate a reduced susceptibility or resistance to infection in these species. However, small sample sizes and targeted PCR assays may have impacted our results. Combined, only 30 lamprophiids, elapids, and vipers were tested and all were negative. Additionally, only 8 boas and 1 colubrid were found to be serpentovirus-positive out of 79 and

116, respectively. Only 5 ophidian serpentovirus sequences longer than 250 base pairs were available in the GenBank database at the initiation of this project, all of which had been detected in pythons. Therefore, our PCR assays were designed using python serpentoviruses. This may have resulted in a higher detection rate of more similar viruses and limited our detection of more divergent viruses. This is further supported by our metagenomic sequencing results that detected serpentoviruses in boas and a colubrid that were undetectable or variably detectable with PCR. Our findings signify a need for increased testing in non-python snakes, especially by unbiased methods such as metagenomic sequencing, for the generation of a more comprehensive database of ophidian serpentoviruses and development of sensitive pan-serpentovirus diagnostics. Overall, our conclusions regarding species susceptibility and species specificity in non-python snakes must be interpreted with caution.

What can be concluded from our results is that non-python snakes are likely less susceptible or resistant to infection by serpentoviruses that readily infect pythons. Phylogenetic analysis revealed that python serpentoviruses can infect multiple genera of pythons. In contrast, the viruses found in boas and colubrids (and reticulated pythons) belonged to a distinct evolutionary lineage from those found in pythons. Therefore, although python serpentoviruses appear to cross python genera, the species barrier may be too great for infection in boas or colubrids, and vice versa. Interestingly, evolutionarily distinct serpentoviruses found in reticulated pythons were more closely related to viruses from boas and colubrids and an evolutionarily distinct serpentovirus found in a Dumeril's boa was more closely related to viruses from pythons (non-reticulated). It is possible these viruses pose a greater risk for cross-species transmission and infection between different families of snakes. Clinical disease was consistently observed for all virus genotypes detected in the clade of python-associated serpentoviruses, whereas clinical disease was absent in snakes from the clade of boas/colubrids/reticulated pythons. This could be an indication of reduced susceptibility to disease in these species or reduced pathogenicity of these viruses. The virus detected in a Dumeril's boa was the only virus associated with clinical disease in a boa species. Its closer relation to python viruses may provide evidence that certain genotypic lineages are more likely to cause disease in

snakes, but this theory will likely be altered as a greater number of serpentoviruses in non-python species or divergent serpentoviruses are discovered.

The single serpentovirus found in a colubrid in the study (L25) was most closely related to other viruses found within colubrids as well as snake-associated nematodes. We propose that the serpentoviruses detected in nematodes [57] actually represent viruses from the snake host rather than true infection of the nematode (possibly virus particles or virus RNA in the snake gut ingested by the nematodes). This speculative interpretation warrants further investigation.

Previous studies evaluating the prevalence of viral infections or respiratory disease in pythons and boas found a greater prevalence in pythons, as well as correlations with older age and specific husbandry practices [132,213,214]. Similarly, our study found older snakes were more likely to be infected, but increasing age did not increase the likelihood of clinical disease. Therefore, infection in older animals is suspected to be due to increasing time of potential exposure, rather than physiologic changes that accompany age. Husbandry was not directly assessed in our study but it is a significant variable in the health of captive reptiles and suboptimal practices can result in stress and alterations in immunity [215,216]. If one can assume similar husbandry practices within a collection, it would be expected that snakes of the same species infected with the same or highly similar viruses would exhibit similar degrees of clinical disease. In some collections, this trend was observed (e.g. Collection H), whereas in others, clinical disease was more variable (e.g. Collection A). It is unknown if husbandry played a role in disease during this study.

Another study from Germany that evaluated the prevalence of viral diseases in boas from “healthy” collections found a correlation between imported snakes (not bred in Germany) and prevalence of paramyxovirus infection [213], another cause of respiratory disease in snakes [192]. It was speculated that imported snakes were more likely to have had multiple owners and/or more contacts with other snakes, increasing the potential for exposure to infectious agents. In our study, all collections in which acquisition practices were known were considered open collections (i.e. at least some snakes had been acquired from outside sources rather than breeding and maintaining snakes within the collection without outside introduction). This practice similarly brings with it a higher likelihood of pathogen introduction. Our

phylogenetic analysis found nearly all positive collections contained 2 or more different viral genotypes. This open collection practice is likely a contributing factor to multiple serpentovirus introductions into collections and coinfections within individual snakes.

Coinfections with different viral genotypes have been documented in natural infections with viruses related to serpentoviruses, such as toroviruses and coronaviruses, and have been associated with viral recombination and evolution [217,218]. This study marks the first documented incidence of coinfection with multiple serpentoviruses. The snake in which coinfection was detected died from severe respiratory disease, but it is unknown if coinfection altered the disease course or pathologic progression. Additional studies are warranted to determine the rate of coinfection with ophidian serpentoviruses, the host and viral factors that allow for coinfection, potential effects on disease course and prognosis, and the consequences in viral evolution. The short serpentovirus sequences we generated from most infected snakes had a low power to detect recombinant genotypes. Coinfections with other known and unknown non-serpentovirus snake pathogens may also have played roles in disease progression. These snakes reflected natural infection in captive pet populations in the USA. Other agents including paramyxoviruses, orthoreoviruses, sunshine virus, and *Mycoplasma* species have been associated with respiratory disease in snakes [108,109,205,214]. The ecological interactions of serpentoviruses with other pathogens and the host immune system merits further study.

One of the primary goals of this project was to assess aspects of disease that may lend themselves to better management strategies for disease prevention and spread. One significant finding was the lower rate of infection in the main collection when infected snakes were spatially separated. Collection A and H removed infected snakes (and snakes that had been in direct contact with infected snakes) from the main collection and placed them in separate quarantine buildings. In both cases, infection rates were high in quarantined snakes (68-100%) and remained low (less than 5%) in the main collection. These findings indicate that transmission occurs at a higher rate between snakes of close-proximity, for instance by fecal-oral or respiratory fomite transmission, and that spread can be minimized by quarantine and physical separation.

Phylogenetic analysis of a single collection (A) over time revealed that existing infected snakes and introduced infected snakes could both contribute to overall serpentovirus burden. Furthermore, longitudinal testing of this same collection revealed that serpentovirus infection is chronic and virus can be persistently detected in snakes over time. In this study, intermittent negative results in a low number of snakes were initially thought to represent viral clearance, but sampling of these snakes over time revealed continued evidence of infection. Negative PCR results could represent episodes of viral clearance followed by re-infection or periods of reduced shedding below the limit of detection. We did not observe a snake transition from consistently positive to consistently negative test results, indicating complete clearance may not be possible. Technical factors could also play a role in “false-negative” results, such as insufficient swabbing or sample handling. Independent of the underlying cause of intermittent negative results, these findings highlight the need to perform multiple tests over time to ensure true negativity in individual snakes, and to follow rigorous quarantine protocols when introducing new pythons into an established collection.

Vertical transmission is a natural route of spread for some nidoviruses (e.g. equine arteritis virus, gill-associated virus) [219,220]. In this study, we tested for vertical transmission by evaluating serpentovirus-positive mating pairs, eggs, and offspring. We found that in all but one case (1/19) offspring remained negative following hatching. In the one positive offspring, the viral genotype was more closely related to the male parent than the female parent. Therefore, our findings may support vertical transmission of serpentoviruses from the male, but at a significantly lower rate than horizontal transmission. Our findings do not rule out the possibility of horizontal transmission in this case and our small sample size is not sufficient to confirm vertical transmission, but our findings do warrant further investigation of possible transmission routes. Furthermore, in this study eggs were artificially incubated and sterilized with UV or a quaternary ammonium compound and hatchlings were housed separately from other infected snakes. The prevalence of infection in offspring hatched under natural conditions was not examined but could provide insight into the likelihood of horizontal transmission from parent to offspring.

Serpentoviruses are significant respiratory pathogens of pythons and introduction into collections can be devastating. Due to the chronicity and variability in clinical signs during infection with

serpentoviruses, stringent management strategies are recommended. These include prolonged quarantine practices with multiple negative test results prior to introduction into the collection, immediate removal or separation of any positive snakes from the main collection, and sterilization and separation of eggs from parents when breeding serpentovirus-positive snakes. The clinical importance of serpentovirus infection in boas and colubrids remains poorly understood, but infection is possible and should be perceived as a potential respiratory pathogen. Serpentovirus infection in other snake species continues to be an ongoing field of research.

CHAPTER 5: RESPIRATORY DISEASE IN VEILED CHAMELEONS (*CHAMAELEO CALYPTRATUS*) ASSOCIATED WITH SERPENTOVIRUS INFECTION

5.1: Introduction

Viruses are well-represented causes of respiratory disease in captive and wild reptiles [192]. Most recently, serpentoviruses have been established as important causes of respiratory disease in snakes, but their association with disease in other reptile species is limited to a few reports [131,134]. In 2016, a serpentovirus was discovered in wild shingleback lizards in Australia [131]. This was the first description of a serpentovirus in a non-snake species and some infected lizards showed clinical evidence of respiratory disease similar to that described in snakes. However, further evidence of disease causation was not explored. In this study, we describe two novel serpentoviruses associated with an outbreak of respiratory disease in veiled chameleons (*Chamaeleo calyptratus*), providing additional support for the hypothesis that serpentoviruses are significant respiratory pathogens of lizards.

5.2: Case History

In September 2017, eight captive-bred juvenile (1-2 months) veiled chameleons were purchased from a commercial breeding facility in the United States as part of a biological research project. Within 3-4 weeks of arriving in the research facility all animals began to exhibit respiratory signs: wheezing and vertical head tilting with gasping, increased mucus in the oral cavity, anorexia, and reduced water intake. All 8 chameleons died within 1-1.5 months of arrival. After the loss of chameleons, the enclosures and items in the enclosures were washed with soap and water prior to the introduction of new chameleons, but disinfectants were not used.

Between October 2017 and January 2018, seventeen additional captive-bred veiled chameleons (4 subadults [3-12 months] and 13 juveniles) were obtained from three different U.S. commercial breeders. Shortly after their introduction into the same enclosures as above, all but two juveniles exhibited similar signs of respiratory disease and died or were euthanized; the subadults did not show clinical signs during

this time. In February 2017, the two remaining juveniles from this group, one male with clinical signs of respiratory disease (VC1; 2 months old) and one clinically normal female (VC2; 2.5 months old), were evaluated by an exotic animal veterinarian. On presentation, VC1 weighed 6.3 grams, was quiet, alert and responsive, had an appropriate body condition score (BCS 4/9), was well hydrated, the mucous membranes were pink and moist, ophthalmic examination was unremarkable, and no abnormalities were found in the oral cavity, nares, on the integument, the musculoskeletal system, the cloaca, or on coelomic palpation. However increased respiratory effort (respiratory rate 3/min), wheezing and gasping for air was detected. VC2 weighed 4.6 grams, was bright, alert and responsive, in appropriate body condition (BCS 4/9) and no abnormalities were found on physical examination. Both animals were euthanized with 0.2mg pentobarbital sodium (FATAL-PLUS solution, Vortech Pharmaceuticals[®]) IV in the ventral coccygeal vein and submitted for necropsy (see Postmortem Evaluation below). No diagnostics or treatments had been performed prior to this.

At this time, an environmental problem was considered a possible cause. Too high humidity was initially suspected resulting in the addition of a dehumidifier in the housing area. Despite this modification, mortalities continued (3 subadults). Subsequently, the ceiling vents were completely closed to prevent to air exchange and the room temperature was increased to 80°F, which resulted in no further mortalities; 1 subadult chameleon remained alive at this time.

In October 2018, 5 additional veiled chameleons were obtained (2 wild caught in Florida and 3 captive). These chameleons were housed with the one remaining chameleon from the previous group, resulting in a total of 6 chameleons. Mild respiratory signs were noted in one chameleon, including slight crusting around the eyes bilaterally and mildly increased mucus within the oral cavity. Additional lizard species in the collection that were temporarily housed in the same room as chameleons (bearded dragons [*Pogono vitticeps*], n=6) or housed in the same facility in a separate room (common leopard geckos [*Eublepharis macularius*], n=3; ocelot geckos [*Paroedura pictus*] n=3) were clinically healthy.

Husbandry practices at the facility were as follows: chameleons were housed in a room with 30-50% humidity. The enclosures were 18" x 18" x 36" screen mesh enclosure with no substrate on the bottom.

Juveniles and small subadults were housed 2-3 per enclosure with large subadults and adults housed singly. The enclosures had a UVB bulb (Repti-Glo 5.0 Fluorescent Lamp, 40W, 48inches, Exo Terra[®]), and a heat lamp. The temperature in the enclosure was a minimum of 75° F with a maximum basking area of 90-100° F. The animals were sprayed with Reverse Osmosis water 2-4 times per day. The diet consisted of crickets dusted with calcium (Calcium powder, Rep-Cal[®]) 3-4 times per week, calcium with vitamin D3 (Calcium with Vitamin D3 powder, Rep-Cal[®]) twice a month, as well as dusted with vitamin and mineral powder (Herptivite Multivitamin, Rep-Cal[®]) two times a month. Occasionally, mealworms were offered.

5.3: Materials and Methods

5.3.1: Postmortem Evaluation and Diagnostics

In February 2017, VC1 and VC2 were submitted for necropsy and histopathology at a veterinary diagnostic laboratory (see case history). Fresh-frozen tissues were collected and stored at -80°C. Fresh-frozen lung from VC1 was submitted for reptile paramyxovirus PCR. VC1 and VC2 samples were submitted separately for bacterial and parasitic evaluation: liver tissue, lung swabs, and colon contents were submitted separately for aerobic culture; liver and lung samples were pooled for enriched culture of *Salmonella* species; feces was submitted for fecal flotation. Fresh-frozen lung, liver, and kidney from VC1 and VC2, along with an entire frozen carcass from a third chameleon (VC3) that had died in the same collection, were shipped overnight to the Stenglein laboratory on dry ice and ice packs for metagenomic sequencing. Individual animal information can be found in Table 5.1.

5.3.2: Antemortem Sampling

In December 2018, oral swabs were taken from remaining veiled chameleons (n=6; VC4-9) in the same collection. Oral swabs were also collected for the central bearded dragons (n=6, CBD1-CBD6) temporarily housed in the same room as chameleons, and from common leopard geckos (n=3, LG1-LG3) and ocelot geckos (n=3, OG1-OG3) housed separately in the same research facility. Oral swabs were

collected with sterile cotton-tipped swabs and placed directly in viral transport medium (modified phosphate-buffered sucrose with aminoglycosides) [221]. Swabs were placed directly on ice and then frozen at -80°C within 4 hours of collection. Samples were subsequently shipped overnight on dry ice and ice packs to the Stenglein laboratory for virological examination. Individual animal information can be found in Table 5.1.

5.3.3: Metagenomic Sequencing and Data Analysis

Methods can be referenced in section 4.2.8. Total RNA was extracted from fresh-frozen lung, liver, and kidney pools (VC1 and VC2) and oral mucosa, trachea, and lung pool (VC3). An RNA-sequencing library was prepared using the RNA Kapa HyperPrep kit, as previously described. The RNA-seq libraries were sequenced using a dual indexed, single end, 1x150 method on an Illumina NextSeq 500 instrument with a NextSeq 500/550 High Output Kit v2 (150 cycles). A second round of metagenomic sequencing was performed on the same samples using a library preparation method with enrichment of double-stranded RNA (University of Colorado, Boulder, Parker laboratory). This was run on the same platform using a dual indexed, paired end, 2x75 sequencing method. Data analysis was performed as previously described; host filtration was performed using the green anole genome (*Anolis carolinensis* AnoCar2.0).

Sequences generated by metagenomic sequencing were utilized for phylogenetic analysis. Nucleotide and protein sequences were aligned using MAFFT software with default parameters (E-INS-i algorithm, 200PAM / k=2 scoring matrix, gap open penalty of 3, and offset value of 0) in Geneious 11.0.4 [209,210]. Phylogenetic trees were generated using the protein alignments with PhyML (3.3.20180621) in Geneious: Le Gascuel (LG) substitution model with 1000 bootstrap replicates [211].

Table 5.1. Animals sampled for serpentovirus testing from a single collection. M, male. F, female. U, unknown. PM, postmortem. AM, antemortem. Lu, lung. Li, Liver. Kid, kidney. OM, oral mucosa. MGS, metagenomic sequencing. PCR, polymerase chain reaction.

ID	Common Name	Scientific Name	Sex	Age	Sample Type	Sample Tissue	Analysis
VC1	Veiled chameleon	<i>Chameleo calypratus</i>	M	Juvenile	PM	Lu, Li, Kid Pool	MGS
VC2	Veiled chameleon	<i>Chameleo calypratus</i>	F	Juvenile	PM	Lu, Li, Kid Pool	MGS
VC3	Veiled chameleon	<i>Chameleo calypratus</i>	U	Subadult	PM	Lu, Tr, OM Pool	MGS
VC4	Veiled chameleon	<i>Chameleo calypratus</i>	U	U	AM	Oral swab	PCR
VC5	Veiled chameleon	<i>Chameleo calypratus</i>	U	Adult	AM	Oral swab	PCR
VC6	Veiled chameleon	<i>Chameleo calypratus</i>	U	U	AM	Oral swab	PCR
VC7	Veiled chameleon	<i>Chameleo calypratus</i>	F	Subadult	AM	Oral swab	PCR
VC8	Veiled chameleon	<i>Chameleo calypratus</i>	F	Subadult	AM	Oral swab	PCR
VC9	Veiled chameleon	<i>Chameleo calypratus</i>	F	Subadult	AM	Oral swab	PCR
BD1	Central bearded dragon	<i>Pogona vitticeps</i>	F	Adult	AM	Oral swab	PCR
BD2	Central bearded dragon	<i>Pogona vitticeps</i>	F	Adult	AM	Oral swab	PCR
BD3	Central bearded dragon	<i>Pogona vitticeps</i>	M	Adult	AM	Oral swab	PCR
BD4	Central bearded dragon	<i>Pogona vitticeps</i>	F	Adult	AM	Oral swab	PCR
BD5	Central bearded dragon	<i>Pogona vitticeps</i>	M	Adult	AM	Oral swab	PCR
BD6	Central bearded dragon	<i>Pogona vitticeps</i>	F	Adult	AM	Oral swab	PCR
LG1	Common leopard gecko	<i>Eublepharis macularius</i>	U	U	AM	Oral swab	PCR
LG2	Common leopard gecko	<i>Eublepharis macularius</i>	U	U	AM	Oral swab	PCR
LG3	Common leopard gecko	<i>Eublepharis macularius</i>	U	U	AM	Oral swab	PCR
OG1	Ocelot gecko	<i>Paroedura pictus</i>	U	U	AM	Oral swab	PCR
OG2	Ocelot gecko	<i>Paroedura pictus</i>	U	U	AM	Oral swab	PCR
OG3	Ocelot gecko	<i>Paroedura pictus</i>	U	U	AM	Oral swab	PCR

5.3.4: PCR Analysis for Viral RNA

Methods can be referenced in section 4.2.6. RNA was extracted from oral swabs. RNA from oral swabs and tissue pools (above) were reverse transcribed into complementary DNA (cDNA) as previously described. Primers were designed to the RNA dependent RNA polymerase (RdRp) of ORF1b (highly conserved region) of seropetovirus sequences: MDS-1518F 5' TACACCTACTTTCAAGGMGA 3' and MDS-1519R 5' GTTGTWGCATCACASWGGGA 3' as forward and reverse primers, respectively. PCR was performed using Luna Universal qPCR Master Mix. Twelve microliter reactions included a final concentration of 1x Luna Universal Master Mix and 0.4 μ M of each primer mixed with 5 μ l of cDNA diluted 1:10 in water. Reaction mixtures were run with the following cycle parameters: 95°C for 1 minute; 95°C for 15 seconds and 60°C for 60 seconds with 45 cycles; and a melting curve. PCR products were run on a 1.5% agarose gel with ethidium bromide for confirmation of amplification and assessment of amplicon size (expected 753 bp). DNA bands were gel extracted (Zymo Gel DNA Recovery Kit) according to the manufacturer's instructions. Bands were Sanger sequenced by GENEWIZ (San Diego, CA) using the forward primer. Sanger sequencing of PCR amplicons yielded 708 bp sequences following removal of poor-quality base calls and primer sequences. These were aligned in Geneious 11.0.4 for assessment of percentage nucleotide identity.

RNA from tissues and oral swabs were reverse transcribed as previously described but replacing the initial incubation at 65°C for 5 minutes to 95°C for 5 minutes to allow for denaturation of double stranded RNA viruses and better yield of reovirus cDNA. PCR was performed as described above with broad orthoreovirus primers [21] as well as primers designed specifically to the polymerase gene of the orthoreovirus detected in this study: MDS-1579F 5' CGTCGGGTAGTGCTGTGATT 3' and MDS-1580R 5' TAGGGTGCCTGCTCACATTG 3' as forward and reverse primers, respectively. Thermocycler parameters were as follows: 95°C for 1 minute; 95°C for 1 minute, 47°C for 1 minute, and 72°C for 1 minute with 45 cycles; and 72°C for 5 minutes.

5.3.5: Virus Isolation

Four cell lines were used for virus isolation attempts: JK cells (boa constrictor kidney) [63], DPHt cells (diamond python heart) [199], IgH2 cells (iguana heart; ATCC, CCL-108), and VH2 (viper heart; ATCC, CCL-140). Pooled tissues (oral mucosa, lung, trachea) from VC3 were homogenated in brain heart infusion (Becton Dickinson) by manual disruption with a plastic sterile pestle in a 1.5 ml Eppendorf tube. The homogenate was filtered (Merck Millipore UltraFree-MC 0.22 µm centrifugal filter) and 40µl was inoculated onto JK, DPHt, IgH2, and VH2 cells at 80% cell confluence in a 6 well tissue-culture plate. Each cell type had 2 devoted wells in the plate: one inoculated with VC3 tissue homogenate and 1 sham inoculated with BHI. Cells were maintained in 2 ml of complete cell medium (MEM/EBSS [HyClone], 10% irradiated FBS [HyClone], 10% Nu-Serum1 [Corning], and 2x penicillin-streptomycin solution [HyClone]) and incubated at 30°C with 5% CO₂. Approximately half the volume of supernatant was collected at 24-hours post-inoculation and stored at -80°C; this volume was replaced with fresh medium. Supernatant was similarly collected every 48 hours for 13 days. On the final collection, cells were trypsinized (200µl of 0.25% trypsin applied directly to rinsed cells and incubated for 2 minutes at 37°C) and both supernatant and cells were stored at -80°C. RNA was extracted and PCR was performed as previously described for all cell inoculation samples at all time points.

5.4: Results

5.4.1: Postmortem Findings

Postmortem evaluation of VC1 (chameleon with clinical evidence of respiratory disease) and VC2 (clinically normal chameleon) was performed. Gross examination of VC1 revealed a scant amount of stomach contents and empty small intestines and colon, consistent with anorexia. No other gross lesions were observed. Histopathology of VC1 (Figure 5.1) revealed severe chronic-active proliferative and catarrhal interstitial pneumonia and tracheitis, moderate chronic lymphocytic and catarrhal rhinitis, and

mild histiocytic and heterophilic colitis. Gross examination of VC2 was unremarkable and histopathologic lesions included mild multifocal heterophilic enterocolitis with focal erosion.

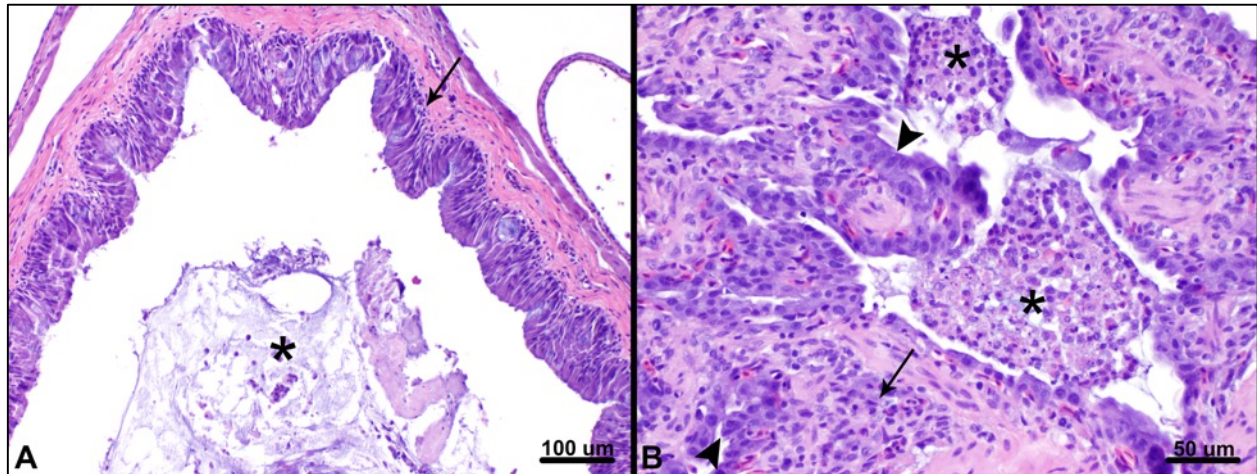


Figure 5.1. Proliferative and catarrhal interstitial pneumonia and rhinitis in a veiled chameleon (VC1). A) Histopathology of the nasal cavity. The lumen contains abundant mucus, low numbers of sloughed epithelial cells, and heterophils (asterisk). There is lymphocytic infiltration of the nasal mucosa and mucosal epithelium (arrow). Hematoxylin and eosin (HE), 100x magnification, 100 μ M scale bar. B) Histopathology of the lungs revealed faveolar lumina (asterisks) and bronchiolar air spaces containing numerous, large accumulations of heterophils admixed with sloughed epithelial cells, mucus and cellular debris. Multifocally, there was marked hypertrophy and hyperplasia of alveolar type II pneumocytes (arrowheads) and expansion of interstitial spaces by mononuclear and heterophilic inflammation (arrow). The trachea (not shown) was similarly affected. HE, 200x magnification, 500 μ M scale bar.

Paramyxovirus PCR of lung tissue from VC1 was negative. Aerobic culture of liver, lung, and colon and fecal flotation were negative for bacteria and parasites in both VC1 and VC2. *Salmonella* was detected in the liver and lung pool by enrichment culture in VC1 and was found to have broad antibiotic sensitivity; *Salmonella* culture was negative in VC2.

5.4.2: Metagenomic Sequencing Findings

Metagenomic sequencing was performed to identify potential infectious agents in diseased chameleons. In the first sequencing run performed, the average number of individual reads per sample was 3×10^6 . On average, 91%, 18%, and 9% of sequences remained following adaptor and quality filtering,

collapsing to unique reads, and filtration of chameleon derived sequences, respectively. Sequences of two genotypically distinct veiled chameleon serpentoviruses (VCSV) were detected in VC1 (VCSV-B) and VC3 (coinfection with VCSV-A and B); no sequences were detected in VC2. In the second sequencing run performed (enriching for dsRNA), the average number of paired reads per sample was 24.2×10^6 , with an average of 90%, 19%, and 17% sequences remaining after filtration. The same serpentoviruses were detected in VC1 (B) and VC3 (A and B); 1 read pair aligned to VCSV-B in VC2. Additionally, sequences aligning to a novel veiled chameleon orthoreovirus (VCOrV) were detected in all three chameleon samples, with the highest number of reads detected in VC2. Sequencing results for each sample are summarized in Table 5.2.

Table 5.2. Summary of sequencing depth and aligning reads to VCSV and VCOrV. The total number of sequences generated per sample was calculated. Seq1 refers to the first round of RNA-seq by standard methods. Seq2 refers to RNA-seq with enrichment for dsRNA. A) Number of initial reads (single, Seq1; paired, Seq2). B) Number of reads remaining after removing low quality sequences. C) Number of reads remaining after collapsing non-unique sequences into a single read. D) Number of reads remaining after removing host-derived sequences. The total number of reads aligning to VCSVs and VCOrV are included.

Sample and Seq Run		Total Reads (A)	Remove low quality reads (B)	Collapse to unique reads (C)	Host filter (D)	VCSV Reads (#)	VCOrV Reads (#)
Seq1	VC1	6.4×10^6	5.7×10^6 (89%)	1×10^6 (15%)	0.5×10^6 (8%)	914	0
	VC2	1.5×10^6	1.4×10^6 (91%)	0.3×10^6 (19%)	0.1×10^6 (9%)	0	0
	VC3	1.1×10^6	1×10^6 (92%)	0.2×10^6 (20%)	0.1×10^6 (10%)	212	0
Seq2	VC1	16.9×10^6	15.7×10^6 (93%)	2.7×10^6 (16%)	2.6×10^6 (15%)	901	39
	VC2	42.7×10^6	38.5×10^6 (90%)	6.6×10^6 (16%)	6×10^6 (14%)	11	2,921
	VC3	13.1×10^6	11.4×10^6 (87%)	3.1×10^6 (24%)	3×10^6 (23%)	11,881	11

5.4.3: Chameleon Serpentoviruses: Genomic and Phylogenetic Analysis

Contigs were assembled from reads using SPAdes genome assembler (version 3.5.0). A complete coding genome of VCSV-A and a partial coding genome of VCSV-B were obtained. Both genomes have an overlapping ORF1ab gene with a ribosomal frameshift signal (-1;AAAAC) followed by a spike protein gene. The 3' end of VCSV-B contained 6 ORFs with an identifiable transmembrane protein, matrix protein,

and nucleocapsid protein. Geneious alignment of ORF1b revealed 51% nucleotide and 48% amino acid identity between VCSV-A and B. Nucleotide and protein alignments of ORF1b from VCSV-A to other serpentoviruses (Figure 5.2) resulted in 47-55% nucleotide and 40-53% amino acid identity; ORF1b from VCSV-B exhibited 47-51% nucleotide and 40-48% amino acid identity. A phylogenetic tree of the protein alignment revealed VCSVs closely related to serpentoviruses in other reptiles (snakes, lizards, and turtles).

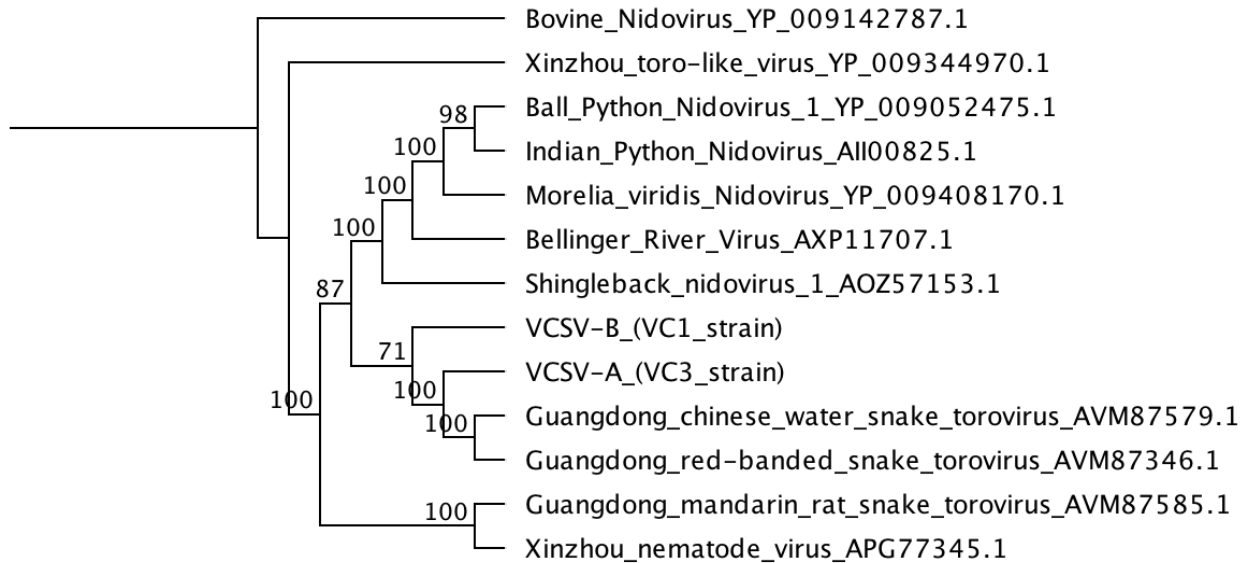


Figure 5.2. Cladogram of veiled chameleon serpentoviruses and other reptilian serpentoviruses. The entirety of ORF1b amino acid sequences were aligned and a phylogenetic tree constructed. Veiled chameleon serpentovirus (VCSV) was compared to known serpentoviruses found in snakes (ball python, Indian python, *Morelia viridis*, Guangdong snake nidoviruses/toroviruses), lizards (shingleback nidovirus), turtles (Bellinger river virus), and snake-associated nematodes (Xinzhou viruses) as well as a remotovirus (bovine nidovirus) of the same *Tobnavirinae* family. GenBank accession numbers are included to the right of the virus name. Maximum likelihood tree constructed using PhyML, LG substitution model, and 1000 bootstrap replicates; bootstrap values (percent) represented at each node. Bovine nidovirus outgroup.

5.4.4: Chameleon Orthoreoviruses: Genomic and Phylogenetic Analysis

A complete coding genome of an orthoreovirus was obtained from VC2. The orthoreovirus consisted of 10 segments: 3 long (L) segments, 3 medium (M) segments, and 4 small (S) segments. Nucleotide and protein sequence alignments of each segment using BLASTn and BLASTx revealed highest percent identity to reptilian orthoreoviruses (GenBank sequences: GCA_000919495.1 and AY238886 to AY238887). All segments aligned with 71-87% nucleotide and 81-94% amino acid identity to reptilian

orthoreovirus (with greater than 95% query coverage) except M1. Segment M1 had 71% nucleotide identity (23% query coverage) and 53% amino acid identity (96% query coverage) to reptilian orthoreovirus. Genome data can be referenced in Table 5.3. A phylogenetic analysis of protein alignments for L3 (RdRp) revealed reptilian orthoreoviruses (isolated from vipers) as the closest evolutionary relation (Figure 5.3).

Table 5.3. General features of the veiled chameleon orthoreovirus genome. The long (L), medium (M), and short (S) encoded genes are indicated. The nucleotide length of each segment is indicated, as is the amino acid length of the encoded protein.

Segment	Gene	Size (bp)	Protein size (aa)
L1	Lambda A	4000	1131
L2	Lambda C	3685	872
L3	Lambda B (RdRp)	3795	1165
M1	Mu Ns	2467	793
M2	Mu A	2289	754
M3	Mu B	2091	613
S1	P14 (fusion), Sigma C	1463	126, 350
S2	Sigma A	1260	390
S3	Sigma B	1252	388
S4	Sigma NS	1129	282

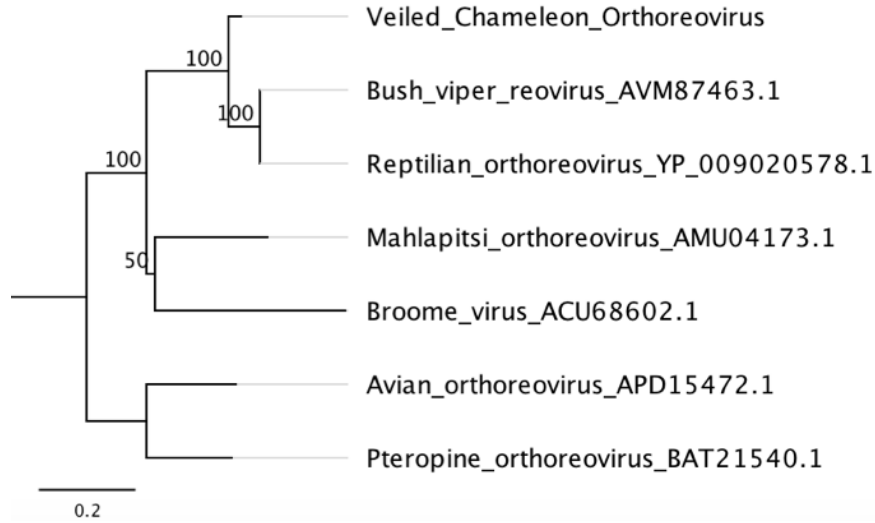


Figure 5.3. Phylogenetic tree of veiled chameleon orthoreovirus and orthoreoviruses of reptiles, mammals, and birds. The amino acid sequences of L3 segments were aligned and a phylogenetic tree constructed. Veiled chameleon orthoreovirus was compared to known reoviruses found in snakes (reptilian orthoreovirus and bush viper reovirus), bats (Broome virus and pteropine orthoreovirus), bat flies (Mahlapitsi orthoreovirus), and birds (avian orthoreovirus). GenBank accession numbers are included to the right of the virus name. Maximum likelihood tree constructed using PhyML, LG substitution model, and 1000 bootstrap replicates; bootstrap values (percent) represented at each node. The tree was arbitrarily rooted.

5.4.5: Targeted Viral RNA Detection

Following the discovery of two novel serpentovirus sequences in veiled chameleons, degenerate primers were designed for PCR detection of both virus genotypes. Initial metagenomic sequencing (seq1) detected serpentovirus sequence in VC1 and VC3, but not VC2. In contrast, PCR detected serpentovirus nucleic acid in all three chameleons (Figure 5.4). Sanger sequencing of PCR amplicons targeting the RdRp matched VCSV-A and B found by metagenomics. VC1 and VC2 shared >99% nucleotide identity to each other and to VCSV-B; they shared 67% nucleotide identity with VCSV-A. The Sanger sequencing of VC3 yielded poor quality sequence due to coinfection, as observed by metagenomics, but the nucleotide fluorescent tracing revealed similarities to VCSV-A and B.

Subsequently, the oral swabs from 6 additional chameleons (VC4-9), 6 bearded dragons (BD1-6), 3 leopard geckos (LG1-3) and 3 ocelot geckos (OG1-3) were analyzed by PCR for the presence of serpentovirus. Five out of 6 chameleons were positive (VCA4, 6-9) for VCSVs, whereas all the bearded

dragons and geckos were negative (Figure 5.4). Sanger sequences from VC7-9 aligned to VCSV-A with 100% nucleotide identity and VCSV-B with 67% nucleotide identity. VC4 and VC6 had poor quality tracings.

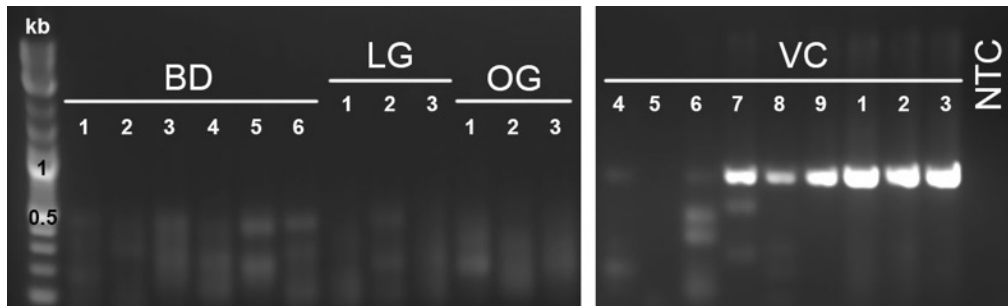


Figure 5.4. Gel electrophoresis of serpentovirus PCR. VC, veiled chameleons. BD, bearded dragons. LG, leopard geckos. OG, ocelot geckos. NTC, no template control (negative). Expected amplicon size of 752 bp detected in VC 1-4 and 6-9.

Attempts at detecting orthoreovirus nucleic acid within chameleon tissues and swabs, even those positive by metagenomic sequencing (VC1-3), were unsuccessful, an occurrence that has been previously reported [222].

5.4.6: Virus Isolation

Reptile cell lines inoculated with tissue homogenate did not exhibit cytopathic effects (cell death or syncytial cell formation). Serpentovirus was not detected by PCR at any time points post-inoculation. Orthoreovirus was also not detected. However, only VC1, 2, and 3 were confirmed to be infected with orthoreovirus and tissue samples were only available from VC3, which had low viral nucleic acid detection compared to VC2 based on metagenomic data, indicating a reduced viral load.

5.5: Discussion

Novel serpentoviruses have recently been found in snake, lizard, and turtle species associated with respiratory or systemic disease and a serpentovirus has been confirmed as a cause of respiratory disease in

pythons (Chapter 3) [9,111,112,131,133,134,199]. However, our study is the first to describe novel serpentoviruses in veiled chameleons associated with respiratory disease, and only the second to describe serpentoviruses in lizards, globally.

In 2016, a respiratory disease in wild shingleback lizards in Australia was found in association with serpentovirus infection [131]. Clinical signs were characterized as excessive oral mucus secretions and serous to mucopurulent discharge from the nares and eyes, pale mucous membranes, sneezing, lethargy, anorexia, depression, and poor body condition. Lizards were tested by antemortem swabbing of the oral cavity; histologic lesions associated with viral infection were not evaluated. In our study, clinical signs of respiratory disease were similar to those found in shingleback lizards as well as those described in serpentovirus-infected snakes [9,111,112,199]. Histologic lesions in chameleons were also like those found in snakes: interstitial proliferative and catarrhal pneumonia, rhinitis, and tracheitis [9,111,112,133,199]. These findings likely indicate a similar pathogenesis.

Our study detected serpentoviruses in chameleons with clinical and histologic evidence of respiratory disease, as well as clinically healthy animals lacking microscopic disease. Serpentovirus infections in shingleback lizards [131] and snakes (Chapter 4) have also been described in clinically healthy animals. This provides further evidence that disease manifestation following serpentovirus infection is multifactorial. Infection in “healthy” animals may represent sampling during the incubation period or a carrier state. In Chapter 4, five pythons (*Morelia* species) that were consecutively tested for over two years were positive for serpentovirus but never exhibited clinical signs during this time. Our findings in chameleons could represent a similar phenomenon, but infection status over longer periods of time are necessary to support this claim.

Serpentovirus infection was also investigated in bearded dragons, leopard geckos, and ocelot geckos from the same collection; PCR for VCSVs were negative. This suggests that either transmission of VCSVs did not occur, or these lizards have a reduced susceptibility or resistance to infection with VCSVs. Our primers were designed to specifically target the VSCVs identified in this study, therefore, our results do not rule out the possibility of divergent serpentovirus infection in these additional lizard species. As

observed in snakes (Chapter 4), divergent serpentoviruses may be present that are not detectable by our current targeted diagnostics. Metagenomic sequencing from these animals may provide additional insight into the presence or absence of viral infection.

Similar to our findings in snakes (Chapter 4), coinfection with different virus genotypes appears to be a natural phenomenon for at least some reptile serpentoviruses. In this study, we identified one definitive case of coinfection by metagenomic sequencing and two additional cases of suspected coinfection based on Sanger sequencing. The chameleon with confirmed coinfection (VC3) died on its own but was not assessed clinically or histologically, therefore, the relationship of coinfection and pathologic progression could not be inferred.

In addition to coinfection with multiple serpentoviruses, a novel orthoreovirus closely related to known reptilian orthoreoviruses was also detected in some of these chameleons, indicating coinfection with multiple different viral pathogens. Orthoreoviruses are non-enveloped, segmented, double-stranded RNA viruses that have been associated with disease in mammals, birds, and reptiles [105,122]. In reptiles, including lizards, orthoreoviruses have been found in healthy animals as well as being associated with several disease processes [105,223–227]. However, the link between orthoreovirus infection and disease in lizards, including chameleons, remains circumstantial [228,229]. In contrast to lizards, orthoreoviruses have been definitively associated with respiratory disease in snakes. In this single study, an orthoreovirus was isolated in culture from beauty snakes (*Orthriophis taeniurus*) and ratsnakes (*Elaphe moellendorffi*) with fatal respiratory disease. Subsequent experimental infection in black ratsnakes (*Elaphe obsoleta obsoleta*) resulted in disease, confirming causation [108]. Histologic lesions in orthoreovirus-infected snakes included proliferative interstitial pneumonia and tracheitis with syncytial cell formation [108]. Reoviruses were associated with syncytial formation both in cell culture and in tissue [108,222,229]. Proliferative lesions are common sequelae to respiratory pathogens in reptiles, [109,203–205,214], however, syncytial cells are a unique feature attributed to few viral infections, including reoviruses [108,230]. In veiled chameleons from our study, syncytial cells were not detected in cell culture or on histologic examination.

Coinfection of chameleons with multiple serpentoviruses and an orthoreovirus pose a dilemma as to the probable cause of respiratory disease in this study. Sequences aligning to the orthoreovirus were detected in all three chameleons tested by metagenomic sequencing. However, the highest number of viral sequences were found in VC2, likely indicating a greater viral load. Interestingly, VC2 was clinically normal, did not have evidence of respiratory disease histologically, and had the fewest number of sequences aligning to VCSV. These findings, along with the lack of syncytial cell formation on histopathology, suggest orthoreovirus may not be playing the primary role in respiratory disease, but rather as a secondary contributor or incidental finding. Reoviruses have occurred as coinfection in other reptiles and have been suggested to be secondary in nature [105,222]. Furthermore, based on serological evidence, orthoreovirus infection in lizards may be commonplace, supporting its role as an incidental infection [223,226].

Multiple introductions occurred within the examined collection between 2017 and 2018, including three different “generations” of chameleons being housed in the same facility and each of these generations being composed of several chameleon groups purchased from multiple locations. Between introductions, proper disinfection was not performed and surviving chameleons that had been exposed to diseased animals were subsequently placed with newly arriving stock. This report emphasizes the importance of adequate disinfection in facilities, especially those following an outbreak. Furthermore, clinical and diagnostic assessment of both established and newly arriving animals prior to entry into the collection, as well as implementation of quarantine practices, is exceedingly important for preventing the spread of infectious diseases.

In conclusion, this study describes respiratory disease associated with novel serpentoviruses in a collection of veiled chameleons. This is the first description of a serpentovirus infection in any chameleon species. Based on the similarities between the disease described in this study and the previous descriptions of serpentoviruses in lizards and snakes, a causal relationship is considered probable. The significance of coinfection with orthoreovirus is currently unknown. Future studies are necessary to determine the role serpentoviruses and possibly orthoreoviruses played in respiratory-disease manifestation and to establish a causal relationship between infection and disease.

CHAPTER 6: CONCLUDING REMARKS

Thorough discussions have been provided in each chapter regarding the major findings of this dissertation. The following are closing thoughts concerning metagenomic-based pathogen discovery projects for the future, the value of pursuing metagenomic projects beyond basic genomic characterization, and unresolved questions regarding serpentoviruses in reptiles.

6.1: Learning from Metagenomic Studies

Next generation sequencing technology is rapidly advancing and is becoming more affordable each year. This has resulted in increased application of NGS in the research and diagnostic setting, including the use of metagenomics. However, as with any new technology, it is important to understand the proper uses and limitations for best application practices.

One of the primary limitations and frustrations of metagenomic sequencing is how to interpret the data that is generated. As demonstrated by the examples included in this dissertation, much can depend on the selection of case and control samples, the type of starting nucleic acid, the method of library preparation, and the disease process itself. Guidelines are presented below describing some important aspects to consider before beginning a metagenomic-based pathogen discovery project.

1. Pathogen discovery projects should be chosen wisely. In most cases, the disease should have a high likelihood of being infectious in origin and conventional methods of microbial detection should be exhausted prior to metagenomic investigation. If an infectious cause is questionable, as observed with canine MUO, having a thorough understanding of the disease process or methodically considering the potential outcomes of metagenomic analysis is an important first step.
2. Case samples should be good quality and be representative of the disease and tissue of interest. Sufficient confidence in samples reduces the likelihood of negative results based on poor quality or improper sample selection.

3. Appropriate negative controls should be included. A water control (no nucleic acid input) should always be performed to assess contamination from the sample preparation and sequencing method. Furthermore, matched samples from healthy individuals provides additional confidence in results and is necessary to establish an association with diseased versus non-diseased cases.
4. RNA-seq has the benefit of sampling the entire transcriptome and is expected to detect transcripts of DNA-based organisms as well as RNA genomes of viruses. However, this may not be universally applicable. If a DNA virus or other organism is suspected, performing both RNA-seq and DNA-seq may provide a more comprehensive assessment of total infectious agents.
5. The method of nucleic acid preparation for sequencing can influence the results. If an RNA virus is suspected, enrichment for dsRNA or subtraction of common RNAs (e.g. rRNA) may improve overall virus detection. Furthermore, standard library preparation kits and methods may be inadequate for detecting dsRNA viruses without modifications.
6. If a sample has a low nucleic acid content (e.g. CSF), sensitive amplification methods can improve library quantity, but can also increase biases and reduce the total number of non-unique reads available for downstream analysis. Therefore, the sequencing platform and achievable depth should be thoroughly considered in the context of sample type and library preparation methods prior to sequencing.
7. Expect the unexpected and anticipate the need for follow-up, independent of the findings. Metagenomic sequencing should only be considered as the first step in the route to pathogen discovery and the characterization of diseases of unknown origin.

Although this is by no means an all-inclusive list, including these steps in metagenomic sequencing projects of pathogen discovery could improve results, interpretation, and overall success.

6.2: The Value of Establishing Disease Causation

Reptilian serpentoviruses were initially described in association with disease outbreaks, and despite significant evidence supporting disease-association, true causation had not been established. Our

subsequent investigation of this pathogen drastically advanced our knowledge of serpentovirus disease in snakes and other reptiles.

By fulfilling Koch's postulates, serpentoviruses are now a proven cause of disease in pythons. This elevates their status as a disease differential in cases of respiratory disease and (ideally) improves the probability of disease diagnosis. Future studies can also be interpreted on the basis of causation. For instance, our epidemiologic investigation in captive snakes resulted in the identification of numerous clinically healthy pythons with serpentovirus infection. This finding could be misinterpreted as counter-evidence to disease causation in snakes, but instead we understand that disease manifestation is multifactorial. Our evaluation of serpentoviruses can now focus on why there is variability of disease in infected snakes (e.g. age, sex, species, environment, virus genotype).

Establishing causation between a pathogen and disease also sets a precedence for related pathogens and their likelihood of disease causation. Our epidemiologic study identified serpentoviruses in many new snake species, indicating these viruses have a broader host range than previously known. Boa and colubrid snakes are now known to be infected with serpentoviruses, but their association with disease remains open. Knowing that related serpentoviruses in pythons cause disease indirectly implicates boa and colubrid serpentoviruses as possible respiratory pathogens. This also prompts the investigation of genotypic variations between disease-causing serpentoviruses and those currently unassociated with disease.

The same precedent applied to serpentoviruses of snakes can also be applied in other reptiles. Researchers in Australia have identified serpentovirus in shingleback lizards with respiratory disease similar to that described in serpentovirus-infected snakes [131]. We additionally identified serpentoviruses in veiled chameleons exhibiting similar clinical and histologic disease to other lizards and snakes. Causation remains circumstantial, but our findings, provide further evidence that, like in snakes, serpentoviruses cause respiratory disease in lizards.

6.3: Going Forward: The Future of Serpentovirus Research

The primary goal of this dissertation was to inform virologists, biologists, veterinarians, and reptile owners of the impact serpentoviruses can have on the health of reptiles. The studies presented in this dissertation provide a solid foundation to this goal, but many unanswered questions remain; most importantly, the role of serpentoviruses in disease causation for non-python snake species and captive and wild populations of reptiles in general.

Our investigations have been limited to captive populations, but the artificial environment and close-proximity of snakes in captivity is an inadequate model for the wild. The stress of captivity and sometimes poor mimicry of natural environments is a common cause of immunosuppression and predisposition to infection in captive animals [215,216]. Furthermore, greater exposure of animals to one another (such as co- or adjacent housing or breeding introductions) increases the likelihood of disease transmission. Therefore, the microcosm of captive collections likely exacerbates viral infection and disease far beyond what may be evident in the wild. Serpentovirus infection has been found in wild reptiles associated with disease (lizards and turtles) [131,134]. However, the presence of serpentoviruses in wild snakes has not been investigated nor have general surveillance studies been performed. We identified serpentoviruses in boas and colubrids in captive collections in the US (Chapter 4). Threatened and endangered native snake species in North America include colubrids and boas, indicating a potential risk for wild snakes [231]. It is important that attention be applied to wild, and especially vulnerable, populations of reptiles to gauge the risk serpentoviruses pose in a natural environment.

We established a basic understanding of serpentovirus infection in captive snakes and characterized new chameleon serpentoviruses as possible respiratory pathogens. However, the extent of serpentovirus susceptibility in reptile species and the association of these viruses with disease is still an open question of investigation. At the current rate of serpentovirus discovery the list of affected species is sure to grow. Future efforts should be applied to a range of reptile species and beyond. With the discovery of a closely related tobanivirus in cattle with respiratory disease, the family *Tobaniviridae* (which includes

serpentoviruses) should be considered as a group of emerging pathogens with significant implications for animal, and possibly human health [130].

REFERENCES

1. de Kruif P. *Microbe hunters*. New York, NY: Harcourt, Brace Co.; 1926.
2. Gest H. The discovery of microorganisms by Robert Hooke and Antoni Van Leeuwenhoek, fellows of the Royal Society. *Notes Rec R Soc Lond*. 2004;58: 187–201. doi:10.1098/rsnr.2004.0055
3. Olofinlade O, Adeonigbagbe O, Karowe M, Robilotti J, Gualtieri N, Cacciarelli A, et al. The diagnostic value of electron microscopy in human immunodeficiency virus-positive patients with gastrointestinal disease. *Scand J Gastroenterol*. 2000;35: 329–332.
4. Fischer SA, Graham MB, Kuehnert MJ, Kotton CN, Srinivasan A, Marty FM, et al. Transmission of lymphocytic choriomeningitis virus by organ transplantation. *N Engl J Med*. 2006;354: 2235–2249. doi:10.1056/NEJMoa053240
5. Geisbert TW, Jahrling PB, Hanes MA, Zack PM. Association of Ebola-related Reston virus particles and antigen with tissue lesions of monkeys imported to the United States. *J Comp Pathol*. 1992;106: 137–152.
6. Ksiazek TG, Erdman D, Goldsmith CS, Zaki SR, Peret T, Emery S, et al. A novel coronavirus associated with severe acute respiratory syndrome. *N Engl J Med*. 2003;348: 1953–1966. doi:10.1056/NEJMoa030781
7. Goldsmith CS, Miller SE. Modern Uses of Electron Microscopy for Detection of Viruses. *Clin Microbiol Rev*. 2009;22: 552. doi:10.1128/CMR.00027-09
8. Iwanowicz LR, Goodwin AE. A new bacilliform fathead minnow rhabdovirus that produces syncytia in tissue culture. *Arch Virol*. 2002;147: 899–915. doi:10.1007/s00705-001-0793-z
9. Stenglein MD, Jacobson ER, Wozniak EJ, Wellehan JFX, Kincaid A, Gordon M, et al. Ball python nidovirus: a candidate etiologic agent for severe respiratory disease in *Python regius*. *mBio*. 2014;5: e01484-01414. doi:10.1128/mBio.01484-14
10. Rodriguez-Hernandez CO, Torres-Garcia SE, Olvera-Sandoval C, Ramirez-Castillo FY, Muro AL, Avelar-Gonzalez FJ, et al. Cell Culture: History, Development, and Prospects. *Int J Curr Res Acad Rev*. 2014;2: 188–200.
11. Gao SJ, Moore PS. Molecular approaches to the identification of unculturable infectious agents. *Emerg Infect Dis*. 1996;2: 159–167. doi:10.3201/eid0203.960301
12. Haelewaters D, Gorczak M, Pfliegler WP, Tartally A, Tischer M, Wrzosek M, et al. Bringing Laboulbeniales into the 21st century: enhanced techniques for extraction and PCR amplification of DNA from minute ectoparasitic fungi. *IMA Fungus*. 2015;6: 363–372. doi:10.5598/imafungus.2015.06.02.08
13. Lawson AJ. Discovering new pathogens: culture-resistant bacteria. *Methods Mol Biol Clifton NJ*. 2004;266: 305–322. doi:10.1385/1-59259-763-7:305

14. Munang'andu HM, Mugimba KK, Byarugaba DK, Mutoloki S, Evensen Ø. Current Advances on Virus Discovery and Diagnostic Role of Viral Metagenomics in Aquatic Organisms. *Front Microbiol.* 2017;8: 406–406. doi:10.3389/fmicb.2017.00406
15. Casas I, Tenorio A, Echevarria JM, Klapper PE, Cleator GM. Detection of enteroviral RNA and specific DNA of herpesviruses by multiplex genome amplification. *J Virol Methods.* 1997;66: 39–50.
16. Lipkin WI. Microbe Hunting. *Microbiol Mol Biol Rev.* 2010;74: 363. doi:10.1128/MMBR.00007-10
17. Nichol ST, Spiropoulou CF, Morzunov S, Rollin PE, Ksiazek TG, Feldmann H, et al. Genetic identification of a hantavirus associated with an outbreak of acute respiratory illness. *Science.* 1993;262: 914–917.
18. Shirato K, Nishimura H, Saijo M, Okamoto M, Noda M, Tashiro M, et al. Diagnosis of human respiratory syncytial virus infection using reverse transcription loop-mediated isothermal amplification. *J Virol Methods.* 2007;139: 78–84. doi:10.1016/j.jviromet.2006.09.014
19. Tumpey TM, Basler CF, Aguilar PV, Zeng H, Solorzano A, Swayne DE, et al. Characterization of the reconstructed 1918 Spanish influenza pandemic virus. *Science.* 2005;310: 77–80. doi:10.1126/science.1119392
20. Mullis K, Faloona F, Scharf S, Saiki R, Horn G, Erlich H. Specific enzymatic amplification of DNA in vitro: the polymerase chain reaction. *Cold Spring Harb Symp Quant Biol.* 1986;51 Pt 1: 263–273.
21. Wellehan JFXJ, Childress AL, Marschang RE, Johnson AJ, Lamirande EW, Roberts JF, et al. Consensus nested PCR amplification and sequencing of diverse reptilian, avian, and mammalian orthoreoviruses. *Vet Microbiol.* 2009;133: 34–42. doi:10.1016/j.vetmic.2008.06.011
22. Lipkin WI. The changing face of pathogen discovery and surveillance. *Nat Rev Microbiol.* 2013;11: 133.
23. McLoughlin KS. Microarrays for pathogen detection and analysis. *Brief Funct Genomics.* 2011;10: 342–353. doi:10.1093/bfgp/elr027
24. Bialynicki-Birula R. The 100th anniversary of Wassermann-Neisser-Bruck reaction. *Clin Dermatol.* 2008;26: 79–88. doi:10.1016/j.clindermatol.2007.09.020
25. Houpiikian P, Raoult D. Traditional and molecular techniques for the study of emerging bacterial diseases: one laboratory's perspective. *Emerg Infect Dis.* 2002;8: 122–131. doi:10.3201/eid0802.010141
26. Lustig A, Levine AJ. One hundred years of virology. *J Virol.* 1992;66: 4629–4631.
27. Peiris J, Lai S, Poon L, Guan Y, Yam L, Lim W, et al. Coronavirus as a possible cause of severe acute respiratory syndrome. *The Lancet.* 2003;361: 1319–1325. doi:10.1016/S0140-6736(03)13077-2

28. Choi HMT, Schwarzkopf M, Fornace ME, Acharya A, Artavanis G, Stegmaier J, et al. Third-generation in situ hybridization chain reaction: multiplexed, quantitative, sensitive, versatile, robust. *Dev Camb Engl*. 2018;145. doi:10.1242/dev.165753
29. Cohen C, Lawson D, Jiang J, Siddiqui MT. Automated in situ hybridization for human papilloma virus. *Appl Immunohistochem Mol Morphol AIMM*. 2014;22: 619–622. doi:10.1097/PAI.0b013e3182a501a2
30. McNicol AM, Farquharson MA. In situ hybridization and its diagnostic applications in pathology. *J Pathol*. 1997;182: 250–261. doi:10.1002/(SICI)1096-9896(199707)182:3<250::AID-PATH837>3.0.CO;2-S
31. Montone KT, Guarner J. In situ hybridization for rRNA sequences in anatomic pathology specimens, applications for fungal pathogen detection: a review. *Adv Anat Pathol*. 2013;20: 168–174. doi:10.1097/PAP.0b013e31828d187d
32. Strickler JG, Manivel JC, Copenhaver CM, Kubic VL. Comparison of in situ hybridization and immunohistochemistry for detection of cytomegalovirus and herpes simplex virus. *Hum Pathol*. 1990;21: 443–448. doi:10.1016/0046-8177(90)90208-M
33. Aslam B, Basit M, Nisar MA, Rasool MH, Khurshid M. Proteomics: Technologies and Their Applications. *J Chromatogr Sci*. 2017;55: 182–196.
34. Biswas S, Rolain J-M. Use of MALDI-TOF mass spectrometry for identification of bacteria that are difficult to culture. *J Microbiol Methods*. 2013;92: 14–24. doi:10.1016/j.mimet.2012.10.014
35. Wang X, Fu Y-F, Wang R-Y, Li L, Cao Y-H, Chen Y-Q, et al. Identification of clinically relevant fungi and prototheca species by rRNA gene sequencing and multilocus PCR coupled with electrospray ionization mass spectrometry. *PloS One*. 2014;9: e98110. doi:10.1371/journal.pone.0098110
36. Trauger SA, Junker T, Siuzdak G. Investigating Viral Proteins and Intact Viruses with Mass Spectrometry. In: Schalley CA, editor. *Modern Mass Spectrometry*. Berlin, Heidelberg: Springer Berlin Heidelberg; 2003. pp. 265–282. doi:10.1007/3-540-36113-8_8
37. Bloch KC, Glaser C. Diagnostic approaches for patients with suspected encephalitis. *Curr Infect Dis Rep*. 2007;9: 315–322.
38. Glaser CA, Honarmand S, Anderson LJ, Schnurr DP, Forghani B, Cossen CK, et al. Beyond viruses: clinical profiles and etiologies associated with encephalitis. *Clin Infect Dis Off Publ Infect Dis Soc Am*. 2006;43: 1565–1577. doi:10.1086/509330
39. Glaser CA, Gilliam S, Schnurr D, Forghani B, Honarmand S, Khetsuriani N, et al. In search of encephalitis etiologies: diagnostic challenges in the California Encephalitis Project, 1998-2000. *Clin Infect Dis Off Publ Infect Dis Soc Am*. 2003;36: 731–742. doi:10.1086/367841
40. Watson JD, Crick FH. Molecular structure of nucleic acids; a structure for deoxyribose nucleic acid. *Nature*. 1953;171: 737–738.
41. Maxam AM, Gilbert W. A new method for sequencing DNA. *Proc Natl Acad Sci U S A*. 1977;74: 560–564.

42. Sanger F, Nicklen S, Coulson AR. DNA sequencing with chain-terminating inhibitors. *Proc Natl Acad Sci U S A*. 1977;74: 5463–5467.
43. Lander ES, Linton LM, Birren B, Nusbaum C, Zody MC, Baldwin J, et al. Initial sequencing and analysis of the human genome. *Nature*. 2001;409: 860–921.
44. Venter JC, Adams MD, Myers EW, Li PW, Mural RJ, Sutton GG, et al. The sequence of the human genome. *Science*. 2001;291: 1304–1351. doi:10.1126/science.1058040
45. McCombie WR, McPherson JD, Mardis ER. Next-Generation Sequencing Technologies. *Cold Spring Harb Perspect Med*. 2018; doi:10.1101/cshperspect.a036798
46. Voelkerding KV, Dames SA, Durtschi JD. Next-generation sequencing: from basic research to diagnostics. *Clin Chem*. 2009;55: 641–658. doi:10.1373/clinchem.2008.112789
47. Heather JM, Chain B. The sequence of sequencers: The history of sequencing DNA. *Genomics*. 2016;107: 1–8. doi:10.1016/j.ygeno.2015.11.003
48. Eid J, Fehr A, Gray J, Luong K, Lyle J, Otto G, et al. Real-time DNA sequencing from single polymerase molecules. *Science*. 2009;323: 133–138. doi:10.1126/science.1162986
49. Haque F, Li J, Wu H-C, Liang X-J, Guo P. Solid-State and Biological Nanopore for Real-Time Sensing of Single Chemical and Sequencing of DNA. *Nano Today*. 2013;8: 56–74. doi:10.1016/j.nantod.2012.12.008
50. Hoenen T, Groseth A, Rosenke K, Fischer RJ, Hoenen A, Judson SD, et al. Nanopore Sequencing as a Rapidly Deployable Ebola Outbreak Tool. *Emerg Infect Dis*. 2016;22: 331–334. doi:10.3201/eid2202.151796
51. Guo L-Y, Feng W-Y, Guo X, Liu B, Liu G, Dong J. The advantages of next-generation sequencing technology in the detection of different sources of abscess. *J Infect*. 2019;78: 75–86. doi:10.1016/j.jinf.2018.08.002
52. Head SR, Komori HK, LaMere SA, Whisenant T, Van Nieuwerburgh F, Salomon DR, et al. Library construction for next-generation sequencing: overviews and challenges. *BioTechniques*. 2014;56: 61-passim. doi:10.2144/000114133
53. Manso CF, Bibby DF, Mbisa JL. Efficient and unbiased metagenomic recovery of RNA virus genomes from human plasma samples. *Sci Rep*. 2017;7: 4173–4173. doi:10.1038/s41598-017-02239-5
54. Barba M, Czosnek H, Hadidi A. Historical Perspective, Development and Applications of Next-Generation Sequencing in Plant Virology. *Viruses*. 2014;6. doi:10.3390/v6010106
55. Wang D. Fruits of Virus Discovery: New Pathogens and New Experimental Models. Sullivan CS, editor. *J Virol*. 2015;89: 1486. doi:10.1128/JVI.01194-14
56. Shi M, Lin X-D, Chen X, Tian J-H, Chen L-J, Li K, et al. The evolutionary history of vertebrate RNA viruses. *Nature*. 2018;556: 197–202. doi:10.1038/s41586-018-0012-7

57. Shi M, Lin X-D, Tian J-H, Chen L-J, Chen X, Li C-X, et al. Redefining the invertebrate RNA virosphere. *Nature*. 2016; doi:10.1038/nature20167
58. Chiu CY. Viral pathogen discovery. *Curr Opin Microbiol*. 2013;16: 468–478. doi:10.1016/j.mib.2013.05.001
59. Lipkin WI, Hornig M. Diagnostics and Discovery in Viral Central Nervous System Infections. *Brain Pathol Zurich Switz*. 2015;25: 600–604. doi:10.1111/bpa.12277
60. Palacios G, Druce J, Du L, Tran T, Birch C, Briese T, et al. A new arenavirus in a cluster of fatal transplant-associated diseases. *N Engl J Med*. 2008;358: 991–998. doi:10.1056/NEJMoa073785
61. Briese T, Paweska JT, McMullan LK, Hutchison SK, Street C, Palacios G, et al. Genetic detection and characterization of Lujo virus, a new hemorrhagic fever-associated arenavirus from southern Africa. *PLoS Pathog*. 2009;5: e1000455. doi:10.1371/journal.ppat.1000455
62. Stenglein MD, Sanchez-Migallon Guzman D, Garcia VE, Layton ML, Hoon-Hanks LL, Boback SM, et al. Differential Disease Susceptibilities in Experimentally Reptarenavirus-Infected Boa Constrictors and Ball Pythons. *J Virol*. 2017;91. doi:10.1128/JVI.00451-17
63. Stenglein MD, Sanders C, Kistler AL, Ruby JG, Franco JY, Reavill DR, et al. Identification, characterization, and in vitro culture of highly divergent arenaviruses from boa constrictors and annulated tree boas: candidate etiological agents for snake inclusion body disease. *mBio*. 2012;3: e00180-00112. doi:10.1128/mBio.00180-12
64. Honkavuori KS, Shivaprasad HL, Williams BL, Quan PL, Hornig M, Street C, et al. Novel borna virus in psittacine birds with proventricular dilatation disease. *Emerg Infect Dis*. 2008;14: 1883–1886. doi:10.3201/eid1412.080984
65. Koch R. *Ueber bakteriologische Forschung*. August Hirschwald, Berlin, Germany; 1891.
66. Evans AS. Causation and disease: the Henle-Koch postulates revisited. *Yale J Biol Med*. 1976;49: 175–195.
67. Fredericks DN, Relman DA. Sequence-based identification of microbial pathogens: a reconsideration of Koch's postulates. *Clin Microbiol Rev*. 1996;9: 18. doi:10.1128/CMR.9.1.18
68. Rivers T. Viruses and Koch's postulates. *J Bacteriol*. 1937;33: 1–12.
69. Brüggemann H, Bäumer S, Fricke WF, Wiezer A, Liesegang H, Decker I, et al. The genome sequence of *Clostridium tetani*, the causative agent of tetanus disease. *Proc Natl Acad Sci*. 2003;100: 1316. doi:10.1073/pnas.0335853100
70. Segelke B, Knapp M, Kadkhodayan S, Balhorn R, Rupp B. Crystal structure of *Clostridium botulinum* neurotoxin protease in a product-bound state: Evidence for noncanonical zinc protease activity. *Proc Natl Acad Sci U S A*. 2004;101: 6888. doi:10.1073/pnas.0400584101
71. Steere AC. Lyme disease. *N Engl J Med*. 2001;345: 115–125.

72. Cao-Lormeau VM, Blake A, Mons S, Lastere S, Roche C, Vanhomwegen J, et al. Guillain-Barré Syndrome outbreak associated with Zika virus infection in French Polynesia: a case-control study. *Lancet Lond Engl.* 2016;387: 1531–1539. doi:10.1016/S0140-6736(16)00562-6
73. Pichichero ME. Group A beta-hemolytic streptococcal infections. *Indian J Pediatr.* 1998;65: 881–881. doi:10.1007/BF02831353
74. zur Hausen H. Papillomaviruses and cancer: from basic studies to clinical application. *Nat Rev Cancer.* 2002;2: 342–350. doi:10.1038/nrc798
75. Gentile G, Micozzi A. Speculations on the clinical significance of asymptomatic viral infections. *Clin Microbiol Infect Off Publ Eur Soc Clin Microbiol Infect Dis.* 2016;22: 585–588. doi:10.1016/j.cmi.2016.07.016
76. Orenstein JM, Fox C, Wahl SM. Macrophages as a Source of HIV During Opportunistic Infections. *Science.* 1997;276: 1857. doi:10.1126/science.276.5320.1857
77. McCullers JA, Bartmess KC. Role of neuraminidase in lethal synergism between influenza virus and *Streptococcus pneumoniae*. *J Infect Dis.* 2003;187: 1000–1009. doi:10.1086/368163
78. Ziebuhr J, Baric RS, Baker S, de Groot RJ, Drosten C, Gulyaeva A, et al. Reorganization of the family Coronaviridae into two families, Coronaviridae (including the current subfamily Coronavirinae and the new subfamily Letovirinae) and the new family Tobaniviridae (accommodating the current subfamily Torovirinae and three other subfamilies), revision of the genus rank structure and introduction of a new subgenus rank. *International Committee on Taxonomy of Viruses*; 2018.
79. Gibbons JW, Scott DE, Ryan TJ, Buhlmann KA, Tuberville TD, Metts BS, et al. The Global Decline of Reptiles, Déjà Vu Amphibians Reptile species are declining on a global scale. Six significant threats to reptile populations are habitat loss and degradation, introduced invasive species, environmental pollution, disease, unsustainable use, and global climate change. *BioScience.* 2000;50: 653–666. doi:10.1641/0006-3568(2000)050[0653:TGDORD]2.0.CO;2
80. Reading CJ, Luiselli LM, Akani GC, Bonnet X, Amori G, Ballouard JM, et al. Are snake populations in widespread decline? *Biol Lett.* 2010;6: 777. doi:10.1098/rsbl.2010.0373
81. Fritts TH, Rodda GH. The role of introduced species in the degradation of island ecosystems: A case history of Guam. *Annu Rev Ecol Syst.* 1998;29: 113–140. doi:10.1146/annurev.ecolsys.29.1.113
82. Winne CT, Willson JD, Todd BD, Andrews KM, Gibbons JW. Enigmatic Decline of a Protected Population of Eastern Kingsnakes, *Lampropeltis Getula*, in South Carolina. *Copeia.* 2007;2007: 507–519. doi:10.1643/0045-8511(2007)2007[507:EDOAPP]2.0.CO;2
83. Allender MC, Raudabaugh DB, Gleason FH, Miller AN. The natural history, ecology, and epidemiology of *Ophidiomyces ophiodiicola* and its potential impact on free-ranging snake populations. *Fungal Ecol.* 2015;17: 187–196.
84. Daszak P, Berger L, Cunningham AA, Hyatt AD, Green DE, Speare R. Emerging infectious diseases and amphibian population declines. *Emerg Infect Dis.* 1999;5: 735–748.

85. James K. Jancovich, Elizabeth W. Davidson, J. Frank Morado, Bertram L. Jacobs, James P. Collins. Isolation of a lethal virus from the endangered tiger salamander *Ambystoma tigrinum stebbinsi*. *Dis Aquat Organ*. 1997;31: 161–167.
86. Robinson JE, Griffiths RA, St. John FAV, Roberts DL. Dynamics of the global trade in live reptiles: Shifting trends in production and consequences for sustainability. *Biol Conserv*. 2015;184: 42–50. doi:10.1016/j.biocon.2014.12.019
87. Schumacher J. Selected Infectious Diseases of Wild Reptiles and Amphibians. *J Exot Pet Med*. 2006;15: 18–24. doi:10.1053/j.jepm.2005.11.004
88. Cowan ML. Diseases of the Respiratory System. *Reptile Medicine and Surgery in Clinical Practice*. John Wiley & Sons, Ltd; 2017. pp. 299–306. doi:10.1002/9781118977705.ch21
89. Hyndman T, Marschang RE. Infectious Diseases and Immunology. *Reptile Medicine and Surgery in Clinical Practice*. John Wiley & Sons, Ltd; 2017. pp. 197–216. doi:10.1002/9781118977705.ch16
90. Blaylock RS. Normal oral bacterial flora from some southern African snakes. *Onderstepoort J Vet Res*. 2001;68: 175–182.
91. Goldstein EJ, Agyare EO, Vagvolgyi AE, Halpern M. Aerobic bacterial oral flora of garter snakes: development of normal flora and pathogenic potential for snakes and humans. *J Clin Microbiol*. 1981;13: 954–956.
92. Plenz B, Schmidt V, Grosse-Herrenthey A, Kruger M, Pees M. Characterisation of the aerobic bacterial flora of boid snakes: application of. *Vet Rec*. 2015;176: 285. doi:10.1136/vr.102580
93. Brown DR. Mycoplasmosis and immunity of fish and reptiles. *Front Biosci J Virtual Libr*. 2002;7: d1338-1346.
94. Mitchell MA. Mycobacterial infections in reptiles. *Veterinary Clin North Am Exot Anim Pract*. 2012;15: 101–111, vii. doi:10.1016/j.cvex.2011.10.002
95. Taylor-Brown A, Ruegg S, Polkinghorne A, Borel N. Characterisation of *Chlamydia pneumoniae* and other novel chlamydial infections in captive snakes. *Vet Microbiol*. 2015;178: 88–93. doi:10.1016/j.vetmic.2015.04.021
96. Franklinos LHV, Lorch JM, Bohuski E, Rodriguez-Ramos Fernandez J, Wright ON, Fitzpatrick L, et al. Emerging fungal pathogen *Ophidiomyces ophiodiicola* in wild European snakes. *Sci Rep*. 2017;7: 3844. doi:10.1038/s41598-017-03352-1
97. Foley J, Clifford D, Castle K, Cryan P, Ostfeld RS. Investigating and managing the rapid emergence of white-nose syndrome, a novel, fatal, infectious disease of hibernating bats. *Conserv Biol J Soc Conserv Biol*. 2011;25: 223–231. doi:10.1111/j.1523-1739.2010.01638.x
98. Lorch JM, Knowles S, Lankton JS, Michell K, Edwards JL, Kapfer JM, et al. Snake fungal disease: an emerging threat to wild snakes. *Philos Trans R Soc Lond B Biol Sci*. 2016;371: 20150457. doi:10.1098/rstb.2015.0457

99. Schmidt V, Klasen L, Schneider J, Hubel J, Cramer K. Pulmonary fungal granulomas and fibrinous pneumonia caused by different hypocrealean fungi in reptiles. *Vet Microbiol.* 2018;225: 58–63. doi:10.1016/j.vetmic.2018.09.008
100. Jacobson ER. *Infectious Diseases and Pathology of Reptiles. Chapter 12. Parasites and Parasitic Diseases of Reptiles: CRC Press; 2007.*
101. Ippen R, Zwart P. Infectious and parasitic disease of captive reptiles and amphibians, with special emphasis on husbandry practices which prevent or promote diseases. *Rev Sci Tech Int Off Epizoot.* 1996;15: 43–54.
102. Upton SJ, McAllister CT, Freed PS, Barnard SM. *Cryptosporidium* spp. in wild and captive reptiles. *J Wildl Dis.* 1989;25: 20–30. doi:10.7589/0090-3558-25.1.20
103. Grego KF, Gardiner CH, Catao-Dias JL. Comparative pathology of parasitic infections in free-ranging and captive pit vipers (*Bothrops jararaca*). *Vet Rec.* 2004;154: 559–562.
104. Paiva PRSO, Grego KF, Lima VMF, Nakamura AA, da Silva DC, Meireles MV. Clinical, serological, and parasitological analysis of snakes naturally infected with *Cryptosporidium serpentis*. *Vet Parasitol.* 2013;198: 54–61. doi:10.1016/j.vetpar.2013.08.016
105. Marschang RE. Viruses infecting reptiles. *Viruses.* 2011;3: 2087–2126. doi:10.3390/v3112087
106. Folsch DW, Leloup P. [Fatal endemic infection in a serpentarium. Diagnosis, treatment and preventive measures]. *Tierarztl Prax.* 1976;4: 527–536.
107. Jacobson ER, Adams HP, Geisbert TW, Tucker SJ, Hall BJ, Homer BL. Pulmonary lesions in experimental ophidian paramyxovirus pneumonia of Aruba Island rattlesnakes, *Crotalus unicolor*. *Vet Pathol.* 1997;34: 450–459. doi:10.1177/030098589703400509
108. Lamirande EW, Nichols DK, Owens JW, Gaskin JM, Jacobson ER. Isolation and experimental transmission of a reovirus pathogenic in ratsnakes (*Elaphe* species). *Virus Res.* 1999;63: 135–141.
109. Hyndman TH, Marschang RE, Wellehan JFXJ, Nicholls PK. Isolation and molecular identification of Sunshine virus, a novel paramyxovirus found in Australian snakes. *Infect Genet Evol J Mol Epidemiol Evol Genet Infect Dis.* 2012;12: 1436–1446. doi:10.1016/j.meegid.2012.04.022
110. Hyndman TH, Shilton CM, Doneley RJT, Nicholls PK. Sunshine virus in Australian pythons. *Vet Microbiol.* 2012;161: 77–87. doi:10.1016/j.vetmic.2012.07.030
111. Uccellini L, Ossiboff RJ, de Matos REC, Morrisey JK, Petrosov A, Navarrete-Macias I, et al. Identification of a novel nidovirus in an outbreak of fatal respiratory disease in ball pythons (*Python regius*). *Virology.* 2014;11: 144. doi:10.1186/1743-422X-11-144
112. Bodewes R, Lempp C, Schurch AC, Habierski A, Hahn K, Lamers M, et al. Novel divergent nidovirus in a python with pneumonia. *J Gen Virol.* 2014;95: 2480–2485. doi:10.1099/vir.0.068700-0
113. De Groot R, Cowley J, Enjuanes L, Faaberg K, Perlman S, Rottier P, et al. Order - Nidovirales. In: King AM, Adams MJ, Carstens EB, Lefkowitz EJ, editors. *Virus taxonomy: classification and nomenclature of viruses: Ninth Report of the International Committee on Taxonomy of Viruses.*

1st ed. San Diego: Elsevier; 2012. pp. 784–794. Available:
<http://www.sciencedirect.com/science/article/pii/B9780123846846000665>

114. Graham RL, Donaldson EF, Baric RS. A decade after SARS: strategies for controlling emerging coronaviruses. *Nat Rev Micro*. 2013;11: 836–848.
115. Lauber C, Ziebuhr J, Junglen S, Drosten C, Zirkel F, Nga PT, et al. Mesoniviridae: a proposed new family in the order Nidovirales formed by a single species of mosquito-borne viruses. *Arch Virol*. 2012;157: 1623–1628. doi:10.1007/s00705-012-1295-x
116. Masters PS, Perlman S. Coronaviridae. In: Knipe DM, Howley PM, editors. *Fields Virology*. 6th ed. Lippincott Williams & Wilkins; 2013. pp. 825–858.
117. Snijder EJ, Kikkert M, Fang Y. Arterivirus molecular biology and pathogenesis. *J Gen Virol*. 2013;94: 2141–2163.
118. Snijder EJ, Kikkert M. Arteriviruses. In: Knipe DM, Howley PM, editors. *Fields Virology*. 6th ed. Lippincott Williams & Wilkins; 2013. pp. 859–879.
119. Cowley JA, Dimmock CM, Wongteerasupaya C, Boonsaeng V, Panyim S, Walker PJ. Yellow head virus from Thailand and gill-associated virus from Australia are closely related but distinct prawn viruses. *Dis Aquat Organ*. 1999;36: 153–157. doi:10.3354/dao036153
120. Vasilakis N, Guzman H, Firth C, Forrester NL, Widen SG, Wood TG, et al. Mesoniviruses are mosquito-specific viruses with extensive geographic distribution and host range. *Virol J*. 2014;11: 97–97. doi:10.1186/1743-422X-11-97
121. Gorbalenya AE, Enjuanes L, Ziebuhr J, Snijder EJ. Nidovirales: evolving the largest RNA virus genome. *Virus Res*. 2006;117: 17–37. doi:10.1016/j.virusres.2006.01.017
122. Fields BN, Knipe DM (David M, Howley PM. *Fields virology*. 6th ed.. Philadelphia: Philadelphia : Wolters Kluwer/Lippincott Williams & Wilkins Health; 2013.
123. Saberi A, Gulyaeva AA, Brubacher JL, Newmark PA, Gorbalenya AE. A planarian nidovirus expands the limits of RNA genome size. *PLOS Pathog*. 2018;14: e1007314. doi:10.1371/journal.ppat.1007314
124. Fehr AR, Perlman S. Coronaviruses: an overview of their replication and pathogenesis. *Methods Mol Biol Clifton NJ*. 2015;1282: 1–23. doi:10.1007/978-1-4939-2438-7_1
125. Lightner DV. Virus diseases of farmed shrimp in the Western Hemisphere (the Americas): A review. *Dis Edible Crustac*. 2011;106: 110–130. doi:10.1016/j.jip.2010.09.012
126. Batts WN, Goodwin AE, Winton JR. Genetic analysis of a novel nidovirus from fathead minnows. *J Gen Virol*. 2012;93: 1247–1252. doi:10.1099/vir.0.041210-0
127. Pradesh U, Chikitsa PDDUP, Vishwa V, Dhcirnci C, Izcitncigcir B. Toroviruses affecting animals and humans: A review. *Asian J Anim Vet Adv*. 2014;9: 190–201.
128. Hoet AE, Cho K-O, Chang K-O, Loerch SC, Wittum TE, Saif LJ. Enteric and nasal shedding of bovine torovirus (Breda virus) in feedlot cattle. *Am J Vet Res*. 2002;63: 342–348.

129. Gorbalenya AE, Brinton MA, Cowley J, De Groot RJ, Gulyaeva A, Lauber C, et al. Reorganization and expansion of the order Nidovirales at the family and sub-order ranks. *International Committee on Taxonomy of Viruses*; 2018.
130. Tokarz R, Sameroff S, Hesse RA, Hause BM, Desai A, Jain K, et al. Discovery of a novel nidovirus in cattle with respiratory disease. *J Gen Virol*. 2015;96: 2188–2193. doi:10.1099/vir.0.000166
131. O’Dea MA, Jackson B, Jackson C, Xavier P, Warren K. Discovery and Partial Genomic Characterisation of a Novel Nidovirus Associated with Respiratory Disease in Wild Shingleback Lizards (*Tiliqua rugosa*). *PloS One*. 2016;11: e0165209. doi:10.1371/journal.pone.0165209
132. Marschang RE, Kolesnik E. Detection of nidoviruses in live pythons and boas. *Tierarztl Prax Ausg K Kleintiere Heimtiere*. 2017;45: 22–26. doi:10.15654/TPK-151067
133. Dervas E, Hepojoki J, Laimbacher A, Romero-Palomo F, Jelinek C, Keller S, et al. Nidovirus-Associated Proliferative Pneumonia in the Green Tree Python (*Morelia viridis*). *J Virol*. 2017; doi:10.1128/JVI.00718-17
134. Zhang J, Finlaison DS, Frost MJ, Gestier S, Gu X, Hall J, et al. Identification of a novel nidovirus as a potential cause of large scale mortalities in the endangered Bellinger River snapping turtle (*Myuchelys georgesi*). *PloS One*. 2018;13: e0205209. doi:10.1371/journal.pone.0205209
135. Kuwabara M, Wada K, Maeda Y, Miyazaki A, Tsunemitsu H. First Isolation of Cytopathogenic Bovine Torovirus in Cell Culture from a Calf with Diarrhea. *Clin Vaccine Immunol*. 2007;14: 998. doi:10.1128/CVI.00475-06
136. Grgic H, Hunter DB, Hunton P, Nagy E. Pathogenicity of infectious bronchitis virus isolates from Ontario chickens. *Can J Vet Res Rev Can Rech Veterinaire*. 2008;72: 403–410.
137. Schunk MK, Percy DH, Rosendal S. Effect of time of exposure to rat coronavirus and *Mycoplasma pulmonis* on respiratory tract lesions in the Wistar rat. *Can J Vet Res Rev Can Rech Veterinaire*. 1995;59: 60–66.
138. Maestre AM, Garzón A, Rodríguez D. Equine Torovirus (BEV) Induces Caspase-Mediated Apoptosis in Infected Cells. *PLOS ONE*. 2011;6: e20972. doi:10.1371/journal.pone.0020972
139. Hoon-Hanks LL, McGrath S, Tyler KL, Owen C, Stenglein MD. Metagenomic Investigation of Idiopathic Meningoencephalomyelitis in Dogs. *J Vet Intern Med*. 2017; doi:10.1111/jvim.14877
140. Coates JR, Jeffery ND. Perspectives on Meningoencephalomyelitis of Unknown Origin. *Adv Vet Neurol*. 2014;44: 1157–1185. doi:10.1016/j.cvsm.2014.07.009
141. Talarico LR, Schatzberg SJ. Idiopathic granulomatous and necrotising inflammatory disorders of the canine central nervous system: a review and future perspectives. *J Small Anim Pract*. 2010;51: 138–149. doi:10.1111/j.1748-5827.2009.00823.x
142. Cordy DR, Holliday TA. A necrotizing meningoencephalitis of pug dogs. *Vet Pathol*. 1989;26: 191–194. doi:10.1177/030098588902600301
143. Tipold A, Fatzer R, Jaggy A, Zurbriggen A, Vandeveld M. Necrotizing encephalitis in Yorkshire terriers. *J Small Anim Pract*. 1993;34: 623–628. doi:10.1111/j.1748-5827.1993.tb02598.x

144. Stalis IH, Chadwick B, Dayrell-Hart B, Summers BA, Van Winkle TJ. Necrotizing meningoencephalitis of Maltese dogs. *Vet Pathol.* 1995;32: 230–235. doi:10.1177/030098589503200303
145. Timmann D, Konar M, Howard J, Vandeveld M. Necrotising encephalitis in a French bulldog. *J Small Anim Pract.* 2007;48: 339–342. doi:10.1111/j.1748-5827.2006.00239.x
146. Cantile C, Chianini F, Arispici M, Fatzer R. Necrotizing Meningoencephalitis Associated with Cortical Hippocampal Hamartia in a Pekingese Dog. *Vet Pathol.* 2001;38: 119–122. doi:10.1354/vp.38-1-119
147. Aresu L. Canine Necrotizing Encephalitis Associated with Anti-glomerular Basement Membrane Glomerulonephritis. *J Comp Pathol.* 2007;v. 136: 279–282. doi:10.1016/j.jcpa.2007.02.008
148. Tipold A. Diagnosis of inflammatory and infectious diseases of the central nervous system in dogs: a retrospective study. *J Vet Intern Med.* 1995;9: 304–314.
149. Kipar A, Baumgärtner W, Vogl C, Gaedke K, Wellman M. Immunohistochemical Characterization of Inflammatory Cells in Brains of Dogs with Granulomatous Meningoencephalitis. *Vet Pathol.* 1998;35: 43–52. doi:10.1177/030098589803500104
150. Fluehmann G, Doherr MG, Jaggy A. Canine neurological diseases in a referral hospital population between 1989 and 2000 in Switzerland. *J Small Anim Pract.* 2006;47: 582–587. doi:10.1111/j.1748-5827.2006.00106.x
151. Schatzberg SJ, Haley NJ, Barr SC, de Lahunta A, Sharp NJH. Polymerase chain reaction screening for DNA viruses in paraffin-embedded brains from dogs with necrotizing meningoencephalitis, necrotizing leukoencephalitis, and granulomatous meningoencephalitis. *J Vet Intern Med.* 2005;19: 553–559.
152. Barber RM, Porter BF, Li Q, May M, Claiborne MK, Allison AB, et al. Broadly reactive polymerase chain reaction for pathogen detection in canine granulomatous meningoencephalomyelitis and necrotizing meningoencephalitis. *J Vet Intern Med.* 2012;26: 962–968. doi:10.1111/j.1939-1676.2012.00954.x
153. Schwab S, Herden C, Seeliger F, Papaioannou N, Psalla D, Polizopoulou Z, et al. Non-suppurative meningoencephalitis of unknown origin in cats and dogs: an immunohistochemical study. *J Comp Pathol.* 2007;136: 96–110. doi:10.1016/j.jcpa.2006.11.006
154. Li L, Diab S, McGraw S, Barr B, Traslavina R, Higgins R, et al. Divergent astrovirus associated with neurologic disease in cattle. *Emerg Infect Dis.* 2013;19: 1385–1392. doi:10.3201/eid1909.130682
155. Wilson MR, Naccache SN, Samayoa E, Biagtan M, Bashir H, Yu G, et al. Actionable diagnosis of neuroleptospirosis by next-generation sequencing. *N Engl J Med.* 2014;370: 2408–2417. doi:10.1056/NEJMoa1401268
156. Grubaugh ND, Smith DR, Brackney DE, Bosco-Lauth AM, Fauver JR, Campbell CL, et al. Experimental evolution of an RNA virus in wild birds: evidence for host-dependent impacts on population structure and competitive fitness. *PLoS Pathog.* 2015;11: e1004874. doi:10.1371/journal.ppat.1004874

157. Stenglein MD, Jacobson ER, Chang L-W, Sanders C, Hawkins MG, Guzman DS-M, et al. Widespread recombination, reassortment, and transmission of unbalanced compound viral genotypes in natural arenavirus infections. *PLoS Pathog.* 2015;11: e1004900. doi:10.1371/journal.ppat.1004900
158. Martin M. Cutadapt removes adapter sequences from high-throughput sequencing reads. *EMBnet journal.* 2011;17. Available: <http://journal.embnet.org/index.php/embnetjournal/article/view/200>
159. Li W, Godzik A. Cd-hit: a fast program for clustering and comparing large sets of protein or nucleotide sequences. *Bioinforma Oxf Engl.* 2006;22: 1658–1659. doi:10.1093/bioinformatics/btl158
160. Langmead B, Salzberg SL. Fast gapped-read alignment with Bowtie 2. *Nat Methods.* 2012;9: 357–359. doi:10.1038/nmeth.1923
161. Bankevich A, Nurk S, Antipov D, Gurevich AA, Dvorkin M, Kulikov AS, et al. SPAdes: a new genome assembly algorithm and its applications to single-cell sequencing. *J Comput Biol.* 2012;19: 455–477.
162. Altschul SF, Gish W, Miller W, Myers EW, Lipman DJ. Basic local alignment search tool. *J Mol Biol.* 1990;215: 403–410. doi:10.1016/S0022-2836(05)80360-2
163. Camacho C, Coulouris G, Avagyan V, Ma N, Papadopoulos J, Bealer K, et al. BLAST+: architecture and applications. *BMC Bioinformatics.* 2009;10: 421. doi:10.1186/1471-2105-10-421
164. BLAST+ Command Line Applications User Manual [Internet]. Available: <http://www.ncbi.nlm.nih.gov/bookshelf/br.fcgi?book=helpblast>
165. Zhao Y, Tang H, Ye Y. RAPSearch2: a fast and memory-efficient protein similarity search tool for next-generation sequencing data. *Bioinformatics.* 2012;28: 125–126. doi:10.1093/bioinformatics/btr595
166. Wu TD, Nacu S. Fast and SNP-tolerant detection of complex variants and splicing in short reads. *Bioinforma Oxf Engl.* 2010;26: 873–881. doi:10.1093/bioinformatics/btq057
167. Johnson M, Zaretskaya I, Raytselis Y, Merezhuk Y, McGinnis S, Madden TL. NCBI BLAST: a better web interface. *Nucleic Acids Res.* 2008;36: W5-9. doi:10.1093/nar/gkn201
168. NCBI BLAST web site [Internet]. Available: <https://blast.ncbi.nlm.nih.gov/Blast.cgi>
169. Grubaugh ND, Sharma S, Krajacich BJ, Fakoli Iii LS, Bolay FK, Diclaro Ii JW, et al. Xenosurveillance: a novel mosquito-based approach for examining the human-pathogen landscape. *PLoS Negl Trop Dis.* 2015;9: e0003628. doi:10.1371/journal.pntd.0003628
170. Xu GJ, Kula T, Xu Q, Li MZ, Vernon SD, Ndung'u T, et al. Viral immunology. Comprehensive serological profiling of human populations using a synthetic human virome. *Science.* 2015;348: aaa0698. doi:10.1126/science.aaa0698

171. Li H, Keller J, Knowles DP, Crawford TB. Recognition of another member of the malignant catarrhal fever virus group: an endemic gammaherpesvirus in domestic goats. *J Gen Virol*. 2001;82: 227–232.
172. Plowright W, Ferris RD, Scott GR. Blue wildebeest and the aetiological agent of bovine malignant catarrhal fever. *Nature*. 1960;188: 1167–1169.
173. Klieforth R, Maalouf G, Stalis I, Terio K, Janssen D, Schrenzel M. Malignant catarrhal fever-like disease in Barbary red deer (*Cervus elaphus barbarus*) naturally infected with a virus resembling alcelaphine herpesvirus 2. *J Clin Microbiol*. 2002;40: 3381–3390.
174. Baxter SI, Pow I, Bridgen A, Reid HW. PCR detection of the sheep-associated agent of malignant catarrhal fever. *Arch Virol*. 1993;132: 145–159.
175. Li H, Cunha CW, Taus NS, Knowles DP. Malignant Catarrhal Fever: Inching Toward Understanding. *Annu Rev Anim Biosci*. 2014;2: 209–233. doi:10.1146/annurev-animal-022513-114156
176. Li H, Dyer N, Keller J, Crawford TB. Newly recognized herpesvirus causing malignant catarrhal fever in white-tailed deer (*Odocoileus virginianus*). *J Clin Microbiol*. 2000;38: 1313–1318.
177. Gasper D, Barr B, Li H, Taus N, Peterson R, Benjamin G, et al. Ibex-Associated Malignant Catarrhal Fever–Like Disease in a Group of Bongo Antelope (*Tragelaphus euryceros*). *Vet Pathol*. 2011;49: 492–497. doi:10.1177/0300985811429306
178. Okeson DM, Garner MM, Taus NS, Li H, Coke RL. Ibex-associated malignant catarrhal fever in a bongo antelope (*Tragelaphus euryceros*). *J Zoo Wildl Med Off Publ Am Assoc Zoo Vet*. 2007;38: 460–464. doi:10.1638/06-046.1
179. Crawford TB, Li H, Rosenberg SR, Norhausen RW, Garner MM. Mural folliculitis and alopecia caused by infection with goat-associated malignant catarrhal fever virus in two sika deer. *J Am Vet Med Assoc*. 2002;221: 843–847, 801.
180. Dettwiler M, Stahel A, Krüger S, Gerspach C, Braun U, Engels M, et al. A possible case of caprine-associated malignant catarrhal fever in a domestic water buffalo (*Bubalus bubalis*) in Switzerland. *BMC Vet Res*. 2011;7: 78–78. doi:10.1186/1746-6148-7-78
181. Keel MK, Gage PJ, Noon TH, Bradley GA, Collins JK. Caprine Herpesvirus-2 in Association with Naturally Occurring Malignant Catarrhal Fever in Captive Sika Deer (*Cervus Nippon*). *J Vet Diagn Invest*. 2003;15: 179–183. doi:10.1177/104063870301500215
182. Li H, Cunha CW, Taus NS. Malignant catarrhal fever: understanding molecular diagnostics in context of epidemiology. *Int J Mol Sci*. 2011;12: 6881–6893. doi:10.3390/ijms12106881
183. Li H, Wunschmann A, Keller J, Hall DG, Crawford TB. Caprine herpesvirus-2-associated malignant catarrhal fever in white-tailed deer (*Odocoileus virginianus*). *J Vet Diagn Investig Off Publ Am Assoc Vet Lab Diagn Inc*. 2003;15: 46–49. doi:10.1177/104063870301500110
184. Vikoren T, Li H, Lillehaug A, Jonassen CM, Bockerman I, Handeland K. Malignant catarrhal fever in free-ranging cervids associated with OvHV-2 and CpHV-2 DNA. *J Wildl Dis*. 2006;42: 797–807. doi:10.7589/0090-3558-42.4.797

185. Zhu H, Huang Q, Hu X, Chu W, Zhang J, Jiang L, et al. Caprine herpesvirus 2-associated malignant catarrhal fever of captive sika deer (*Cervus nippon*) in an intensive management system. *BMC Vet Res.* 2018;14: 38–38. doi:10.1186/s12917-018-1365-8
186. Li H, Westover WC, Crawford TB. Sheep-associated malignant catarrhal fever in a petting zoo. *J Zoo Wildl Med Off Publ Am Assoc Zoo Vet.* 1999;30: 408–412.
187. Schultheiss PC, Van Campen H, Spraker TR, Bishop C, Wolfe L, Podell B. Malignant catarrhal fever associated with ovine herpesvirus-2 in free-ranging mule deer in Colorado. *J Wildl Dis.* 2007;43: 533–537. doi:10.7589/0090-3558-43.3.533
188. Falk K, Batts WN, Kvellestad A, Kurath G, Wiik-Nielsen J, Winton JR. Molecular characterisation of Atlantic salmon paramyxovirus (ASPV): a novel paramyxovirus associated with proliferative gill inflammation. *Virus Res.* 2008;133: 218–227. doi:10.1016/j.virusres.2008.01.006
189. Kvellestad A, Dannevig BH, Falk K. Isolation and partial characterization of a novel paramyxovirus from the gills of diseased seawater-reared Atlantic salmon (*Salmo salar* L.). *J Gen Virol.* 2003;84: 2179–2189.
190. Woo PCY, Lau SKP, Martelli P, Hui S-W, Lau CCY, Fan RYY, et al. Fatal systemic necrotizing infections associated with a novel paramyxovirus, anaconda paramyxovirus, in green anaconda juveniles. *J Clin Microbiol.* 2014;52: 3614–3623. doi:10.1128/JCM.01653-14
191. Gogoi P, Ganar K, Kumar S. Avian Paramyxovirus: A Brief Review. *Transbound Emerg Dis.* 2017;64: 53–67. doi:10.1111/tbed.12355
192. Jacobson ER. *Infectious Diseases and Pathology of Reptiles. Chapter 9. Viruses and Viral Diseases of Reptiles: CRC Press; 2007.*
193. Péntzes JJ, de Souza WM, Agbandje-McKenna M, Gifford RJ. An ancient lineage of highly divergent parvoviruses infects both vertebrate and invertebrate hosts. *bioRxiv.* 2019; 571109. doi:10.1101/571109
194. Roediger B, Lee Q, Tikoo S, Cobbin JCA, Henderson JM, Jormakka M, et al. An Atypical Parvovirus Drives Chronic Tubulointerstitial Nephropathy and Kidney Fibrosis. *Cell.* 2018;175: 530-543.e24. doi:10.1016/j.cell.2018.08.013
195. Beineke A, Puff C, Seehusen F, Baumgärtner W. Pathogenesis and immunopathology of systemic and nervous canine distemper. *Vet Immunol Immunopathol.* 2009;127: 1–18. doi:10.1016/j.vetimm.2008.09.023
196. Stuetzer B, Hartmann K. Feline parvovirus infection and associated diseases. *Spec Issue Feline Infect Dis.* 2014;201: 150–155. doi:10.1016/j.tvjl.2014.05.027
197. Szentiks CA, Tsangaras K, Abendroth B, Scheuch M, Stenglein MD, Wohlsein P, et al. Polar bear encephalitis: establishment of a comprehensive next-generation pathogen analysis pipeline for captive and free-living wildlife. *J Comp Pathol.* 2014;150: 474–488. doi:10.1016/j.jcpa.2013.12.005

198. Prüss H, Leubner J, Wenke NK, Czirják GÁ, Szentiks CA, Greenwood AD. Anti-NMDA Receptor Encephalitis in the Polar Bear (*Ursus maritimus*) Knut. Sci Rep. 2015;5: 12805–12805. doi:10.1038/srep12805
199. Hoon-Hanks LL, Layton ML, Ossiboff RJ, Parker JSL, Dubovi EJ, Stenglein MD. Respiratory disease in ball pythons (*Python regius*) experimentally infected with ball python nidovirus. Virology. 2018;517: 77–87. doi:10.1016/j.virol.2017.12.008
200. Runckel C, Flenniken ML, Engel JC, Ruby JG, Ganem D, Andino R, et al. Temporal Analysis of the Honey Bee Microbiome Reveals Four Novel Viruses and Seasonal Prevalence of Known Viruses, Nosema, and Crithidia. PLOS ONE. 2011;6: e20656. doi:10.1371/journal.pone.0020656
201. Buchfink B, Xie C, Huson DH. Fast and sensitive protein alignment using DIAMOND. Nat Methods. 2015;12: 59–60. doi:10.1038/nmeth.3176
202. Ariel E. Viruses in reptiles. Vet Res. 2011;42: 100.
203. Bodetti TJ, Jacobson E, Wan C, Hafner L, Pospischil A, Rose K, et al. Molecular evidence to support the expansion of the hostrange of *Chlamydophila pneumoniae* to include reptiles as well as humans, horses, koalas and amphibians. Syst Appl Microbiol. 2002;25: 146–152. doi:10.1078/0723-2020-00086
204. Jacobson ER. Infectious Diseases and Pathology of Reptiles. Chapter 5. Host response to infectious agents and identification of pathogens in tissue section.: CRC Press; 2007.
205. Penner JD, Jacobson ER, Brown DR, Adams HP, Besch-Williford CL. A novel *Mycoplasma* sp. associated with proliferative tracheitis and pneumonia in a Burmese python (*Python molurus bivittatus*). J Comp Pathol. 1997;117: 283–288.
206. Starck JM, Weimer I, Aupperle H, Muller K, Marschang RE, Kiefer I, et al. Morphological Pulmonary Diffusion Capacity for Oxygen of Burmese Pythons (*Python molurus*): a Comparison of Animals in Healthy Condition and with Different Pulmonary Infections. J Comp Pathol. 2015;153: 333–351. doi:10.1016/j.jcpa.2015.07.004
207. Hoon-Hanks LL, Ossiboff RJ, Bartolini P, Fogelson SB, Perry SM, Stöhr AC, et al. An epidemiologic investigation of serpentovirus (nidovirus) infection in captive snake populations. Front Vet Sci. 2019;Submitted.
208. Rampacci E, Masi M, Origgi FC, Stefanetti V, Bottinelli M, Selleri P, et al. First molecular detection of ball python nidovirus in Italy - Short communication. Acta Vet Hung. 2019;67: 127–134. doi:10.1556/004.2019.014
209. Katoh K, Standley DM. MAFFT Multiple Sequence Alignment Software Version 7: Improvements in Performance and Usability. Mol Biol Evol. 2013;30: 772–780. doi:10.1093/molbev/mst010
210. Misawa K, Katoh K, Kuma K, Miyata T. MAFFT: a novel method for rapid multiple sequence alignment based on fast Fourier transform. Nucleic Acids Res. 2002;30: 3059–3066. doi:10.1093/nar/gkf436

211. Guindon S, Dufayard J-F, Lefort V, Anisimova M, Hordijk W, Gascuel O. New Algorithms and Methods to Estimate Maximum-Likelihood Phylogenies: Assessing the Performance of PhyML 3.0. *Syst Biol.* 2010;59: 307–321. doi:10.1093/sysbio/syq010
212. Hasegawa M, Kishino H, Yano T. Dating of the human-ape splitting by a molecular clock of mitochondrial DNA. *J Mol Evol.* 1985;22: 160–174.
213. Pees M, Schmidt V, Marschang RE, Heckers KO, Krautwald-Junghanns M-E. Prevalence of viral infections in captive collections of boid snakes in Germany. *Vet Rec.* 2010;166: 422. doi:10.1136/vr.b4819
214. Schmidt V, Marschang RE, Abbas MD, Ball I, Szabo I, Helmuth R, et al. Detection of pathogens in Boidae and Pythonidae with and without respiratory disease. *Vet Rec.* 2013;172: 236. doi:10.1136/vr.100972
215. DeNardo D. Chapter 9 - Stress in Captive Reptiles A2 - Mader, Douglas R. *Reptile Medicine and Surgery (Second Edition)*. Saint Louis: W.B. Saunders; 2006. pp. 119–123. doi:10.1016/B0-72-169327-X/50013-4
216. Murray MJ. Chapter 65 - Pneumonia and Lower Respiratory Tract Disease A2 - Mader, Douglas R. *Reptile Medicine and Surgery (Second Edition)*. Saint Louis: W.B. Saunders; 2006. pp. 865–877. doi:10.1016/B0-72-169327-X/50069-9
217. Chu DKW, Peiris JSM, Chen H, Guan Y, Poon LLM. Genomic characterizations of bat coronaviruses (1A, 1B and HKU8) and evidence for co-infections in *Miniopterus* bats. *J Gen Virol.* 2008;89: 1282–1287.
218. Smits SL, Lavazza A, Matiz K, Horzinek MC, Koopmans MP, de Groot RJ. Phylogenetic and Evolutionary Relationships among Torovirus Field Variants: Evidence for Multiple Intertypic Recombination Events. *J Virol.* 2003;77: 9567. doi:10.1128/JVI.77.17.9567-9577.2003
219. Cowley JA, Hall MR, Cadogan LC, Spann KM, Walker PJ. Vertical transmission of gill-associated virus (GAV) in the black tiger prawn *Penaeus monodon*. *Dis Aquat Organ.* 2002;50: 95–104.
220. Vaala WE, Hamir AN, Dubovi EJ, Timoney PJ, Ruiz B. Fatal, congenitally acquired infection with equine arteritis virus in a neonatal Thoroughbred. *Equine Vet J.* 1992;24: 155–158. doi:10.1111/j.2042-3306.1992.tb02803.x
221. Bovarnick MR, Miller JC, Snyder JC. The influence of certain salts, amino acids, sugars, and proteins on the stability of rickettsiae. *J Bacteriol.* 1950;59: 509–522.
222. Abbas MD, Marschang RE, Schmidt V, Kasper A, Papp T. A unique novel reptilian paramyxovirus, four atadenovirus types and a reovirus identified in a concurrent infection of a corn snake (*Pantherophis guttatus*) collection in Germany. *Vet Microbiol.* 2011;150: 70–79.
223. Marschang RE, Donahoe S, Manvell R, Lemos-Espinal J. Paramyxovirus and reovirus infections in wild-caught Mexican lizards (*Xenosaurus* and *Abronia* spp.). *J Zoo Wildl Med Off Publ Am Assoc Zoo Vet.* 2002;33: 317–321.
224. Blahak S, Ott I, Vieler E. Comparison of 6 different reoviruses of various reptiles. *Vet Res.* 1995;26: 470–476.

225. Ahne W, Thomsen I, Winton J. Isolation of a reovirus from the snake, *Python regius*. Brief report. *Arch Virol*. 1987;94: 135–139.
226. Gravendyck M, Ammermann P, Marschang RE, Kaleta EF. Paramyxoviral and reoviral infections of iguanas on Honduran Islands. *J Wildl Dis*. 1998;34: 33–38.
227. Raynaud A, Adrian M. [Cutaneous lesions with papillomatous structure associated with viruses in the green lizard (*Lacerta viridis* Laur.)]. *Comptes Rendus Hebd Seances Acad Sci Ser Sci Nat*. 1976;283: 845–847.
228. Drury SEN, Gough RE, Welchman D de B. Isolation and identification of a reovirus from a lizard, *Uromastyx hardwickii*, in the United Kingdom. *Vet Rec*. 2002;151: 637–638.
229. Marschang RE, Papp T. Isolation and Partial Characterization of Three Reoviruses from Lizards. *J Herpetol Med Surg*. 2009;19: 13–15. doi:10.5818/1529-9651.19.1.13
230. Clark HF, Lief FS, Lunger PD, Waters D, Leloup P, Foelsch DW, et al. Fer de Lance virus (FDLV): a probable paramyxovirus isolated from a reptile. *J Gen Virol*. 1979;44: 405–418. doi:10.1099/0022-1317-44-2-405
231. Endangered species. Environmental conservation online system. [Internet]. U.S. Fish and Wildlife Service; Available: <https://ecos.fws.gov/>

APPENDIX

Chapter 2 Supplemental Tables

Supplemental Table 2.1. Average reads per canine sample and sequencing analysis summary. The average number of sequences generated per canine sample was calculated for all RNA-derived and DNA-derived libraries, as well as the total average depth per sample (RNA and DNA together). A) Average number of initial reads. B) Average number of reads remaining after removing low quality sequences. C) Average number of reads remaining after collapsing non-unique sequences into a single read. D) Average number of reads remaining after removing host-derived sequences.

	Total Reads (A)	Remove low quality reads (B)	Collapse to unique reads (C)	Host filter (D)
RNA	11.8 x 10 ⁶	8.6 x 10 ⁶ (74.1%)	1.9 x 10 ⁶ (16.2%)	0.2 x 10 ⁶ (1.3%)
DNA	11.3 x 10 ⁶	10.3 x 10 ⁶ (90.7%)	8.5 x 10 ⁶ (74.9%)	0.4 x 10 ⁶ (3.2%)
Total	11.6 x 10 ⁶	9.6 x 10 ⁶ (82.2%)	5.2 x 10 ⁶ (44.9%)	0.3 x 10 ⁶ (2.2%)

Supplemental Table 2.2. Positive control sequencing analysis summary. Positive control samples that had been previously sequenced using either metagenomic NGS (python) or targeted NGS (crow and robin) were used to validate our sequencing pipeline. Expected results were based on the known viral agents previously detected by sequencing. All expected agents were detected during this metagenomic NGS study, except within the robin, which was later confirmed WNV positive by PCR. The total read depth for the sample as well as the number of unique individual sequences that aligned to the known agent are provided within the table. NGS, next generation sequencing.

Sample	Known infectious agent	Total reads (depth)	Number of aligned sequences
Green tree python (RNA)	Python serpentovirus	8.7 x 10 ⁶	2,077
American Crow (RNA)	West Nile virus	12.4 x 10 ⁶	832
American Robin (RNA)	West Nile virus	7.6 x 10 ⁶	0

Supplemental Table 2.3: Oligonucleotides used in this study. Oligonucleotides are listed in the order they occur in the genome sequence (5' to 3'). F, forward; R, reverse; M, presumptive matrix protein; Fu, presumptive fusion protein; HN, presumptive hemagglutinin-neuraminidase protein; Pol, presumptive large polymerase protein.

Name	Sequence 5'-3'	F/R	Target
MDS-1417	CTCCAAAGTCTGTCCCTCTA	F	M
MDS-1418	AGATGGTCTTGGATTCCGTT	R	Fu
MDS-1389	AAATGATCTGGGCTGCGGTG	F	Fu
MDS-1390	TCATACCTTGCTCCATCACG	R	Fu
MDS-1387	CGTGATGGAGCAAGGTATGA	F	Fu
MDS-1388	ACCTGGTACTACTGAAATCC	R	Fu
MDS-1419	GGGCAGTGAATGGATTTCAG	F	Fu
MDS-1443	TCTGCTCTGTCAACTGGATC	R	HN
MDS-1420	ATACCGTCAATGTTTAGCAG	R	HN
MDS-1385	GGTGGATGTGAGGGAAGTAC	F	HN
MDS-1386	CGAGCAAAGGTAAGGTAGTA	R	Pol
MDS-1356	AGGATGAAGGGACAAAATAC	F	Pol
MDS-1357	AACCATGTCCCAAACGGTAT	R	Pol
MDS-1358	CAAGAACAGACGCCTAGGGA	F	Pol
MDS-1359	ATAACCTTTGGCTTCGGTCC	R	Pol
MDS-1424	CCGGTAAAGGAATGGTAGTG	R	Pol
MDS-1425	GATTCATGAAATTCCTCGAGCC	F	Pol
MDS-1446	TTCTTGAGGTTGGCTTGGGT	R	Pol
MDS-1447	GCCAAACATGACCCTGCATA	F	Pol
MDS-1448	ATGGACTTTGCTGCAGAGGT	R	Pol
MDS-1449	AATGGCCTGGCTCCTATAGT	F	Pol
MDS-1452	GTAGCATATCTGGAGACCCT	R	Pol

Chapter 4 Supplemental Tables

Supplemental Table 4.1. Summary table of each study collection. Sampling type: longitudinal (tested consecutively over time) or single (tested once). Portion of collection sampled: partial or complete or unknown. Status of serpentovirus in collection: present (known to be in collection prior to testing) or unknown. M, male. F, female. U, unknown. N/Av, not available. N/A, not applicable. Age was estimated for snakes designated as hatchlings (0.1 years) and juveniles (0.5 years). Respiratory score: 0-absent, 1-mild, 2-moderate, 3-severe. *Respiratory score count includes 1 uninfected snake; **Respiratory score count includes 2 uninfected snakes; ***Respiratory score count includes all uninfected snakes.

Collection A													
Type of sampling: Longitudinal													
Portion of collection sampled: Partial (91 of >200)													
Status of serpentoviruses in collection: Present													
Common Name	Scientific Name	Snake Family	Total Tested	Total Positive	Sex (Total #)			Age range (years)	Mean Age (years)	Respiratory Score (Total #)			
					M	F	U			0	1	2	3
Blackhead python	<i>Aspidites melanocephalus</i>	Pythonidae	2	0	1	1	0	3	3	2	0	0	0
Savu python	<i>Liasis mackloti savuensis</i>	Pythonidae	2	0	1	1	0	3	3	2	0	0	0
Olive python	<i>Liasis olivaceus</i>	Pythonidae	2	0	1	1	0	4	4	2	0	0	0
Rough scaled python	<i>Morelia carinata</i>	Pythonidae	2	2	1	1	0	5	5	0	0	2	0
Jungle carpet python	<i>Morelia spilota cheynei</i>	Pythonidae	8	6	4	2	2	0.1-4	2.5	4	0	3	1
Inland carpet python	<i>Morelia spilota metcalfei</i>	Pythonidae	2	2	1	1	0	4	4	0	1	0	1
Diamond python	<i>Morelia spilota spilota</i>	Pythonidae	2	2	1	1	0	4	4	0	0	0	2
Green tree python	<i>Morelia viridis</i>	Pythonidae	45	27	6	8	31	0.1-12	2.2	23	6	5	11
Ball python	<i>Python regius</i>	Pythonidae	1	1	0	1	0	2	N/A	0	0	0	1
Death adder	<i>Acanthophis rogosus</i>	Elapidae	1	0	0	0	1	0.5	N/A	1	0	0	0
Angolan coral cobra	<i>Aspidelaps lubricus cowlesi</i>	Elapidae	1	0	0	1	0	3	N/A	1	0	0	0
Shield nose cobra	<i>Aspidelaps s. scutatus</i>	Elapidae	1	0	0	0	1	0.5	N/A	1	0	0	0
Blackbacked Jameson mamba	<i>Dendroaspis j. jamesoni</i>	Elapidae	3	0	1	2	0	3	3	2	0	0	1*
Black mamba	<i>Dendroaspis polylepis</i>	Elapidae	1	0	0	0	1	3	N/A	1	0	0	0
Western green mamba	<i>Dendroaspis viridis</i>	Elapidae	3	0	2	1	0	3	3	3	0	0	0
Eastern green mamba	<i>Dendroaspis angusticeps</i>	Elapidae	1	0	0	1	0	3	N/A	1	0	0	0
Rinkhal's spitting cobra	<i>Hemachatus haemachatus</i>	Elapidae	1	0	0	1	0	3	N/A	1	0	0	0
Usambara bush viper	<i>Atheris ceratophora</i>	Viperidae	3	0	0	2	1	0.5-3	2.2	3	0	0	0
Mexican nomad Viper	<i>Atropoides nummifer</i>	Viperidae	1	0	0	0	1	0.5	N/A	1	0	0	0
Speckled forest pit viper	<i>Bothriopsis taeniata</i>	Viperidae	4	0	1	3	0	3	3	4	0	0	0
Brazilian lancehead pitviper	<i>Bothrops moojeni</i>	Viperidae	2	0	0	0	2	3	3	2	0	0	0
Sri Lankan palm pit viper	<i>Trimeresurus trigonocephalus</i>	Viperidae	3	0	1	2	0	3	3	3	0	0	0
TOTALS			91	40	21	30	40	0.1-12	2.6	57	7	10	17

Collection B													
Type of sampling: Single													
Portion of collection sampled: Unknown													
Status of serpentoviruses in collection: Unknown													
Common Name	Scientific Name	Snake Family	Total Tested	Total Positive	Sex (Total #)			Age range (years)	Mean Age (years)	Respiratory Score (Total #)			
					M	F	U			0	1	2	3
Carpet python	<i>Morelia spilota</i>	Pythonidae	5	5	0	1	4	N/Av	N/A	N/Av			
Green tree python	<i>Morelia viridis</i>	Pythonidae	2	2	1	0	1	N/Av	N/A	N/Av			
TOTALS			7	7	1	1	5	N/Av	N/A	N/Av			

Collection C													
Type of sampling: Single													
Portion of collection sampled: Complete													
Status of serpentoviruses in collection: Unknown													
Common Name	Scientific Name	Snake Family	Total Tested	Total Positive	Sex (Total #)			Age range (years)	Mean Age (years)	Respiratory Score (Total #)			
					M	F	U			0	1	2	3
Green tree python	<i>Morelia viridis</i>	Pythonidae	15	7	2	2	11	1-6	2.5	11	2	0	2
Emerald tree boa	<i>Corallus caninus</i>	Boidae	5	3	2	2	1	0.5-5	3.7	5	0	0	0
TOTALS			20	10	4	4	12	0.5-6	2.9	16	2	0	2

Collection D													
Type of sampling: Single													
Portion of collection sampled: Unknown													
Status of serpentoviruses in collection: Unknown													
Common Name	Scientific Name	Snake Family	Total Tested	Total Positive	Sex (Total #)			Age range (years)	Mean Age (years)	Respiratory Score (Total #)			
					M	F	U			0	1	2	3
Green tree python	<i>Morelia viridis</i>	Pythonidae	5	5	0	0	5	N/Av	N/A	N/Av			
TOTALS			5	5	0	0	5	N/Av	N/A	N/Av			

Collection E													
Type of sampling: Single													
Portion of collection sampled: Complete													
Status of serpentoviruses in collection: Unknown													
Common Name	Scientific Name	Snake Family	Total Tested	Total Positive	Sex (Total #)			Age range (years)	Mean Age (years)	Respiratory Score (Total #)			
					M	F	U			0	1	2	3
Olive python	<i>Liasis olivaceus</i>	Pythonidae	1	0	0	0	1	3	N/A	1	0	0	0
Green tree python	<i>Morelia viridis</i>	Pythonidae	10	10	0	0	10	0.5-3	2.8	10	0	0	0
Ball python	<i>Python regius</i>	Pythonidae	2	0	0	0	2	0.5	0.5	2	0	0	0
Boa constrictor	<i>Boa constrictor</i>	Boidae	3	0	0	0	3	0.5-3	2.2	3	0	0	0

Emerald tree boa	<i>Corallus caninus</i>	Boidae	24	2	0	0	24	0.5-3	1.9	24	0	0	0
Amazon tree boa	<i>Corallus hortulanus</i>	Boidae	2	1	0	0	2	0.5	0.5	2	0	0	0
Cornsnake	<i>Pantherophis guttatus</i>	Colubridae	9	0	0	0	9	3	3	9	0	0	0
TOTALS			51	13	0	0	51	1-3	2.2	51	0	0	0
Collection F													
Type of sampling: Single													
Portion of collection sampled: Complete													
Status of serpentoviruses in collection: Present													
Common Name	Scientific Name	Snake Family	Total Tested	Total Positive	Sex (Total #)			Age range (years)	Mean Age (years)	Respiratory Score (Total #)			
					M	F	U			0	1	2	3
Green tree python	<i>Morelia viridis</i>	Pythonidae	17	15	7	9	1	4-10	6.8	13	0	2	2
TOTALS			17	15	7	9	1	4-10	6.8	13	0	2	2
Collection G													
Type of sampling: Single													
Portion of collection sampled: Complete													
Status of serpentoviruses in collection: Present													
Common Name	Scientific Name	Snake Family	Total Tested	Total Positive	Sex (Total #)			Age range (years)	Mean Age (years)	Respiratory Score (Total #)			
					M	F	U			0	1	2	3
Anthill python	<i>Antaresia perthensis</i>	Pythonidae	2	1	1	1	0	N/Av	N/A	2	0	0	0
Woma python	<i>Aspidites ramsayi</i>	Pythonidae	2	0	1	1	0	N/Av	N/A	2	0	0	0
Diamond python	<i>Morelia spilota spilota</i>	Pythonidae	2	2	1	1	0	N/Av	N/A	1	0	1	0
Green tree python	<i>Morelia viridis</i>	Pythonidae	14	14	4	8	2	N/Av	N/A	8	1	2	3
Angolan python	<i>Python anchietae</i>	Pythonidae	2	1	1	1	0	N/Av	N/A	1	0	1	0
Ball python	<i>Python regius</i>	Pythonidae	2	2	1	1	0	N/Av	N/A	2	0	0	0
Rosy boa	<i>Lichanura trivirgata</i>	Boidae	1	0	1	0	0	N/Av	N/A	1	0	0	0
CA kingsnake	<i>Lampropeltis getula californiae</i>	Colubridae	2	0	1	1	0	N/Av	N/A	2	0	0	0
Nuevo Leon kingsnake	<i>Lampropeltis mexicana thayeri</i>	Colubridae	13	0	7	5	1	N/Av	N/A	13	0	0	0
AZ mountain kingsnake	<i>Lampropeltis pyromelana</i>	Colubridae	9	0	1	6	2	N/Av	N/A	9	0	0	0
Nelsons milksnake	<i>Lampropeltis t. nelsoni</i>	Colubridae	1	0	0	1	0	N/Av	N/A	1	0	0	0
Sinaloan milksnake	<i>Lampropeltis t. sinaloae</i>	Colubridae	4	0	2	2	0	N/Av	N/A	4	0	0	0
Baja CA mountain kingsnake	<i>Lampropeltis zonata algama</i>	Colubridae	1	0	0	0	1	N/Av	N/A	1	0	0	0
TOTALS			55	20	21	28	6	N/Av	N/A	47	1	4	3
Collection H													
Type of sampling: Single													
Portion of collection sampled: Complete													
Status of serpentoviruses in collection: Present													
Common Name	Scientific Name	Snake Family	Total Tested	Total Positive	Sex (Total #)			Age range (years)	Mean Age (years)	Respiratory Score (Total #)			
					M	F	U			0	1	2	3
Children's python	<i>Antaresia childreni</i>	Pythonidae	1	0	0	1	0	5	N/A	1	0	0	0
Bismarck ring python	<i>Bothrochilus boa</i>	Pythonidae	2	0	1	1	0	3-4	3.5	2	0	0	0
Savu python	<i>Liasis mackloti</i>	Pythonidae	2	0	1	1	0	3	3	2	0	0	0
Carpet python	<i>Morelia spilota</i>	Pythonidae	8	3	2	6	0	4-7	5.8	5	2	0	1
Green tree python	<i>Morelia viridis</i>	Pythonidae	1	1	0	1	0	3	N/A	1	0	0	0
Burmese python	<i>Python bivittatus</i>	Pythonidae	2	0	1	1	0	3-4	3.5	2	0	0	0
Borneo python	<i>Python breitensteini</i>	Pythonidae	20	2	6	14	0	1-4	2.1	19	1*	0	0
Blood python	<i>Python brongersmai</i>	Pythonidae	41	16	14	26	1	1-5	2.8	26	0	14	1
Sumatran python	<i>Python curtus</i>	Pythonidae	18	7	7	11	0	1-5	2.4	12	5**	1	0
Ball python	<i>Python regius</i>	Pythonidae	40	0	12	28	0	1-12	4	40	0	0	0
Reticulated python	<i>Malayopython reticulatus</i>	Pythonidae	7	2	3	4	0	3-4	3.4	5	2**	0	0
Kenyan sand boa	<i>Gongylophis colubrinus</i>	Boidae	3	0	2	1	0	2	2	3	0	0	0
West Africa sand boa	<i>Gongylophis muelleri</i>	Boidae	10	0	4	6	0	3	3	10	0	0	0
TOTALS			155	31	53	101	1	1-12	3.2	128	10	15	2
Collection I													
Type of sampling: Single													
Portion of collection sampled: Complete													
Status of serpentoviruses in collection: Unknown													
Common Name	Scientific Name	Snake Family	Total Tested	Total Positive	Sex (Total #)			Age range (years)	Mean Age (years)	Respiratory Score (Total #)			
					M	F	U			0	1	2	3
Ball python	<i>Python regius</i>	Pythonidae	76	4	35	41	0	0.1-11	1.9	73	0	3	0
Reticulated python	<i>Malayopython reticulatus</i>	Pythonidae	1	0	0	1	0	2	N/A	1	0	0	0
Dumeril's boa	<i>Acrantophis dumerili</i>	Boidae	1	0	1	0	0	4	N/A	1	0	0	0
Boa constrictor	<i>Boa constrictor</i>	Boidae	5	0	4	1	0	2-6	3.8	5	0	0	0
Brazilian rainbow boa	<i>Epicrates cenchrus</i>	Boidae	1	0	1	0	0	1	N/A	1	0	0	0
Kenyan sand boa	<i>Gongylophis colubrinus</i>	Boidae	1	0	0	1	0	0.1	N/A	1	0	0	0
TOTALS			85	4	41	44	0	0.5-11	2.1	82	0	3	0

Collection J													
Type of sampling: Single													
Portion of collection sampled: Partial (80 of 451)													
Status of serpentoviruses in collection: Unknown													
Common Name	Scientific Name	Snake Family	Total Tested	Total Positive	Sex (Total #)			Age range (years)	Mean Age (years)	Respiratory Score (Total #)			
					M	F	U			0	1	2	3
Spotted python	<i>Antaresia maculosa</i>	Pythonidae	3	0	1	2	0	N/Av	N/A	3	0	0	0
Angolan python	<i>Python anchietae</i>	Pythonidae	4	0	2	2	0	2-8	4.8	4	0	0	0
Blood python	<i>Python brongersmai</i>	Pythonidae	4	0	1	3	0	1-6	3	4	0	0	0
Sumatran python	<i>Python curtus</i>	Pythonidae	2	0	1	1	0	3	3	2	0	0	0
Ball python	<i>Python regius</i>	Pythonidae	10	0	8	2	0	1-4	1.8	4	6***	0	0
Boa constrictor	<i>Boa constrictor</i>	Boidae	6	0	3	3	0	1-10	3.8	6	0	0	0
Brazilian rainbow boa	<i>Epicrates cenchria</i>	Boidae	4	0	1	3	0	1-3	2.5	4	0	0	0
Kenyan sand boa	<i>Gongylophis colubrinus</i>	Boidae	7	0	4	3	0	3-5	3.7	7	0	0	0
Rosy boa	<i>Lichanura trivirgata</i>	Boidae	2	0	1	1	0	N/Av	N/A	2	0	0	0
Western hognose	<i>Heterodon nasicus</i>	Colubridae	4	0	1	3	0	4	4	4	0	0	0
Nuevo Leon kingsnake	<i>Lampropeltis mexicana thayeri</i>	Colubridae	4	0	1	3	0	4	4	4	0	0	0
Louisiana milksnake	<i>Lampropeltis t. amaura</i>	Colubridae	2	0	1	1	0	N/Av	N/A	2	0	0	0
Pueblan milksnake	<i>Lampropeltis t. campbelli</i>	Colubridae	3	0	1	2	0	N/Av	N/A	3	0	0	0
Honduran milksnake	<i>Lampropeltis t. hondurensis</i>	Colubridae	3	0	1	2	0	5-8	7	3	0	0	0
Baja CA mountain kingsnake	<i>Lampropeltis zonata algama</i>	Colubridae	2	0	1	1	0	5	5	2	0	0	0
Tricolor hognose	<i>Lystrophis pulcher</i>	Colubridae	7	0	4	2	1	2-4	3.1	7	0	0	0
Cornsnake	<i>Pantherophis guttatus</i>	Colubridae	13	0	4	9	0	4	4	13	0	0	0
TOTALS			80	0	36	43	1	10-Jan	3.5	74	6	0	0
Collection K													
Type of sampling: Single													
Portion of collection sampled: Partial													
Status of serpentoviruses in collection: Unknown													
Common Name	Scientific Name	Snake Family	Total Tested	Total Positive	Sex (Total #)			Age range (years)	Mean Age (years)	Respiratory Score (Total #)			
					M	F	U			0	1	2	3
Ball python	<i>Python regius</i>	Pythonidae	1	0	0	0	1	N/Av	N/A	1	0	0	0
Reticulated python	<i>Malayopython reticulatus</i>	Pythonidae	6	4	1	1	4	0.5-3	1.5	6	0	0	0
Western hognose	<i>Heterodon nasicus</i>	Colubridae	3	0	0	0	3	N/Av	N/A	3	0	0	0
California kingsnake	<i>Lampropeltis getula californiae</i>	Colubridae	14	0	0	0	14	N/Av	N/A	11	3***	0	0
Milksnake	<i>Lampropeltis triangulum</i>	Colubridae	1	0	0	0	1	N/Av	N/A	1	0	0	0
Sinaloa milksnake	<i>Lampropeltis t. sinaloae</i>	Colubridae	2	0	0	0	2	N/Av	N/A	2	0	0	0
Cornsnake	<i>Pantherophis guttatus</i>	Colubridae	12	0	0	0	12	N/Av	N/A	11	1*	0	0
Bullsnake	<i>Pituophis catenifer sayi</i>	Colubridae	2	0	0	0	2	N/Av	N/A	2	0	0	0
Cape gopher snake	<i>Pituophis vertebralis</i>	Colubridae	4	0	0	0	4	N/Av	N/A	4	0	0	0
African house snake	<i>Boaedon filiginosus</i>	Lamprophiidae	4	0	0	0	4	N/Av	N/A	4	0	0	0
TOTALS			49	4	1	1	47	N/Av	N/A	45	4	0	0
Collection L													
Type of sampling: Single													
Portion of collection sampled: N/A													
Status of serpentoviruses in collection: N/A													
Common Name	Scientific Name	Snake Family	Total Tested	Total Positive	Sex (Total #)			Age range (years)	Mean Age (years)	Respiratory Score (Total #)			
					M	F	U			0	1	2	3
Stimsons python	<i>Antaresia stimsoni</i>	Pythonidae	1	1	0	0	1	N/Av	N/A	0	0	1	0
Woma python	<i>Aspidites ramsayi</i>	Pythonidae	1	1	0	0	1	N/Av	N/A	0	0	1	0
Green tree python	<i>Morelia viridis</i>	Pythonidae	11	10	1	3	7	1-7	4.5	0	1	5	5*
Indian rock python	<i>Python molurus</i>	Pythonidae	1	1	0	0	1	10	N/A	0	0	0	1
Ball python	<i>Python regius</i>	Pythonidae	4	0	1	2	1	1-2	1.3	2	0	0	2**
Dumerils boa	<i>Acrantophis dumerili</i>	Boidae	1	1	0	0	1	N/Av	N/A	0	0	1	0
Boa constrictor	<i>Boa constrictor</i>	Boidae	2	0	1	1	0	16-22	19	1	0	0	1*
Puerto Rican boa	<i>Chilabothrus inornatus</i>	Boidae	1	1	0	0	1	3	N/A	1	0	0	0
Honduran milksnake	<i>Lampropeltis t. hondurensis</i>	Colubridae	1	1	0	0	1	3	N/A	1	0	0	0
Sumatran pit viper	<i>Trimeresurus sumatranus</i>	Viperidae	1	0	0	0	1	N/Av	N/A	1	0	0	0
TOTALS			24	16	3	6	15	1-22	6.3	6	1	8	9
TOTALS			639	165	188	267	184	0.1-22	4.2	519	31	42	35

Supplemental Table 4.2. Snakes screened for serpentoviruses by metagenomic sequencing. PCR positive prior to sequencing: yes (Y), no (N), or inconclusive (I). Serpentoviral reads detected with metagenomic sequencing: yes (Y), no (N). Snakes in which results differed between PCR and sequencing are highlighted (black border). Assuming a 32 kilobase genome size (for complete coding sequence), the approximate fraction of the genome covered (as a %) is provided. Approximate percent nucleotide identity to ball python nidovirus 1 (BPNV; NC_024709.1) is provided. If left blank, reference Figure 4.8 for alignment of short sequences. N/A, not applicable. S, Scaffold sequence with short gaps. *Reads only or short contigs, not a full or partial sequence. C, evidence of coinfection.

Common Name	Scientific Name	Collection ID	PCR Positive (Y/N/I)	Metagenomic Sequencing Positive (Y/N)	Approximate genome coverage (%)	Approximate % nucleotide identity to BPNV
Dumeril's boa	<i>Acrantophis dumerili</i>	L22	I	Y	4%*	
Anthill python	<i>Antaresia perthensis</i>	G58	Y	Y	23%*	
Stimson python	<i>Antaresia stimsoni</i>	L21	Y	Y	63%* C	
Woma python	<i>Aspidites ramsayi</i>	L14	Y	Y	76%	94%
Boa constrictor	<i>Boa constrictor</i>	I6	N	N	N/A	
Puerto Rican boa	<i>Chilabothrus inornatus</i>	L24	I	Y	8%*	
Emerald tree boa	<i>Corallus caninus</i>	C16	N	Y	1%*	
Emerald tree boa	<i>Corallus caninus</i>	C18	N	Y	85%	31%
Emerald tree boa	<i>Corallus caninus</i>	C19	N	Y	35% S	43%
Emerald tree boa	<i>Corallus caninus</i>	E18	I	Y	4%*	
Emerald tree boa	<i>Corallus caninus</i>	E32	I	N	N/A	
Emerald tree boa	<i>Corallus caninus</i>	E30	N	N	N/A	
Emerald tree boa	<i>Corallus caninus</i>	E35	N	N	N/A	
Amazon tree boa	<i>Corallus hortulanus</i>	E15	I	Y	17%*	
Kenyan sand boa	<i>Gongylophis colubrinus</i>	H2	N	N	N/A	
Kenyan sand boa	<i>Gongylophis colubrinus</i>	H4	N	N	N/A	
Kenyan sand boa	<i>Gongylophis colubrinus</i>	H6	N	N	N/A	
Kenyan sand boa	<i>Gongylophis colubrinus</i>	J201	N	N	N/A	
Nuevo Leon kingsnake	<i>Lampropeltis mexicana thayeri</i>	G33	N	N	N/A	
Nuevo Leon kingsnake	<i>Lampropeltis mexicana thayeri</i>	G36	N	N	N/A	
Arizona mountain kingsnake	<i>Lampropeltis pyromelana</i>	G19	N	N	N/A	
Honduran milksnake	<i>Lampropeltis triangulum hondurensis</i>	J190	N	N	N/A	
Honduran milksnake	<i>Lampropeltis triangulum hondurensis</i>	L25	N	Y	94%	30%
Reticulated python	<i>Malayopython reticulatus</i>	K48	Y	Y	85%	31%
Green tree python	<i>Morelia viridis</i>	A93	Y	Y	75%	80%
Green tree python	<i>Morelia viridis</i>	A94	Y	Y	86%	63%
Green tree python	<i>Morelia viridis</i>	A95	Y	Y	100%	72%
Green tree python	<i>Morelia viridis</i>	F17	Y	Y	100%	71%
Green tree python	<i>Morelia viridis</i>	L4	Y	Y	100%	63%
Green tree python	<i>Morelia viridis</i>	L8	Y	Y	99%	62%
Green tree python	<i>Morelia viridis</i>	L3	Y	Y	100%	63%
Cornsnake	<i>Pantherophis guttatus</i>	E44	N	N	N/A	
Cornsnake	<i>Pantherophis guttatus</i>	E48	N	N	N/A	
Angolan python	<i>Python anchietae</i>	G61	Y	Y	5%*	
Borneo python	<i>Python breitensteini</i>	H44	Y	Y	13%*	
Blood python	<i>Python brongersmai</i>	H0-1	Y	Y	100%	62%
Blood python	<i>Python brongersmai</i>	H0-2	Y	Y	100% S	63%
Sumatran python	<i>Python curtus</i>	H136	Y	Y	85%* C	
Ball python	<i>Python regius</i>	L1	Y	Y	95%	63%